Vol. 239: 231–232, 2002 | MARINE ECOLOGY PROGRESS SERIES
Mar Ecol Prog Ser | Published August 23

THEME SECTION

The Red Sea Programme: sailing a nutshell of hope in Red Sea waters

Gotthilf Hempel[1,*], Claudio Richter[2]

[1]Senatskanzlei, Freie Hansestadt Bremen, Altenwall 14, 28195 Bremen, Germany
[2]Zentrum für Marine Tropenökologie, Fahrenheitstraße 6, 28359 Bremen, Germany

Contributors to Theme Section: **S. Al-Moghrabi, T. Al-Najjar, M. Al-Qutob, S. Al-Rousan, M. I. Badran, U. G. Berninger, R. Böttger-Schnack, A. Cornils, Z. Dedej, M. El-Absawi, M. El-Gharabawi, A. El-Naggar, R. Gottlieb, H. P. Grossart, W. Hagen, T. Hansen, C. Häse, M. Huettel, M. A. Khalaf, M. Kochzius, H. Li, B. Lazar, J. Pätzold, A. F. Post, M. Rasheed, C. Richter, S. B. Schnack-Schiel, M. Simon, U. Sommer, H. Stibor, D. Stübing, D. N. Thomas, M. M. Tilzer, G. Wefer, S. Wickham**

Science is one of the few areas in which Arabs and Israelis can cooperate on common goals in a non-political context. After the signing of the 1993 Oslo peace agreement, there was widespread optimism that the dialogue and trust created by scientists would support the political peace process. The importance of science for peace was recognized by the German government, which supported the iniative of leading Israeli, German, Egyptian and Palestinian scientists to develop a major project of regional cooperation in marine science in the Red Sea area.

This initiative led to the creation of the 'Red Sea Programme' in 1995, coordinated by the Center for Tropical Marine Ecology in Bremen. With strong financial support from the German Ministry for Research and Technology and under the auspices of the Nobel Laureate Erwin Neher in Göttingen, the programme became one of the major multinational research networks in the area, with about 70 participants, including Jordanians, who joined the activities in 1997. Throughout its existence and beyond its termination, scheduled for 2001, the programme had important spin-offs to other scientific endeavours, such as the 1999 international Red Sea cruise of the RV 'Meteor' and the US-sponsored 'Red Sea Peace Park' between Israel and Jordan.

The Red Sea Programme was built on existing personal contacts between individual Middle East and German scientists and on traditional links between the German marine science community and the research institutions in Red Sea countries. The aim of the programme was to carry out cutting edge research on defined themes using a number of multinational teams. Research centered around: (1) ocean processes of the Gulf of Aqaba and northern Red Sea, (2) coral reef ecology, (3) calcification and palaeoclimate, (4) microbial processes at marine interfaces and (5) neurophysiology and toxins of reef organisms.

Most of the research activities took place at the Interuniversity Institute in Eilat (Israel) and the Aqaba Marine Science Station (Jordan), at opposite sides of the northern Gulf of Aqaba, with short-term cruises and land-based expeditions of individual teams to Egyptian waters. Sophisticated equipment was provided to the Interuniversity Institute in Eilat and its vessel was operated partly out of Red Sea Programme funds.

The RV 'Meteor' cruise leg 44/2, which was also coordinated by the authors with Gotthilf Hempel as chief scientist, provided the unique opportunity to carry out synoptic interdisciplinary research on a wider regional scale. Research focussed on pelagic processes during the winter/spring transition period, particularly on the dynamics of vertical mixing and microbial production in a weakly stratified oligotrophic water column.

The cruise was a real challenge to the coordinators and all participants: when leaving port in the Mediterranean no working permit for the Red Sea had reached us, except for the northernmost tip of the Gulf of Aqaba. While passing the Suez Canal, we still had no assurance as to who of the Middle East partners would

*E-mail: ghempel@marketing.bremen.de

be able to embark in Suez. But finally, programme scientists from all nationalities joined the cruise.

The Gulf of Aqaba is like a bathtub, ca. 165 km long and 15 km wide — not very large for a big research vessel to operate in for 15 d. The freedom of movement was mostly limited to a narrow central strip along the dividing line between Egyptian and Saudi territories. This resulted in a series of repeated transects. Fortunately, the cruise hit the rapid transition from winter to spring hydrographic conditions. This was well reflected in the narrow-meshed spatial and temporal series of samples and data sets.

In addition to closing gaps in our understanding of the ecology of the Red Sea, a major goal of the Red Sea Programme and the RV 'Meteor' cruise was to build the research capacity and infrastructure to enable cooperation on a more equal footing in the region. This involved on-the-job training of students in state-of-the-art research techniques, as well as a broad spectrum of introductory and specialized courses in Eilat and Aqaba with excursions to various coral sites along the Sinai and Jordan coasts. In those courses Arab, Israeli and German students and lecturers worked together. Several young Egyptian and Jordanian scientists obtained their PhD in Germany, while Palestinian PhD students were enrolled at Israeli universities. German MSc and PhD students and PostDocs did their field work in Egypt, Israel and Jordan. Regular scientific conferences served as fora for interdisciplinary discussions, particularly for young scientists. Special attention was given to joint publications reflecting the multinational cooperation under the Red Sea Programme. Human resource development was accompanied by the provision of modern equipment to the partner laboratories, allowing young researchers and postgraduates to carry on collaborative research in their home institutions after the end of the programme. More than 80 PhDs and MScs emerging from the programme or related to it, now constitute the core of a young generation of talented young scientists enriching the science capacity of the region, and of the Arab institutions in particular. The Red Sea Programme contributed to the establishment of a new department of marine science at the Palestinian Al Quds University and to the strengthening of the various branches of the Egyptian National Institute of Oceanography and Fisheries.

The following 7 contributions to *Marine Ecology Progress Series* were selected from a large collection of papers based on the Red Sea Programme and the RV 'Meteor' cruise (the full list is available at www.zmt.uni-bremen.de). They reflect the multinational character and wide scope of these activities, leading from nitrite and phytoplankton dynamics (Al-Qutob et al., Post et al.) to grazing (Sommer et al.) and to the dynamics of bacterioplankton (Grossart & Simon). The reef research is represented by 2 papers on the effects of the reef framework on nutrient cycling (Rasheed et al.) and of shore-based industry on fish populations (Khalaf & Kochzius). Palaeoenvironmental and biological effects on corals are tackled by the closing article (Al-Rousan et al.).

The multinational and multidisciplinary authorship reflects the spirit of the Red Sea Programme and the RV 'Meteor' cruise. We hope that the papers demonstrate that heavy constraints do not rule out good science, provided the scientific partners are willing to bridge gaps and overcome barriers, and provided they find support from some wise administrators.

Acknowledgements. We thank the Red Sea Programme and RV 'Meteor' cruise participants for their support and enthusiasm, the Red Sea Programme Steering Committee for advice and assistance, and the Egyptian, Israeli and Jordanian Authorities for permission to carry out the work. Financial support was granted by the German Ministry of Education and Research (BMBF, grant nos. 03F0151A, 03F0245A) and the German Research Council (DFG, grant no. HE 89/58-1). We are particularly grateful to the Editor O. Kinne for approving the publication of this Theme Section in *Marine Ecology Progress Series*.

Vol. 239: 233–239, 2002 | MARINE ECOLOGY PROGRESS SERIES
Mar Ecol Prog Ser | Published August 23

Phytoplankton drives nitrite dynamics in the Gulf of Aqaba, Red Sea

Mutaz Al-Qutob[1, 2,*], Clivia Häse[3, 4], Max M. Tilzer[5], Boaz Lazar[6, 7]

[1]Department of Biology, Faculty of Science and Technology, Alquds University, Palestinian Authority
[2]Department of Life Sciences, Bar Ilan University, Ramat Gan, Israel
[3]Center for Tropical Marine Ecology—ZMT, Fahrenheitstraße 6, Bremen, 28359 Bremen, Germany
[4]German Aerospace Center—DLR Oberpfaffenhofen, 82230 Wessling, Germany
[5]Aquatic Ecology, University of Constance, 78457 Konstanz, Germany
[6]Institute of Earth Sciences and [7]Moshe Shilo Centre for Marine Biogeochemistry, The Hebrew University of Jerusalem, Givat Ram, 91904 Jerusalem, Israel

ABSTRACT: This study focuses on the seasonal changes in the Gulf of Aquaba, Red Sea, in nitrite concentration and their relationship with phytoplankton activity, which is mainly controlled by an alternation of water-column stratification with vertical mixing. Within the euphotic zone, during thermal summer stratification, nutrient depletion was severe, and no nitrite could be detected in the upper 70 m. However, during stratification, nitrite was always associated with the nutriclines and formed a deep maximum at the bottom of the euphotic zone. In contrast, nitrite accumulated in the mixed water column during winter, closely paralleling the development of phytoplankton biomass. In the Gulf of Aqaba, maximum nitrite accumulation occurred when winter mixing reached its greatest depth, which in turn was coincident with the height of the phytoplankton spring bloom. Thus, our field data suggest that accumulation of nitrite is associated with nutrient-stimulated phytoplankton growth. This hypothesis was supported by nutrient-enrichment bioassays performed concomitantly: only when phytoplankton growth was stimulated by nutrient additions, did nitrite accumulate in the water. In the bioassays, the time-course of nitrite accumulation closely paralleled the development of phytoplankton biomass during the incubation period. We therefore suggest that the accumulation of nitrite in the mixed water column during winter is due to excretion by algal cells. Our field and experimental data show that between 10 and 15% of the total amount of nitrogen entering the mixed-water column is released as nitrite by phytoplankton. Further, our field and experimental data support the hypothesis that nitrite excretion by phytoplankton has a significant role in the formation of the deep nitrite maximum (DNM) during stratification in summer. In the bioassays, phytoplankton cells excreted nitrite even when ammonia was the nitrogen source. This indicates a so far unrecognised physiological pathway involved in nitrite excretion by phytoplankton cells.

KEY WORDS: Nutrients · Nitrogen species · Nitrite · Phytoplankton

INTRODUCTION

Nitrite plays an intermediate role in several biological processes within the oceanic nitrogen cycle, being the net result of different generation and consumption processes (Rakestraw 1936, Vaccaro & Ryther 1960). Surface or subsurface nitrite maxima occur over wide areas of the tropical and temperate oceans. In a stratified water column, the nitrite maximum is found near the bottom of the euphotic zone or, at higher latitudes, often throughout the upper mixed layer (Dore & Karl 1996a,b). In upwelling regions, or as a result of the introduction of nitrate into the euphotic zone by vertical winter mixing, the nitrite concentrations can increase remarkably (Rakestraw 1936, Olson 1981a,b, Dore & Karl 1996a).

*Present address: Department of Life Sciences, Bar Ilan University, Ramat Gan, Israel. E-mail: qutob@planet.edu

In the well-oxygenated water column of the Gulf of Aqaba, the dissimilatory reduction of nitrate to nitrite by denitrifying bacteria is likely to be negligible. Thus, we consider the following processes as potentially responsible for the generation and consumption of ambient nitrite in the Gulf of Aqaba: (1) Excretion of nitrite during nitrate reduction, i.e. incomplete assimilatory reduction of nitrate by phytoplankton and bacteria (Vaccaro & Ruyther 1960, Wada & Hattori, 1971, Miyazzaki et al. 1973, Miyazzaki et al. 1975, Kiefer et al. 1976, Herbland & Voituriez 1979, Olson 1981a, Dore & Karl, 1996b, Collos 1998). (2) Ammonium oxidation to nitrite by autotrophic nitrifying bacteria (Brandhorst 1959, Miyazzaki et al. 1975, Olson 1981a,b, Ward 1986, Dore & Karl 1996b, Enoksson et al. 1996). (3) Nitrite assimilation by phytoplankton and bacteria (Ward et al. 1989). (4) Nitrite oxidation to nitrate by autotrophic nitrifying bacteria (Ward et al. 1989, Dore & Karl 1996b).

Light is known to have a stimulating effect on phytoplankton nitrite excretion during nitrate assimilation (Wada & Hattori 1971), and an inhibitory effect on both ammonium oxidation and nitrite oxidation by nitrifying bacteria (Horrigan et al. 1981, Olson, 1981a,b, Guerrero & Jones 1996).

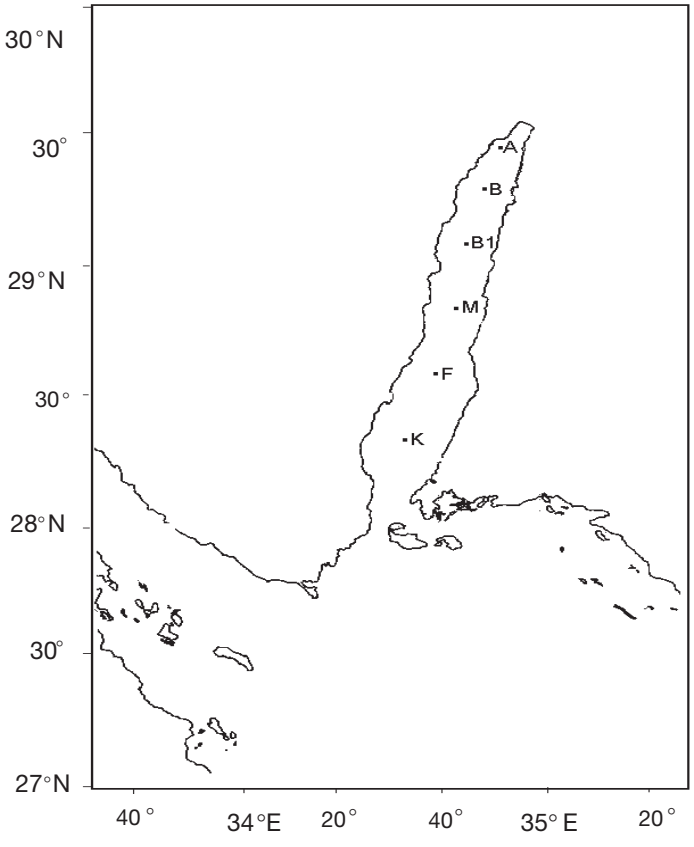

Fig. 1. Gulf of Aqaba and the northern Red Sea, showing Stns A to K in the Gulf

The majority of the studies on nitrite dynamics focus on the deep nitrite maximum in a stratified water column (e.g. Wada & Hattori 1971, Kiefer et al. 1976, Zafiriou et al. 1992, Dore & Karl 1996a,b). The formation of the Deep Nitrite Maximum (DNM) is related to the vertical separation of generation and consumption processes in the water column driven by differential sensitivity to light (Wada & Hattori 1971, Olson 1981a,b, Dore & Karl 1996b). Only a few studies have reported on nitrite accumulation within a mixed water column (e.g. Lipschultz et al. 1996, Collos 1998), although nitrite excretion by phytoplankton is well documented for both cultures and natural populations (Wada & Hattori 1971, Collos 1998).

The present study was conducted in the oligotrophic Gulf of Aqaba at the northern end of the Red Sea. The Gulf, which is located on the fault of the major rift-valley system, is 165 km long and an average of 15 km wide. The maximum depth is 1830 m, the average depth is around 800 m. The Gulf of Aqaba receives nutrient-depleted surface waters from the Indian Ocean through the Gulf of Aden across 2 shallow sills: the Bab al Mandab (ca. 140 m deep), and, 2000 km to the north, the Straits of Tiran (ca. 250 m deep). The Gulf is surrounded by a sparsely inhabited desert and therefore has characteristics that are typical for warm oceanic open waters. It is thus an ideal site for studying nutrient cycling in an oligotrophic ocean. Within the euphotic zone nutrients are depleted almost throughout the year. The vertical distribution of nutrients and phytoplankton in the Gulf of Aqaba is mainly controlled by an annual cycle of stratification in summer and deep mixing in winter. The latter is far deeper in the Gulf of Aqaba than in the Red Sea proper.

The aim of the present study was to identify the mechanisms by which nitrite is accumulated in the Gulf of Aqaba, both in stratified and mixed waters.

MATERIALS AND METHODS

This study is based on data collected during the Red Sea Programme (January 1997 to January 2000) at the routine station (Stn A) in the Gulf of Aqaba, and includes data collected during the cruise of the German RV 'Meteor' to the Gulf and the northern Red Sea in spring 1999 (Fig. 1).

Water samples were collected by a Rosette sampler with twelve 10 l Niskin bottles. Individual water samples were drawn into 14 ml polyethylene test tubes using clean Tygon tubing. For each bottle, the tubing was thoroughly flushed, and each test tube was rinsed 3 times with sample water before filling. Analyses were carried out within 4 h; meanwhile, the samples were kept at 4°C in the dark. Nitrite was measured

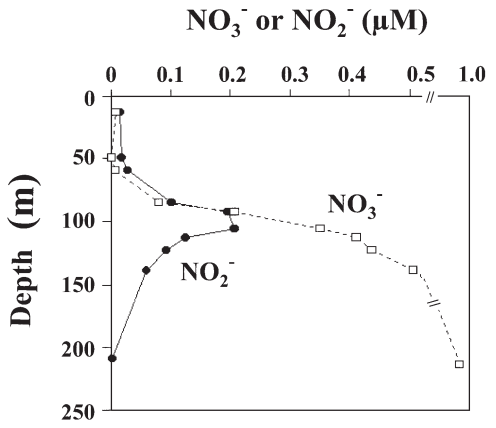

Fig. 2. Examples of typical profiles of nitrite and nitrate during summer stratification in the Gulf of Aqaba at Stn A, 17 July 1998

using a flow injection analyser. After dissociation with sulphanylamide and naphtylethylenediamine, the samples were measured at 550 nm with filtered seawater as a carrier against a zero blank.

Bioassays were performed by adding nutrients to water samples from the sea surface and from the depth of the deep chlorophyll maximum (DCM; ca. 70 to 90 m). Nutrient additions included nitrate and ammonia alone, as well as either nitrate or ammonia together with phosphate. Final concentrations were 6 µM N and 0.4 µM P, respectively. In addition, nutrient-rich deep (600 m) water was added to water samples taken from surface and the DCM. During a long-term experiment conducted in September 1999, water samples from the surface and the DCM layer were incubated *in situ* close to shore at 20 m depth in natural daylight for 8 d. Short-term experiments (24 h) were performed at simulated 20 m light level in basins on board the ship. Temperature was controlled by running surface water. Dark bottles were used as a reference. During the incubation, nitrite concentrations and *in vivo* chlorophyll fluorescence (as a measure of phytoplankton biomass) were monitored in the experimental flasks.

RESULTS AND DISCUSSION

Field data. During summer in the stratified water column, ammonia was present and nitrite formed a deep maximum just below the nitracline. During mixing, ammonia concentrations were unexpectedly low, whereas nitrite was homogeneously distributed throughout the mixed layer.

The low ammonium concentration in the mixed layer suggests either rapid transformation of the excreted ammonium into nitrite that accumulates in the mixed layer or rapid uptake of ammonia by phytoplankton. Our field and experimental data clearly support the second assumption.

Nitrite profiles during summer stratification were characterised by nitrite depletion within the upper euphotic zone and a nitrite maximum (up to 0.15 to 0.2 µM) in the waters below (Fig. 2). The DNM was located between 90 and 110 m depth, which corresponds roughly to the 1% light depth of PAR. The DNM overlapped with the upper part of the nitracline, but was located below the deep chlorophyll maximum. The shape of the nitrite peak altered little over time, and was somewhat asymmetric, tailing off towards deeper water.

The DNM was established shortly after the onset of stratification in April-May. The maximum nitrite concentration decreased during summer, reaching a minimum towards the end of July. By the end of September, the nitrite concentration had begun to rise again, until the peak was eroded by mixing in November.

Diurnal variations in nitrite and nitrate concentration were recorded on 8 July 1997. Nitrite and nitrate concentrations exhibited marked fluctuations in the uppermost 120 m, which can be attributed to both water movements and biological processes. Regardless of the impact of vertical water motions, the nitrite maximum increased towards evening (Fig. 3). In contrast,

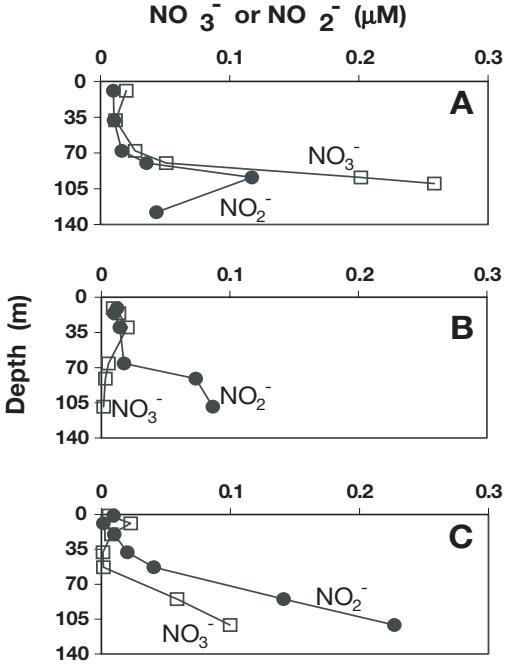

Fig. 3. Vertical nitrite and nitrate profiles observed over 12 h in the Gulf of Aqaba at Stn A, 8 July 1997, during stratification. (A) Cast finished at 07:30 h local time; (B) cast finished at 12:00 h; (C) cast finished at 18:00 h

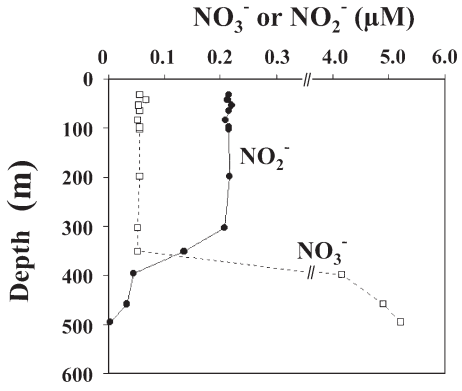

Fig. 4. Examples of typical profiles of nitrite and nitrate during winter mixing in the Gulf of Aqaba at Stn A, 2 February 1998

nitrate concentration decreased in the first half of the daylight period (07:30 to 12:00 h), especially at the bottom of the euphotic zone (Fig. 3). This suggests that nitrate was taken up by phytoplankton cells during that period, and part of it was excreted as nitrite due to nutrient-stimulated growth. Any fluctuation in the nitracline resulting from water motion would only increase nitrate concentration in that region. The increase in nitrate recorded during the second half of the daylight period (12:00 to 18:00 h) is probably related to water motion.

In contrast, during the deep winter mixing, nitrite was homogeneously distributed throughout the mixed layer (Fig. 4). As the mixing deepened, high concentrations of nitrate were entrained into the euphotic zone from deeper water. As a result, phytoplankton growth was stimulated (C. Häse et al. pers. obs.). Concomitantly, the nitrite concentration increased in the mixed layer. This suggests that the accumulation of nitrite in the mixed layer is related to phytoplankton growth, either by release of a small proportion of nitrite generated as an intermediate product of assimilatory nitrate reduction, or by bacterial activity.

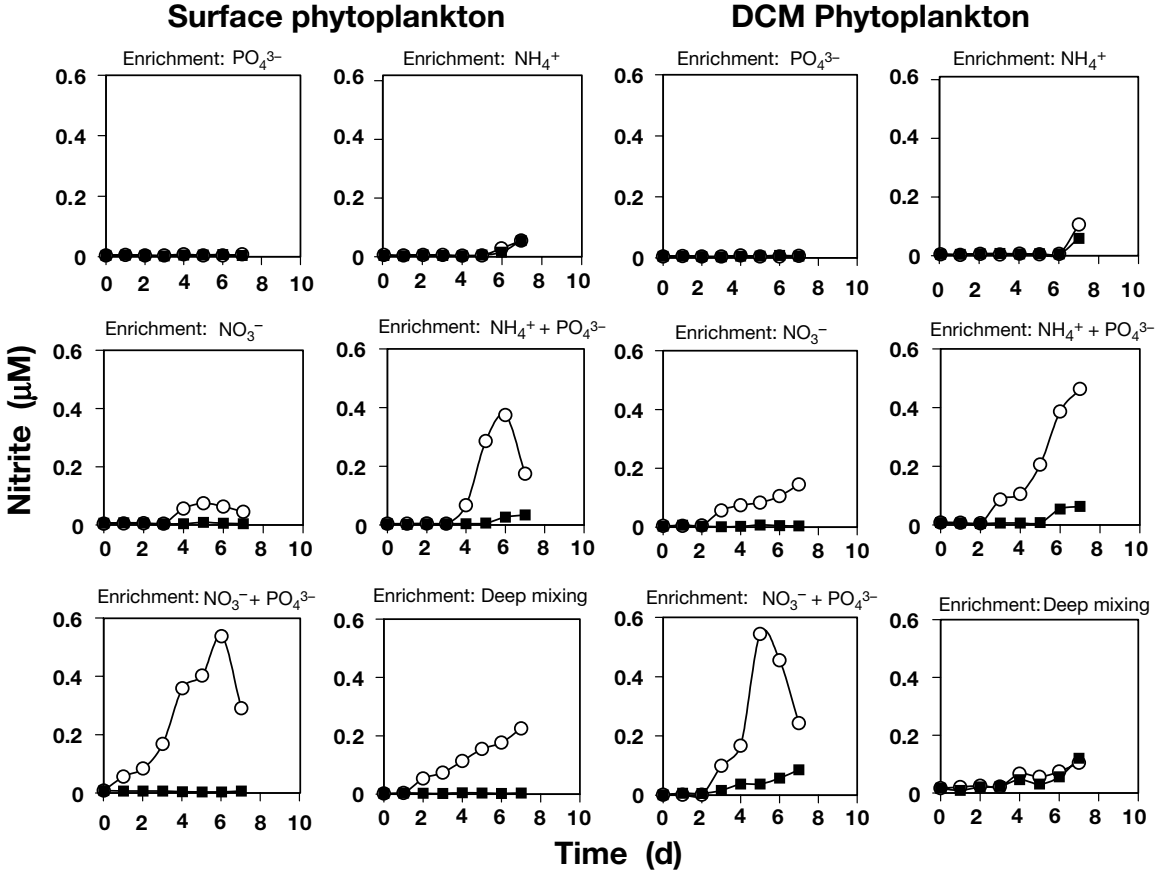

Fig. 5. Time course of nitrite accumulation during 8 d incubation of the nutrient-enrichment bioassays at Stn A. In light-incubated samples (○) only the addition of either nitrate or ammonia together with phosphate, or deep water, had stimulatory effects on nitrite accumulation, whereas neither nitrate nor ammonium alone elicited any response. Dark-incubated samples (■) did not show any response. Experiment began on 7 September 1999. DMC: deep chlorophyll maximum

Bioassay experiments

In the bioassays, nitrite accumulation was observed only when the samples were enriched with both N and P in samples incubated in the light (Fig. 5) (M. Al-Qutob et al. pers. obs.). In contrast, little or no increase was observed in the nitrite concentration after additions of nitrate, ammonium or phosphate alone. Nitrite concentration changes exhibited patterns similar to the development of the phytoplankton biomass (Fig. 6).

Because nitrite release was only observed after additions of both N and P, we conclude that phytoplankton growth plays the key role in nitrite accumulation within the mixed water column. Our experiments clearly indicate that nitrite is accumulated as a result of phytoplankon growth, which needs light and both a nitrogen and a phosphate source.

Our bioassays strongly suggest that the accumulation of nitrite during mixing was coupled to the development of phytoplankton biomass. At the present stage, the underlying mechanism cannot be finally resolved. Indirect coupling could include either excretion of DOM by phytoplankton or grazing and/or decomposition of organic matter, all of which support bacterial growth. However, the bioassays give strong evidence of direct coupling: (1) No consumption of the added ammonium could be observed within the first few days of the long-term experiment; (2) phytoplankton growth and nitrite accumulation occurred simultaneously; (3) nitrite concentrations decreased in parallel with phytoplankton biomass towards the end of the incubation.

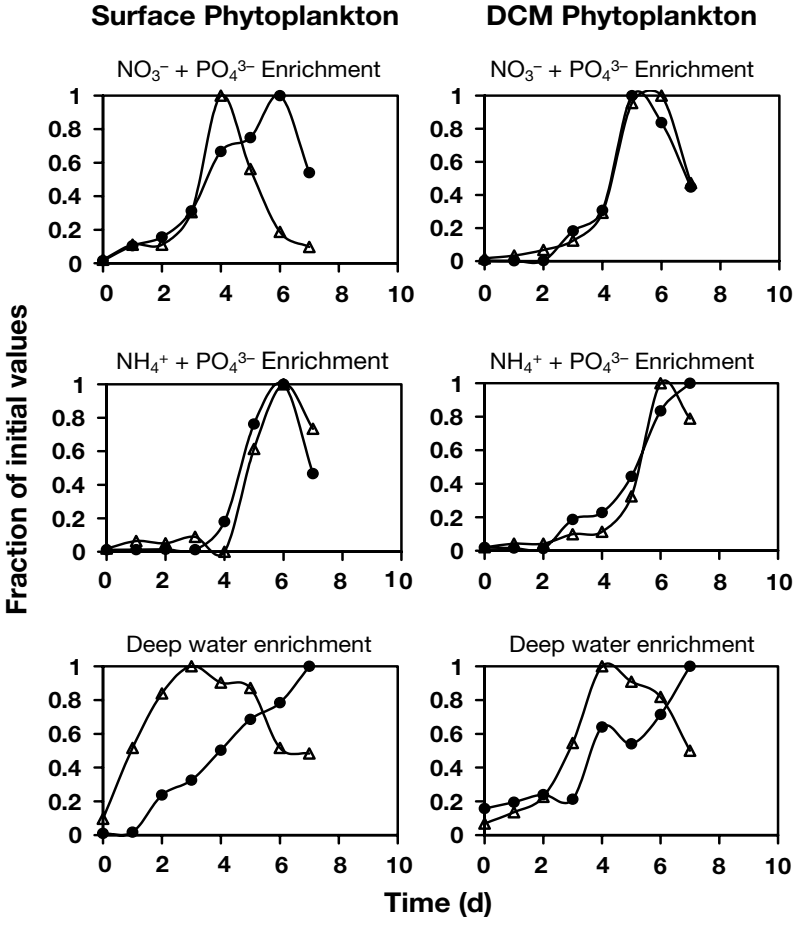

Fig. 6. Time course of nitrite concentrations (●) and *in vivo* fluorescence (▵) during 8 d incubation of the nutrient enrichment bioassays. Only results from assays with dual additions of N plus P are shown, since single additions did not elicit any response

In the bioassays the final concentrations of the added nutrient salts were 6 µM N and 0.4 µM P. In addition, nutrient-rich deep (600 m) water was added to surface and DCM-water, leading to a final concentration of ~1 µM N. After total consumption of the nitrate and phosphate, the former samples contained up to 0.6 µM of nitrite in the incubation bottle, and the latter up to 0.2 µM, implying that 80 to 90% of the nitrate taken up by the phytoplankton was incorporated into biomass, and 10 to 20% was excreted as nitrite. In a year with a typical maximum winter mixing depth of 400 m, a total of about 800 mmol nitrate is entrained into the mixed layer. This corresponds to an average nitrate concentration within the 400 m mixed layer of about 2 µM. The maximum concentration of nitrite in the mixed column reached 0.2 to 0.3 µM towards the end of the mixing season. This confirms that between 10 and 15% of the total amount of nitrate introduced into the mixing column was released as nitrite by the phytoplankton cells *in situ*, the same proportion as in the bioassays. We would emphasise that this amount of nitrite accumulated is the net result of nitrate entrained or enriched on the one side and nitrite accumulated and consumed by bacteria (or even certain phytoplankton species) on the other. After the mixing has stopped, nitrite is completely assimilated from the water column, since new nitrate is no longer entrained.

Nitrification was recently reported to play an important role in nitrogen recycling within the euphotic zone of oligotrophic oceans (Ward et al. 1989, Dore & Karl 1996b). In particular, high ammonia oxidation rates were measured below the DNM peak, whereas above the DNM peak, nitrite release by phytoplankton was a

significant source of nitrite (Wada & Hattori 1971, Dore & Karl 1996b). However, in our bioassays, nitrite accumulation due to nitrification was low, as evident from the dark samples enriched solely with ammonia (Fig. 5). Likewise, nitrite accumulation was quicker in samples with nitrate + phosphate than with ammonia + phosphate additions, indicating that nitrite production from ammonia via nitrification plays only a minor role during mixing. This, and the diurnal dynamics of nitrite and nitrate concentrations (Fig. 3), give strong evidence that during stratification in summer nitrite excretion by phytoplankton does contribute a significant share to the formation of the DNM in the Gulf of Aqaba.

Nitrite release by phytoplankton during nitrate assimilation has been reported by several authors (Vaccaro & Ryther 1960, Wada & Hattori 1971, Collos 1998). However, to our knowledge, this is the first time that nitrite release by phytoplankton is reported for phytoplankton growth stimulated by addition of ammonia. Unlike nitrate, ammonia does not have to be reduced to be incorporated into biomass. Therefore, we conclude that the nitrite released in the bioassays, especially in those with ammonia plus phosphate additions, was not directly related to nutrient assimilation of the algal cells. Thus, a different and so far unrecognised physiological pathway must be responsible.

CONCLUSIONS

The nutrient-enrichment bioassays were performed at the end of the stratification period. At this time, nitrite *in situ* was only present in the deep nitrite maximum below the deep chlorophyll maximum. The results of the bioassays are summarized as follows: (1) Nitrite accumulated in remarkable concentrations only in light samples, not in dark samples; (2) only the addition of both nitrogen and phosphate had stimulatory effects on nitrite accumulation, whereas neither nitrate nor ammonium alone elicited any responses; (3) nitrite accumulation closely paralleled the development of phytoplankton biomass with no time lag, and especially did not occur in those bioassays that showed no change in phytoplankton biomass; (4) surface and DCM samples responded similarly; (5) accumulation was faster in samples with nitrate + phosphate than with ammonia + phosphate additions, indicating that nitrite production from ammonia via nitrification plays only a minor role during mixing.

These results, together with the field data, clearly support the hypothesis that nitrite accumulation during mixing is driven by nutrient-replete phytoplankton growth.

Both field and experimental data have shown that about 10 to 20% of the N introduced into the mixed layer by deep winter mixing is released as nitrite. This process is dependent on phytoplankton photosynthesis, as no nitrite accumulated in the bioassays performed in the dark.

Field and experimental data support the hypothesis that nitrite excretion by phytoplankton has a significant role in the formation of the DNM during stratification in summer.

Finally, our results indicate that there is a so far unrecognised physiological pathway involved in nitrite excretion by phytoplankton cells.

Acknowledgements. We are grateful to the coordinator of the Red Sea Program, G. Hempel. We are also grateful for helpful comments on this manuscript from Z. Dubinsky, J. Erez, N. Stambler and 3 anonymous reviewers. We thank M. Dray and R. Shem-Tov for their support with sampling and logistics. We also would like to thank the captains and the crew of the research vessels 'Meteor', 'Suellyn' and 'Sea Surveyor' and all the members of the Red Sea Program project. This work was supported by the German Ministry for Education and Research (BMBF) within the Red Sea Program. This work was part of the PhD thesis of M.A-Q. at Bar Ilan University, Israel.

LITERATURE CITED

Brandhorst W (1959) Nitrification and denitrification in the eastern tropic North Pacific. J Cons Perm Int Explor Mer 25:2–20

Collos Y (1998) Nitrate uptake, nitrite release and uptake, and new production estimates. Mar Ecol Prog Ser 171: 293–301

Dore JE, Karl DM (1996a) Nitrite distributions and dynamics at station ALOHA. Deep-Sea Res 43:385–402

Dore JE, Karl DM (1996b) Nitrification in the euphotic zone as a source for nitrite, nitrate and nitrous oxide at station ALOHA. Limnol Oceanogr 41:1619–1628

Enoksson V, Fogelqvist E, Fonselius S (1996) Nitrogen speciation and nitrification potential in the Skagerrak area during the SKAGEX IV experiment. Deep-Sea Res 43: 1029–1044

Guerrero MA, Jones RD (1996) Photoinhibition of marine nitrifying bacteria. I. Wavelength-dependent response. Mar Ecol Prog Ser 141:183–192

Herbland A, Voituriez B (1979) Hydrological structure analysis for estimating the primary production in tropical Atlantic Ocean. J Mar Res 37:87–101

Horrigan SG, Carlucci AF, Williams PM (1981) Light inhibition of nitrification in sea surface films. J Mar Res 39: 557–565

Kiefer DA, Olson RJ, Holm-Hansen O (1976) Another look at the nitrite and chlorophyll maxima in the central North Pacific. Deep-Sea Res 23:1199–1208

Lipschultz F, Zafiriou OC, Ball LA (1996) Seasonal fluctuations of nitrite concentration in the deep oligotrophic ocean. Deep-Sea Res Part II 43:403–419

Miyazzaki TE, Wada EA, Hattori (1973) Capacities of shallow waters of Sagami Bay for oxidation and reduction of inorganic nitrogen. Deep-Sea Res 20:571–577

Miyazzaki TE, Wada E, Hattori A (1975) Nitrite production from ammonia and nitrate in the euphotic layer of the western North Pacific. Mar Sci Commun 1:381–394

Olson RJ (1981a) ^{15}N tracer studies of the primary nitrite maximum. J Mar Res 39:203–226

Olson RJ (1981b) Differential photoinhibition of marine nitrifying bacteria: a possible mechanism for the formation of the primary nitrite maximum. J Mar Res 39: 227–238

Rakestraw NW (1936) The occurrence and significance of nitrite in the sea. Biol Bull 71:131–167

Vaccaro RF, Ryther JH (1960) Marine phytoplankton and the distribution of nitrite in the sea. J Cons Int Explor Mer 25: 260–271

Wada E, Hattori A (1971) Nitrite metabolism in the euphotic layer of the central North Pacific Ocean. Limnol Oceanogr 16:766–772

Ward BB (1986) Nitrification in marine environments. In: Prosser JI (ed) Nitrification. IRL Press, Oxford, p 157–184

Ward BB, Kilpatrick KA, Renger EH, Eppley RW (1989) Biological nitrogen cycling in the nitracline. Limnol Oceanogr 34:493–513

Zafiriou OC, Ball LA, Hanley Q (1992) Trace nitrite in oxic waters. Deep-Sea Res 39:1329–1347

Editorial responsibility: Gotthilf Hempel, Bremen, Germany

Submitted: May 3, 2001; Accepted: January 31, 2002
Proofs received from author(s): August 7, 2002

Vol. 239: 241–250, 2002 | MARINE ECOLOGY PROGRESS SERIES
Mar Ecol Prog Ser | Published August 23

Spatial and temporal distribution of *Trichodesmium* spp. in the stratified Gulf of Aqaba, Red Sea

A. F. Post[1,*], Z. Dedej[1], R. Gottlieb[1], H. Li[1], D. N. Thomas[1,2,], M. El-Absawi[3], A. El-Naggar[3], M. El-Gharabawi[3], U. Sommer[4]**

[1]Interuniversity Institute for Marine Science, PO Box 469, 88103 Eilat, Israel
[2]Centre for Marine Tropical Ecology—ZMT, Fahrenheitstraße 6, 28359 Bremen, Germany
[3]National Institute for Oceanography and Fisheries, Kayet Bay, Alexandria, Egypt
[4]Institut für Meereskunde, Düsternbrooker Weg 20, 24105 Kiel, Germany

ABSTRACT: Phytoplankton (>100 µm) abundance was studied in the open waters of the Gulf of Aqaba during the summer stratification period of 1996. A succession took place among the major phytoplankton groups, with diatom numbers decreasing throughout the summer. The diazotrophic cyanobacteria *Trichodesmium* spp. became more prominent as the stratification period progressed; 5 *Trichodesmium* species were identified: *T. thiebautii*, *T. erythraeum* with tuft-shaped colonies and *Trichodesmium* sp. with puff-shaped colonies were common at ~10^2 colonies m^{-3} throughout the stratification period, whereas *T. tenue* and *T. hildebrandtii* were more rare. A bloom of *T. thiebautii* and *T. erythraeum* with >10^6 tuft colonies m^{-3} was observed in coastal waters of the Gulf during fall 1997. Tuft-shaped colonies were dominant near the surface, while puff-shaped colonies of *Trichodesmium* sp. were mainly found in the bottom half of the photic zone. These depth distributions were maintained for more than 2 mo, suggesting that the 2 colony types occupied distinct niches. Puff-shaped colonies were found to have higher chlorophyll *a* contents than tufts, but their photosynthetic activities were not significantly different. Fatty acid analysis of dominant plankton species yielded new trophic relationships for *Trichodesmium* spp. The *Trichodesmium* spp.-specific fatty acid C22:2ω6 was found in *Macrosetella gracilis* (the sole copepod to graze on *Trichodesmium* spp.) and in chaetognaths, suggesting that these carnivorous zooplankton fed on *M. gracilis*. Furthermore, this fatty acid was observed in the filter-feeding *Salpa maxima*, which was abundantly present in the Gulf of Aqaba during June 1997.

KEY WORDS: Red Sea · Phytoplankton · Cyanobacteria · *Trichodesmium* · Nitrogen fixation

INTRODUCTION

The Gulf of Aqaba is an extension of the northern Red Sea, located between the Sinai (Et Tih) Desert and the Western Arabian (An Nefud) Desert. It is a deep basin (1800 m) approximately 165 km in length and an average of 15 km wide. It is separated from the northern Red Sea by a shallow sill (240 m) at the Straits of Tiran. High evaporation rates drive a thermohaline circulation with a continuous advection of nutrient-poor surface waters from the Red Sea into the Gulf, counterbalanced by an efflux of more dense deep waters (Klinker et al. 1976, Murray et al. 1984, Wolf-Vecht et al. 1992). Surface waters are characterized by a shallow but stable thermocline in summer. Lower air temperatures in fall cause a rapid erosion of the thermo-

*E-mail: anton.post@huji.ac.il
**Present address: School of Ocean Sciences, University of Wales Bangor, Menai Bridge LL59 5EY, Wales, UK

cline, leading to deep convective mixing during the winter months. Convective mixing may reach down to depths of 600 m or more in the northern part of the Gulf (Klinker et al. 1976, Wolf-Vecht et al. 1992, Genin et al. 1995, Lindell & Post 1995).

Phytoplankton chlorophyll *a* in the Gulf of Aqaba is low in summer, with surface concentrations fluctuating between 0.02 and 0.04 µg l^{-1} (Klinker et al. 1978, Genin et al. 1995, Yahel et al. 1998), considered characteristic for oligotrophic conditions. Chlorophyll *a* reaches its maximum concentration (1.2 µg l^{-1} on average) at the end of the winter mixing period (Genin et al. 1995). Phytoplankton is made up mostly of ultraphytoplankton, species with a cell diameter of less than 8 µm, which contribute >90% to chlorophyll *a* standing stock (Lindell & Post 1995, Yahel et al. 1998). The deep mixing in winter drives a seasonal succession among the ultraphytoplankton (Lindell & Post 1995). Eukaryotic algae dominate during the mixing event, whereas the cyanobacteria *Synechococcus* spp. and *Prochlorococcus* spp. are dominant during spring and late summer respectively (Lindell & Post 1995). Likewise, one would expect the composition of larger phytoplankton to be affected by water body structure and nutrient availability. Studies of larger phytoplankton in the Gulf of Aqaba have been limited in scope with a focus on symbiotic associations of nitrogen-fixing cyanobacteria with diatoms and dinoflagellates (Kimor et al. 1992, Gordon et al. 1994). Temporal and spatial distribution of microplankton in the Gulf of Aqaba was studied in 1974-1975 and the presence of nitrogen-fixing, bloom-forming *Trichodesmium* spp. colonies in early and late summer was documented (Kimor & Golandsky 1977, Gordon et al. 1994). *Trichodesmium* spp. has been the subject of intense study over the last 2 decades, since it is considered a major contributor to primary production and a significant source of new nitrogen in the ocean surface layers (Capone et al. 1997, Carpenter & Romans 1991). Summer populations and especially blooms of *Trichodesmium* spp. may contribute significantly to the carbon and nitrogen budget of the Gulf of Aqaba during summer stratification. The purpose of this study was to establish temporal and spatial distribution patterns of *Trichodesmium* spp. among the >100 µm phytoplankton size fraction. We further report on chlorophyll contents, photosynthetic activities, nitrogen fixation and trophic relationships of *Trichodesmium* spp. populations in the Gulf of Aqaba.

MATERIALS AND METHODS

During the 1996 summer stratification period we collected samples on board the RV 'University I' at monthly intervals at Sampling Station A (29°28′N, 34°55′E) at the northern tip of the Gulf of Aqaba. During a research cruise from 2 to 10 June on board the same vessel, we visited additional sampling sites with a more central location in the Gulf of Aqaba: Stns B (29°06′N, 34°46′E) and M (28°47′N, 34°43′E), along with Stn R (27°25′N, 34°25′E) in the northern Red Sea (see map in Li et al. 1998). Samples were collected with 100 µm mesh plankton nets. The nets were fitted with a Tsurumi-Seiki flow meter (model #5197) in order to obtain estimates of the total volume of water passed through the net. Vertical hauls were made at a rate of 0.8 m s^{-1}, and a mechanical closing mechanism allowed sampling of desired depth ranges: 0–5, 5–10, 10–30, 30–50, 50–75 and 75–100 m. Horizontal tows were made at a speed of approximately 0.5 m s^{-1} for 7 min duration. Samples were resuspended in 300 to 500 ml filtered seawater. Diel change in the vertical distribution of *Trichodesmium* spp. was studied on samples taken at 00:00, 07:00, 13:00 and 19:00 h local summer time; 50 ml samples were taken for immediate analysis of *Trichodesmium* spp. populations, and colonies were enumerated using a Nikon SMZ-2B dissecting microscope. Colony size was estimated in replicates of 20 colonies suspended in 50 ml GF/F-filtered seawater. Colonies were gently vortexed for 10 to 30 min, until all colonies had disassembled into individual trichomes without disrupting them. Trichomes were counted in a 1 ml Sedgwick-Rafter cell using a Nikon Labophot 2 microscope equipped with an epifluorescence attachment and a B2 filter set (excitation range 450 to 490 nm, a 510 nm dichroic mirror and a 520 nm barrier filter). A 250 to 450 ml sample from each tow was preserved in 2.5% glutaraldehyde and stored in darkness at room temperature. Diatom and dinoflagellate species in these samples were identified and enumerated using both a bright-field inverted microscope (Nikon TMS-F) and a phase-contrast microscope (Nikon Labophot 2).

Analyses. Chlorophyll *a* was determined on samples of 10 to 20 colonies of *Trichodesmium* spp. collected on Whatman GF/F filters and extracted in 90% acetone for 12 to 24 h in the dark at 4°C. Chlorophyll *a* concentrations were determined on a Turner Design model 10-000A fluorometer following the procedure of Venrick et al. (1987). On the June 1996 cruises, samples were also taken to measure the carbon and nitrogen content of *Trichodesmium* colonies and that of the particulate fraction in the water column. For the individual colony contents, between 50 and 70 colonies were collected on precombusted Whatmann GF/F filters which were rinsed in 0.2 µm-filtered seawater. Water-column particulate organic carbon/nitrogen (POC/PON) samples were collected by filtering onto precombusted GF/F filters between 0.5 and 1.5 l samples collected by Niskin bottles or from surface bucket hauls. All POC/

PON filters were acid-fumed (concentrated HCl) overnight to remove carbonate, dried at 40°C, and then stored in a desiccator prior to analysis. POC and PON concentrations were determined with a Europa Scientific CHN analyser, using acetanilide as a standard. Photosynthetic carbon fixation was measured on 10 to 20 *Trichodesmium* spp. colonies collected in glass vials with 20 ml GF/F-filtered seawater while basically following established procedures (Carpenter et al. 1993, Roenneberg & Carpenter 1993, Villareal 1995). Samples were spiked with 10 µCi of $NaH^{14}CO_3$ (Amersham) and immediately transferred to a 24°C incubator for 4 h. Light was provided by 'warm-white' fluorescent tubes at 300 µmol quanta m^{-2} s^{-1}. Light was measured with a Li-COR LI 185 light meter with a LI-195SA quantum sensor. Temperature was maintained at approximately 24°C with running seawater. Dark control bottles were run alongside the samples in each incubation. Samples were filtered on 25 mm GF/F filters, then washed with 10 ml filtered seawater. Thefilters were fumed overnight with HCl in desiccators. The filters were supplied with 5 ml scintillation cocktail (Insta-GelII Plus, Packard) and ^{14}C incorporation was determined during 10 min readings per vial using a Tri-Carb 1600 TR (Packard) scintillation counter. The nitrogen fixation potential of *Trichodesmium* spp. was measured by the acetylene reduction method (Capone et al. 1990). Twenty colonies were placed in darkened 22 ml tubes containing 18 ml of GF/F-filtered seawater. Tubes were crimp-sealed with a teflon/silicon septum (National Scientific), 2 ml of acetylene-saturated seawater was injected through the septum, and the tubes were transferred to the light. Incubation conditions were identical to those of photosynthesis measurements, and the incident light allowed both photosynthesis and nitrogen fixation to occur at their maximal rates. Controls were tubes with GF/F-filtered seawater spiked with acetylene, and dark-incubated samples. Incubations were terminated by injecting either 10^{-6} M DCMU (Sigma) or transfer to darkness. Headspace samples (100 µl) were drawn with a 250 µl gas-tight syringe (Precision Sampling Corporation Pressure-Lock) and analysed on a gas chromatograph (Hewlett 5890, Packard Series II) with a 30 m semi-capillary column of 0.53 mm internal diameter. The contribution of *Trichodesmium* spp. to the marine food web of the Gulf of Aqaba was studied from comparative lipid analyses of both phytoplankton and zooplankton species. Zooplankton samples were taken by vertical tows of a 100 µm mesh plankton net from 150 m depth to the surface. Salps were sampled from surface waters with a bucket. Samples for lipid analysis were taken by picking individual animals from the net sample, placing them on precombusted 45 mm Whatman GF/F-filters, and quickly freezing them in liquid nitrogen. The sample size for calanoid copepods and for the harpacticoid *Macrosetella gracilis* amounted to 15 adult individuals, chaetognaths and doliolids to 8 individuals each, and salps to 5 individuals. The zooplankton samples were lyophylized prior to analysis. Samples for the lipid analysis of cyanobacteria were obtained from exponentially growing pure cultures of *Synechococcus* sp. Strain C129 and *Trichodesmium* sp. Strain RS9602 (Gulf of Aqaba isolates) along with the Sargasso Sea isolates *Synechococcus* sp. Strain WH7803 and *Trichodesmium* sp. Strain IMS101. Fatty acids were extracted and processed according to standard methods (Christie 1982, Kattner & Fricke 1986, Müller-Navarra 1995, Müller-Navarra & Lampert 1996). Known concentrations of synthetic fatty acids of odd chain length (11:0, 13:0, 15:0, 17:0, 19:0, 21:0) were added to the samples to serve as internal standards. Samples were analysed by thin-layer chromatography flame-ionisation detection on a Iatroscan MARK II gas chromatograph with a 30 m DB-FFAP column. Fatty acid composition was expressed as the percent contribution of each individual fatty acid to the total natural (even chain length) fatty acid mass of each sample.

RESULTS

Population dynamics

The phytoplankton (>100 µm) community in the Gulf of Aqaba during summer 1996 was made up by representatives of diatoms, dinoflagellates and cyanobacteria. Both pennate and centric diatoms were observed, the latter group being the most abundant. The diatoms consisted mostly of *Chaetoceros* and *Leptocylindrus* species found throughout the photic layer down to 100 m depth. *Proboscia alata* dominated the phytoplankton community in the upper 10 m, with densities of 30 000 cells m^{-3} recorded at Stn R. Less abundant species included those of the genera *Rhizosolenia* and *Hemiaulus.* Dinoflagellates belonged mostly to the orders Gonyaulacales (genera *Ceratium* and *Protoperidinium*) and Dinophysiales (genera *Dinophysis* and *Ornithocercus*). The genus *Ceratium* was best represented with at least 7 species, of which *C. fusus* and *C. trichoceros* were the most abundant. Cyanobacteria were represented by various species of the genus *Trichodesmium*.

Identification of *Trichodesmium* species is less straightforward than that of diatoms and dinoflagellates because of the lack of distinct and unique morphological characteristics. We distinguished 3 colony types (Table 1): (1) spherically shaped colonies, (2) bow-tie-shaped colonies of trichomes that were densely arranged (puffs), and (3) colonies with trichomes arranged in

Table 1. *Trichodesmium* spp. Morphological characteristics of colonies and trichomes from the Gulf of Aqaba. For the spherical colonies, dimensions are for the central section (core of densely packed trichomes) and the diameter of the colony as a whole; for bow-tie colonies, dimensions are for the central section (center point where trichomes are in tight association) and the exterior section (polar ends of the colony where the trichomes are separated). nd: not determined; l: length; w: width

	Colonies			Trichomes			
Colony shape	Color	Dimensions (µm)		No. per colony	Dimensions (µm)	Cells per trichome	Cell shape (µm)
Spherical (puffs), *Trichodesmium* sp.	Dark-brown to reddish-brown	Central section Colony diam.	150–300 1000–2500	30–150	800–2000 (l) 5–7 (w)	110–270	7.5–15 (l) 5–7 (w)
Bow-tie (*T. tenue*)	Yellow-brown	Central section Exterior section Colony length	20–40 200–250 >1000–2500	nd	1000–2000 (l) 5–6.5 (w)	80–310	8–12 (l) 5–6.5 (w)
Parallel-straight (*T. erythraeum*)	Dark-brown to reddish	Colony diam. Colony length	50–150 1000–2000	35–190	300–800 (l) 6.5–8 (w)	40–130	6–7.5 (l) 6.5–8 (w)
Parallel-twisted (*T. thiebautii*)	Yellow-brown	Colony diam. Colony length	50–300 1800–2500	35–190	1000–2200 (l) 6–7 (w)	55–180	12–17.5 (l) 6–7 (w)

parallel bundles or rafts (tufts). The former 2 colony types were each made up of unitypical trichomes and cells. The bow-tie-shaped colonies were identified as *T. tenue* and the puff-shaped colonies as *Trichodesmium* sp. sensu Janson et al. (1995). Among the tuft-shaped colonies we observed 2 different trichome types with cells that differed in shape and dimensions (Table 1). These types were identified as *T. thiebautii* and *T. erythraeum*. *T. erythraeum* colonies were made up of 35 to 190 trichome bundles arranged parallelly; the colonies were smaller in cross-section, than those of *T. thiebautii*, and contained shorter trichomes with cells that were approximately as long as wide (Table 1). *T. thiebautii* colonies were larger in diameter, with winding trichomes up to 2 mm in length and cells that were significantly longer than wide. On one occasion we found a different trichome type of distinctly larger diameter. This type was tentatively identified as *T. hildebrandtii*.

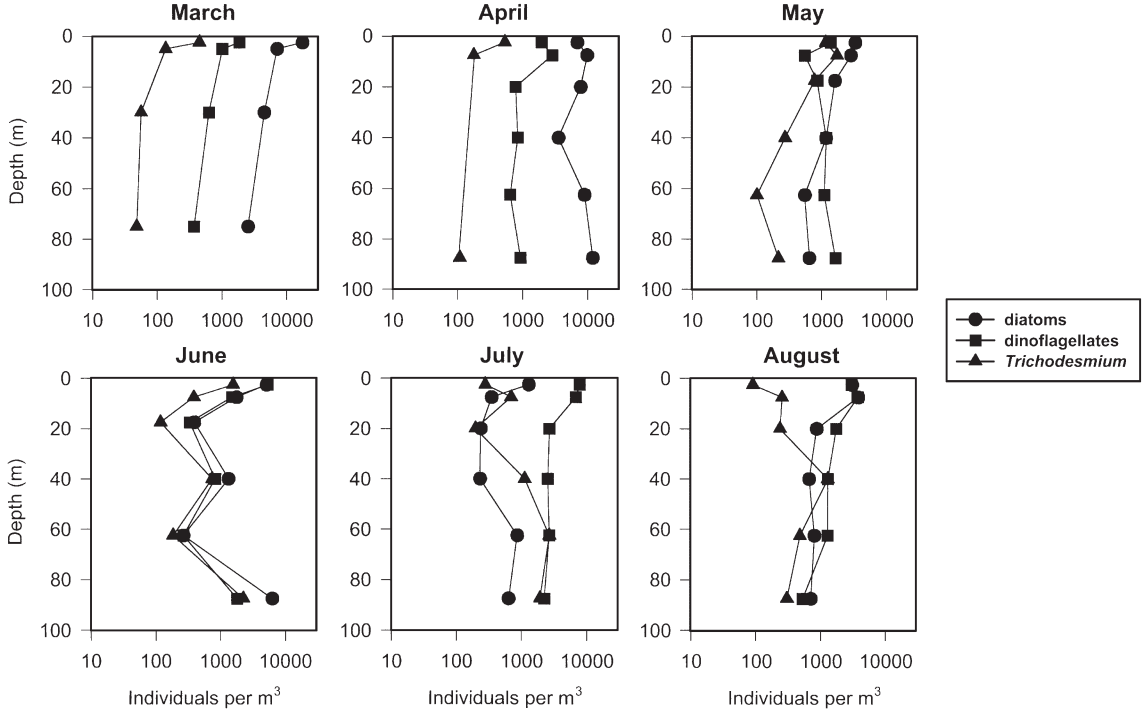

Fig. 1. Depth distributions of diatoms, dinoflagellates and the filamentous cyanobacterium *Trichodesmium* spp. in the open waters of the Gulf of Aqaba during the summer stratification period of 1996

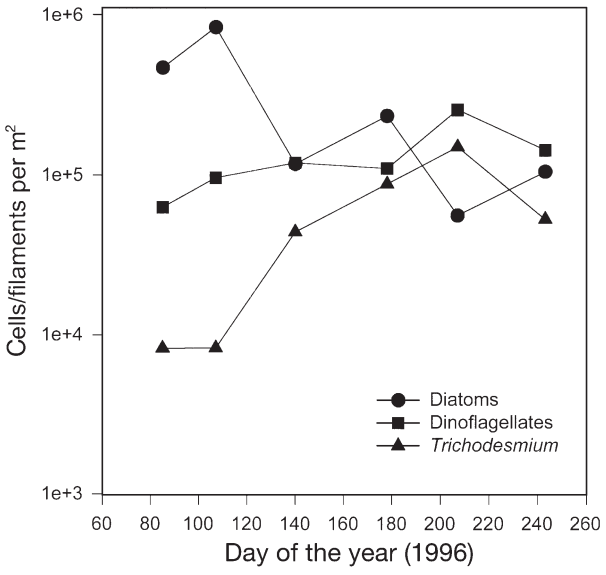

Fig. 2. Changes in total integrated number of diatoms, dinoflagellates cells and filaments of the cyanobacteria *Trichodesmium* spp. in the open waters of the Gulf of Aqaba during summer 1996

Throughout the upper 100 m of the water column, dinoflagellates and diatoms were found at all depths, with their highest numbers near the surface (Fig. 1). *Trichodesmium* spp. trichome numbers were most abundant in the upper 10 m in May and June. During July and August they were found mostly in the 50 to 100 m layer. Depth profiles further indicate a decreasing contribution of diatoms to the phytoplankton community as the summer progressed (Fig. 1). Total integrated numbers show that a succession among the major phytoplankton groups took place during summer stratification (Fig. 2). Diatoms, the most abundant group in the early stage of stratification, decreased in abundance by an order of magnitude. Specifically, *Proboscia alata* declined in May-June, whereas *Rhizosolenia* and *Hemiaulus* sp. appeared during this period. Dinoflagellates maintained their population size throughout the stratification period. *Trichodesmium* spp. populations clearly developed during this period of nutrient-deplete conditions and their trichome numbers increased by an order of magnitude to >100 000 filaments m^{-2} (Fig. 2). The development of *Trichodesmium* spp. was expressed as an increase in colony number. Of the 3 colony types (spherical puffs, bow-tie and parallel tufts) only the latter 2 were quantitatively important. *T. tenue*, with its bow-tie-shaped colonies, was the first to appear in late March, when deep mixing ceased, and was found in low numbers only. This species was rapidly replaced by larger populations of tuft- and puff-shaped colonies of *Trichodesmium* spp. Tuft colonies in the Gulf of Aqaba contained 45 ± 7 trichomes and were significantly smaller those from Stn R in the northern Red Sea, which were made up of 186 ± 6 trichomes. Puff colonies were not observed in samples from Stn R in the northern Red Sea.

Tuft and puff colonies at Stns B and M in the northern part of the Gulf maintained depth distributions, with little overlap between the 2 types (Fig. 3). The vast majority (>95%) of the tuft colonies were localized in the upper 50 m at both locations (Fig. 3) mostly in the upper 10 m; in contrast, 62 to 81% of the puff colonies (41 ± 5 trichomes) were confined to the lower half of the photic zone between 50 and 100 m (Fig. 3). These depth distributions were maintained over the diel cycle, suggesting that both populations were neutrally buoyant.

The depth distribution of the tuft and puff populations described above was maintained throughout the summer at Stn A (Fig. 4). The tuft population appeared in early April. It reached maximum densities/concentrations at the end of May, after which it rapidly declined. The deep puff populations of *Trichodesmium* sp. appeared towards the end of May, later than the tuft colony, but its population maintained itself throughout June and July until its decline at the end of the stratification period (Fig. 4). Since the more

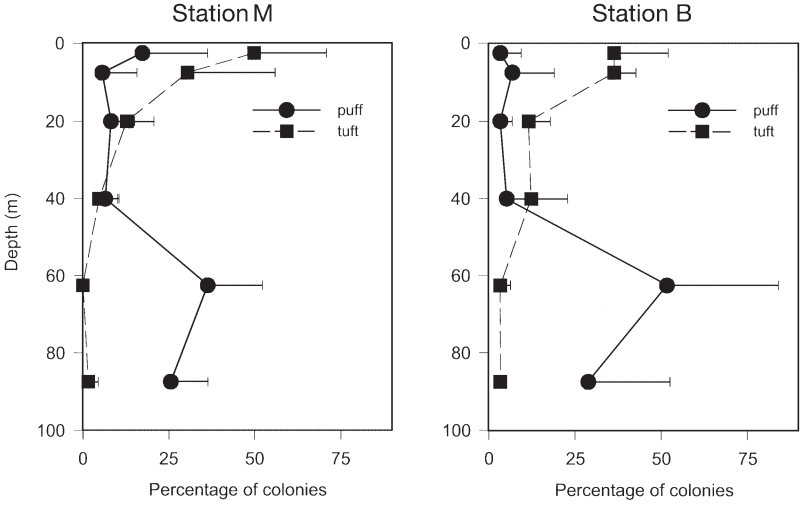

Fig. 3. *Trichodesmium* spp. Depth distributions puff- and tuft-shaped colonies at 2 sampling sites in the northern Gulf of Aqaba (June 1996). Typical colony densities were 15 to 24 colonies m^{-3} for each vertical haul

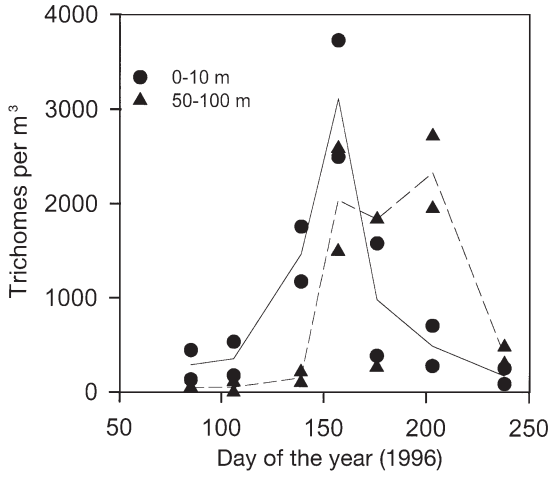

Fig. 4. *Trichodesmium* spp. Succession of shallow (0 to 10 m) and deep (50 to 100 m) populations at Sampling Stn A in the northern Gulf of Aqaba (summer 1996). Shallow populations consisted mainly of tuft-shaped colonies and free filaments of *T. thiebautii/erythraeum* and the deep population of puff-shaped colonies and free filaments of *Trichodesmium* sp. (see also Fig. 3). Lines connect mean values of duplicate samples for each depth range

buoyant tuft colonies accumulate in the surface layer, they were subject to wind action. This caused *Trichodesmium* spp. to accumulate in adjacent coastal waters, and their total population in the Gulf of Aqaba would be underestimated if sampling were to take place in the open waters only. Coastal waters near the Marine Biology Station in Eilat were monitored for *Trichodesmium* spp. populations during the 1996 and 1997 summers (Fig. 5). Modest maxima in late spring and early fall were recorded for 1996, with colony numbers not exceeding 10^2 m^{-3}. A spring maximum was not observed in 1997. However, a *Trichodesmium* spp. bloom with occasional densities of $>10^6$ tuft colonies m^{-3} occurred in early fall of 1997 (Fig. 5). Bloom conditions lasted about 2 wk, after which colony numbers declined, becoming insignificant towards winter.

Table 2. *Trichodesmium* spp. Average (±SD) chlorophyll content (ng colony^{-1}), photosynthetic carbon fixation (nmol C colony^{-1} h^{-1}) and ethylene reduction (nmol colony^{-1} h^{-1}) for puff- and tuft-shaped colonies from the Gulf of Aqaba during the 1996 and 1997 stratification periods. Number of observations in parentheses; nd: not determined

Parameter	1996		1997	
	Puff	Tuft	Puff	Tuft
Chlorophyll *a*	7 ± 1 (5)	3 ± 2 (20)	14 ± 4 (6	4 ± 3 (35)
Photosynthesis	0.3 ± 0.3 (18)	0.4 ± 0.2 (22)	0.8 ± 0.02 (4)	0.5 ± 0.1 (24)
Acetylene reduction	nd	nd	0.004 (1)	0.01 ± 0.01 (5)
C/N ratio	4.3 ± 0.3 (5)	4.1 ± 0.4 (9)	nd	nd

Physiological properties

Surface populations of the tuft and puff colony types differed in chlorophyll content as well as rates of carbon and nitrogen fixation at ambient light (Table 2). Puff colonies had higher chlorophyll contents and higher carbon fixation rates than tuft colonies in both 1996 and 1997. Tuft colonies attained rates of acetylene reduction ranging between 2 and 5% of carbon-fixation rates (Table 2). Cultures of *Trichodesmium* sp. Strain RS9602, which was isolated from the Gulf of Aqaba, had rates of carbon fixation and acetylene reduction of 0.56 nmol C ng^{-1} chlorophyll *a* h^{-1} and 0.017 nmol ethylene ng^{-1} chlorophyll *a* h^{-1} respectively. These rates were similar to those of ethylene reduction and carbon fixation of the tuft colonies among natural populations of *Trichodesmium* spp. in the Gulf. The resulting C/N ratios of *Trichodesmium* spp. colonies did not reflect their carbon and nitrogen fixation potential. The tuft and puff colony types from surface waters had a C/N ratio of 4.1 to 4.3 (Table 2). Such ratios were observed in plankton samples from near the nitracline, whereas C/N ratios of surface plankton samples at the same sites ranged between 7.7 and 8.9 (Fig. 6). Plankton samples taken at 5 to 20 m depth (wind-mixed layer) along a longitudinal transect in the Gulf had C/N ratios of 8.0 ± 1.2 (n = 13), whereas C/N ratios of 10.4 ± 2.2 (n = 4) were determined for the open waters of the northern Red Sea.

Trophic relationships

During spring 1997, *Trichodesmium* spp. were not observed, and the Gulf of Aqaba carried atypically large populations of the jellyfish *Aurelia* (>1 m^2), and the tunicates *Salpa maxima* (>100 m^2) and *Doliolum denticulatum*. This raised the question whether these observations were related. So far, *Macrosetella* has been regarded as the sole grazer of *Trichodesmium* spp.; and we therefore studied the fatty acid signatures of the cyanobacteria *Trichodesmium* spp. and *Synechococcus* and potential grazers to elucidate whether chaetognaths, copepods and tunicates directly or indirectly fed on *Trichodesmium* spp. during spring 1997. The fatty acid analyses revealed interesting differences between the different plankton organisms (Table 3). Both *Synechococcus* spp. strains had an extremely low content of long-chain (>18 C-at.) polyunsaturated fatty acids, which were represented only by 20:5ω3. This is in agreement with the published

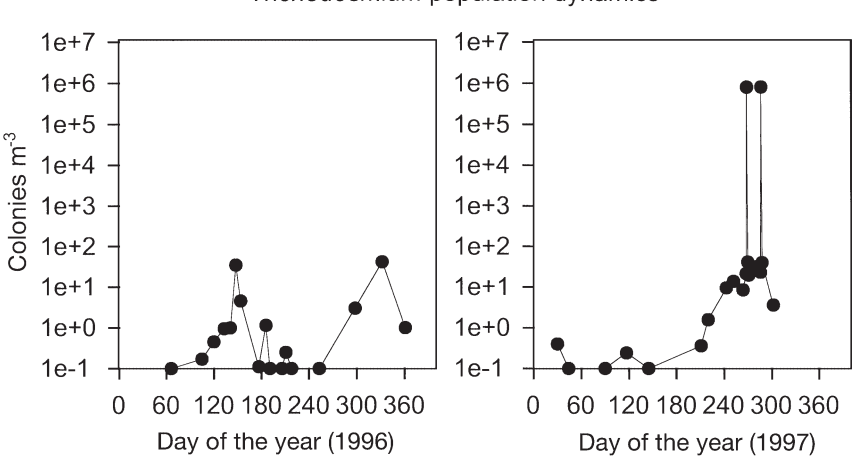

Fig. 5. *Trichodesmium* spp. Seasonal variation in colony numbers of tuft colonies in coastal surface waters (0 to 5 m) near the Marine Biology Station, Eilat, during the summer stratification periods of 1996 and 1997

DISCUSSION

Phytoplankton communities of the Gulf of Aqaba in the summer of 1996 were made up of an assemblage of diatoms, dinoflagellates and the cyanobacteria *Trichodesmium* spp. as is usual for open seas of (sub)tropical regions. Dynamic changes in diatom and *Trichodesmium* spp. abundance have been noted previously for the Gulf of Aqaba (Kimor & Golandsky 1977). The phytoplankton underwent a succession whereby diatom numbers declined over summer, and the prokaryotic *Trichodesmium* spp. became more dominant. This succession is similar to the seasonal succession among ultraphyto-

fatty acid profiles of cyanobacteria (Sargent et al. 1987, Brett & Müller-Navarra 1997). Unlike other cyanobacteria, both strains of *Trichodesmium* spp. had a modest content of 20:5ω3 and of C22:2ω6. The latter fatty acid is either not found or found in very low concentrations (<1% of total fatty acids) in other groups of phytoplankton (Ackman et al. 1968, Harwood & Jones 1989, Reitan et al. 1994, Brett & Müller-Navarra 1997). Large calanoid copepods and the tunicate *D. denticulatum* (solitary gonozoids) contained considerable amounts of C:20ω3, but no C:22ω6. The harpacticoid copepod *Macrosetella gracilis* and the salp *Salpa maxima* (chain-forming blastozoids) contained both C20:5ω3 and C22:2ω6. Results were more ambiguous for chaetognaths: about one-third of the samples contained C22:2ω6 while the other two-thirds did not.

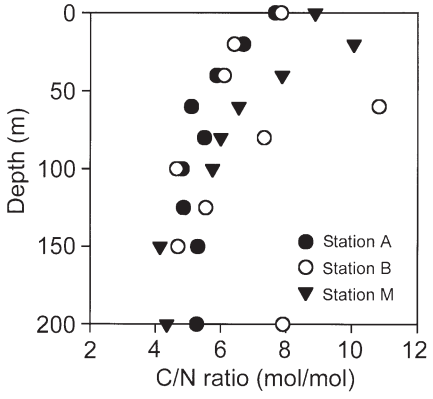

Fig. 6. Depth profiles of C/N ratios of plankton (<100 µm) populations at Sampling Stations A, B and M in the northern part of the Gulf of Aqaba, Red Sea

Table 3. Contents of polyunsaturated fatty acids as percentage of total fatty acids in cultured marine cyanobacteria and invertebrate species abundant in surface waters of the Gulf of Aqaba during the May 1997 cruise

Species	C20:5ω3 mean (min–max)	C22:2ω6 mean (min–max)	n
Trichodesmium sp. Strain RS9602	1.70	2.00	1
Trichodesmium sp. Strain WH9601	3.20	1.70	1
Synechococcus sp. Strain C129	0.22	0	1
Synechococcus sp. Strain WH7803	0.47	0	1
Salpa maxima	5.05 (2.43–11.90)	6.77 (0.65–23.3)	10
Macrosetella gracilis	11.41 (5.60–18.50)	3.33 (2.40–5.15)	5
Doliolum fasciculatum	2.89 (1.95–3.75)	0	4
Calanoid copepods	10.17 (2.50–24.40)	0	12
Chaetognaths	7.44 (2.57–22.80)	0.48 (0[a]–2.24)	10

[a]Seven samples contained no C22:2ω6

plankton (<8 µm) in these waters (Lindell & Post 1995). Both ultraphytoplankton and netphytoplankton successions in the Gulf of Aqaba are probably related to the characteristic, semi-annual variation in water body structure (Genin et al. 1995, Lindell & Post 1995). Such successions are typical of temperate waters (Smayda 1980), in contrast to the relative stability and slight inter-annual variability reported for other

warm, oligotrophic waters of the Sargasso Sea (Smayda 1980) and the Pacific Ocean (Venrick 1990). Phytoplankton composition in the central gyre of the Pacific shows a slow multi-annual trend of change, with *Trichodesmium* spp. populations becoming more prominent over recent years (Karl 1999). *Trichodesmium* spp. were the dominant nitrogen-fixing species in the Gulf of Aqaba, although diatoms such as *Rhizosolenia* sp. and *Hemiaulus* sp. as well as the heterotrophic dinoflagellate *Ornithocercus quadratus* contributed significantly to the phytoplankton in summer. These species often harbor cyanobacterial symbionts capable of nitrogen fixation (Kimor et al. 1992, Gordon et al. 1994), and their abundance is thus consistent with a progressing depletion of N-compounds (Gordon et al. 1994).

Here we report for the first time on the species composition and population dynamics of *Trichodesmium* spp. in the Gulf of Aqaba, Red Sea. Using the morphological characters of Janson et al. (1995) we identified *Trichodesmium* sp, *T. tenue*, *T. erythraeum*, *T. thiebautii* and *T. hildebrandtii* . The colony densities were low compared to reports from the Caribbean and Sargasso Sea (Hulburt 1968, Steven & Glombitza 1972, Carpenter & Price 1977, Villareal 1995), but consistent with reports of 10^3 trichomes m^{-3}, that are apparently typical for the Red Sea (Carpenter 1983). Distinctly different depth distributions for 2 *Trichodesmium* spp. colony types were observed. Puff-colony populations remained in deep parts of the photic zone, while tuft-colony populations were located in the wind-mixed layer (upper 10 to 30 m). While information on buoyancy regulation of colonies is extensive (Walsby 1978, Villareal & Carpenter 1990, Kromkamp & Walsby 1992, Romans et al. 1994), little is known about the capacity of natural populations of *Trichodesmium* spp. to regulate their position along the vertical. Our data suggest that vertical migration of the 2 *Trichodesmium* spp. colony types, if it occurred at all, was confined to bidirectional migration of low numbers of individual colonies. *Trichodesmium* spp. depth distributions at later dates in 1996 were consistent with the observations described above, suggesting that the 2 different *Trichodesmium* spp. types occupy different niches within the photic layer.

It is not known at present whether the deep populations of *Trichodesmium* sp. employ nitrogen fixation or if they meet their nitrogen demand through assimilation of dissolved N-compounds. A C/N ratio of 4.3 for both tuft and puff colony types in surface samples indicates that these were N-sufficient relative to the surrounding plankton community (C/N ratio of ~8). Deep populations of puff colonies do not necessarily depend on N-fixation, but may utilise combined N-sources. Plankton C/N ratios in the bottom half of the photic zone approached those of *Trichodesmium* spp., colonies, suggesting a higher N-supply at these depths. *Trichodesmium* spp. are capable of utilising ammonium and urea (Ohki et al. 1991) and could further explore the nitracline, as nitrate assimilation has previously been identified (Ohki et al. 1991, Wang et al. 2000).

According to the primary production data available for the Gulf of Aqaba (Iluz pers. comm.), *Trichodesmium* spp. contributed 13 to 35% of the surface production by other phytoplankton in early summer months. Primary production by *Trichodesmium* spp. exceeded surface primary production >7-fold during the short bloom period of September 1997. Since *Trichodesmium* spp. are largely limited to the surface layers, they do not contribute significantly to total annual primary production in the Gulf. However, it may impact significantly on C and N fluxes in coastal waters overlying coral reefs. Moreover, the C/N ratios of surface waters in the Gulf of Aqaba tend to be lower than those in the northern Red Sea, where the N-fixing *Trichodesmium* spp. were less abundant. High alkaline phosphatase activities among surface plankton and *Trichodesmium* spp. colonies from the Gulf of Aqaba measured during the same sampling period were indicative of low inorganic phosphate availability and, possibly, P-limitation (Li et al. 1998, Stihl et al. 2001). *Trichodesmium* spp. may thus play a pivotal role in the plankton ecology of the Gulf by alleviating N-depletion and driving the system to more P-deplete conditions.

Trophic relationships can be deduced from profiles of polyunsaturated fatty acids, since these are essential for metazoans, which have a very limited capacity for de novo synthesis (Sargent et al. 1987, Brett & Müller-Navarra 1997). Therefore, the fatty acid-composition of animals reflects the fatty acid composition of their food (Scott & Baynes 1978, StJohn & Lund 1996). In general, phytoplankton have a more constant composition of polyunsaturated fatty acids than organisms from higher trophic levels (Reitan et al. 1994, Brett & Müller-Navarra 1997). Until now, C20:5ω3 fatty acid has been reported as a marker of diatoms, C22:6ω3 as a marker of pigmented flagellates (Prymnesiophyceae, Chrysophyceae, Xanthophyceae, Cryptophyceae), while cyanobacteria and Chlorophyta were found to have negligible polyunsaturated fatty acid contents (Ackman et al. 1968, Sargent et al. 1987, Harwood & Jones 1989, Reitan et al. 1994, Pond & Harris 1996, Brett & Müller-Navarra 1997). Our results indicate that C22:2ω6 serves as a specific biomarker for *Trichodesmium* spp., since it is lacking in *Synechococcus*. We identified the C22:2ω6 marker in the known *Trichodesmium* spp.-feeder *Macrosetella gracilis* (Böttger-Schnack & Schnack

1989, O'Neil 1998) and in the salp *Salpa maxima*. However, it was not found in calanoid copepods which supposedly do not feed on *Trichodesmium* spp. Similarly, no C22:2ω6 was found in the tunicate *Doliolum denticulatum*. From this we conclude that *S. maxima* did feed on *Trichodesmium* spp. populations in the Gulf of Aqaba. It seems improbable that C22:2ω6 entered the food web via degradation of *Trichodesmium* spp., bacterial uptake and subsequent bacteriovory by protozoans. In such case, C22:2ω6 would have been either oxidised during degradation or would have shown up in the calanoid copepods as well. Its appearance in a portion of the chaetognath population is probably due to predation of some chaetognath individuals on *Macrosetellla gracilis*. *S. maxima* is too large to be fed upon by chaetognaths.

In spite of the virtual absence of *Trichodesmium* spp. from the Gulf of Aqaba during spring 1997, *Salpa maxima* must have ingested sufficient colonies to account for the C22:2ω6 signature among salps. Harbison & Gilmer (1976) provided a logarithmic regression of filtration rates on body size of *S. maxima* blastozoids that predict rates of 10.5 l d^{-1} for a mean 25 mm (body length) salp. During the 1997 cruise, several chains of 20 to 40 individuals were observed within 1 m^3 of the surface water. The individual filtration rate and a conservative estimate of 100 salps m^{-3} yields an estimated population filtration rate of 1 colony d^{-1}. This filtration rate cannot be met by the maximal growth rate of *Trichodesmium* spp., and therefore explains adequately why the anticipated *Trichodesmium* spp. spring maximum was lacking in 1997. Similarly, the high growth rates of pelagic tunicates such as *Doliolum denticulatum* (which has C22:2ω6 signatures) enable their populations to control algal blooms (Heron 1972). So far, feeding studies of salps and doliolids have concentrated on bacteria, small and medium-sized algae. The lower size limit of edible particles of ca. 0.5 µm has been well established through the morphology of the mucus filter (Silver & Bruland 1981), while little attention has been given to the upper size limit. However, there is no objective reason why salps and tunicates should not feed on a colonial cyanobacterium such as *Trichodesmium* spp. and thus form a new link in the trophic relationships of the marine food web.

Acknowledgements. We are grateful to Sheba Solomon for assistance in sampling and identification of phytoplankton species. This research was supported financially by US-Israel Binational Science Foundation grant no. 94-146 and 'Red Sea Programme' grant no. 03F0151A provided by the German Ministry for Education, Science, Research and Technology. This study was further supported by the 'Moshe Shilo' Minerva Center for Marine Biogeochemistry, Minerva Stiftung — Gesellschaft für die Forschung, Munich, Germany. R.G. received financial support from Tel Aviv University.

LITERATURE CITED

Ackman RG, Tocher CS, McLachlan J (1968) Marine phytoplankter fatty acids. J Fish Res Board Can 25:1603–1620

Böttger-Schnack R, Schnack D (1989) Vertical distribution and population structure of *Macrosetella gracils* (Copepoda: Harpacticoida) in the Red Sea in relation to the occurrence of *Oscillatoria* (*Trichodesmium* spp.) spp. (Cyanobacteria). Mar Ecol Prog Ser 52:17–31

Brett MT, Müller-Navarra DC (1997) The role of highly unsaturated fatty acids in aquatic foodweb processes. Freshw Biol 38:483–499

Capone DG, O'Neil JM, Zehr J, Carpenter EJ (1990) Basis for diel variation in nitrogenase activity in the marine planktonic cyanobacterium *Trichodesmium* spp. *thiebautii*. Appl Environ Microbiol 56:3532–3536

Capone DG, Zehr JP, Paerl HW, Bergman B, Carpenter EJ (1997) *Trichodesmium* spp., a globally significant marine cyanobacterium. Science 276:1221–1229

Carpenter EJ (1983) Nitrogen fixation by marine *Oscillatoria* (*Trichodesmium* spp.) in the world's oceans. In: Carpenter EJ, Capone DG, Reuter J (eds) Nitrogen in the marine environment. Academic Press, New York, p 65–103

Carpenter EJ, Price CC (1977) Nitrogen fixation, distribution and production of *Oscillatoria* (*Trichodesmium* spp.) *thiebautii* in the eastern Sargasso Sea. Limnol Oceanogr 20: 381–401

Carpenter EJ, Romans K (1991) Major role of the cyanobacterium *Trichodesmium* spp. in nutrient cycling in the North Atlantic Ocean. Science 254:1356–1358

Carpenter EJ, O'Neil JM, Dawson R, Capone DG, Siddiqui PJA, Roenneberg T, Bergman B (1993) The tropical diazotrophic phytoplankter *Trichodesmium* spp.: biological characteristics of two common species. Mar Ecol Prog Ser 95:295–304

Christie WW (1982) Lipid analysis, 2nd edn. Pergamon Press, Oxford

Genin A, Lazar B, Brenner S (1995) Vertical mixing and coral death in the Red Sea following the eruption of mount Pinatubo. Nature 377:507–510

Gordon N, Angel DL, Neori A, Kress N, Kimor B (1994) Heterotrophic dinoflagellates with symbiotic cyanobacteria and nitrogen limitation in the Gulf of Aqaba. Mar Ecol Prog Ser 107:83–88

Harbison GR, Gilmer RW (1976) The feeding rates of the pelagic tunicate *Pegea confederata* and two other salps. Limnol Oceanogr 21:517–528

Harwood JL, Jones AL (1989) Lipid metabolism in algae. Adv Bot Res 16:1–53

Heron AC (1972) Population ecology of a colonizing species: the pelagic tunicate *Thalia demiocratica*. Oecologia 10: 269–293

Hulburt EM (1968) Phytoplankton observations in the western Carribean Sea. Bull Mar Sci 81:168–186

Janson S, Siddiqui PJA, Walsby AE, Romans KM, Carpenter EJ, Bergman B (1995) Cytomorphological characterization of the planktonic diazotrophic cyanobacteria *Trichodesmium* spp. from the Indian Ocean and Carribean and Sargasso Seas. J Phycol 31:463–477

Karl DM (1999) A sea of change: biogeochemical variability in the North Pacific subtropical gyre. Ecosystems 2: 181–274

Kattner G, Fricke HSG (1986) Simple gas-liquid chromatographic method for the simultaneous determination of fatty acid and alcohols in wax esters of marine organisms. J Chromatogr 361:263–268

Kimor B, Golandsky B (1977) Microplankton of the Gulf of Eilat: aspects of seasonal and bathymetric distributions. Mar Biol 42:55–67

Kimor B, Gordon N, Neori A (1992) Symbiotic associations among the microplankton in oligotrophic marine environments, with special reference to the Gulf of Aqaba, Red Sea. J Plankton Res 14:1217–1231

Klinker J, Reiss Z, Kropach C, Levanon I, Harpaz H, Halicz E, Assaf G (1976) Observations on the circulation pattern in the Gulf of Aqaba (Eilat), Red Sea. Isr J Earth Sci 25: 85–103

Klinker J, Reiss Z, Levanon I, Harpaz H, Shapiro Y (1978) Nutrients and biomass distribution in the Gulf of Aqaba (Eilat), Red Sea. Mar Biol 45:53–64

Kromkamp J, Walsby AE (1992) Buoyancy regulation and vertical migration of *Trichodesmium* spp.: a computer-model prediction. In: Carpenter EJ, Capone DG, Rueter JG (eds) Marine pelagic cyanobacteria, *Trichodesmium* spp. and other diazotrophs. Kluwer Academic Publishers, Dordrecht, p 239–248

Li H, Veldhuis MJW, Post AF (1998) Alkaline phosphatase activities among planktonic communities in the northern Red Sea. Mar Ecol Prog Ser 173:107–115

Lindell D, Post AF (1995) Ultraphytoplankton succession is triggered by deep winter mixing in the Gulf of Aqaba (Eilat), Red Sea. Limnol Oceanogr 40:1130–1141

Müller-Navarra DC (1995) Evidence that a highly unsaturated fatty acid limits *Daphnia* growth in nature. Arch Hydrobiol 132:297–307

Müller-Navarra DC, Lampert W (1996) Seasonal patterns of food limitation in *Daphnia galeata*—separating food quantity from food quality effects. J Plankton Res 18: 1137–1157

Murray SP, Hecht A, Babcock A (1984) On the mean flow in the Tiran Strait in winter. J Mar Res 42:265–287

Ohki K, Zehr JP, Falkowski PG, Fujita Y (1991) Regulation of nitrogen-fixation by different nitrogen sources in the marine non-heterocystous cyanobacterium *Trichodesmium* sp. NIBB1067. Arch Microbiol 156:335–337

O'Neill JM (1998) The colonial cyanobacterium *Trichodesmium* spp. as a physical and nutritional substrate for the harpacticoid copepod *Macrosetella gracilis*. J Plankton Res 20:43–59

Pond DW, Harris RP (1996) The lipid composition of the coccolithophore *Emiliana huxleyi* and its possible ecological significance. J Mar Biol Assoc UK 76:579–594

Reitan KI, Rainuzzo JR, Olsen Y (1994) Effect of nutrient limitation on fatty acid and lipid content of marine microalgae. J Phycol 30:972–979

Roenneberg T, Carpenter EJ (1993) Daily rhythm of O_2-evolution in the cyanobacterium *Trichodesmium* spp. *thiebautii* under natural and constant conditions. Mar Biol 117: 693–697

Romans KM, Carpenter EJ, Bergman B (1994) Buoyancy regulation in the colonial diazotrophic cyanobacterium *Trichodesmium* spp. *tenue*: ultrastructure and storage of carbohydrate, polyphosphate and nitrogen. J Phycol 30: 935–942

Sargent JR, Parkes RJ, Müller-Harvey I, Henderson RJ (1987) Lipid biomarkers in marine ecology. In: Sleigh MA (ed) Microbes in the sea. Horwood, Chichester, p 119–138

Scott AP, Baynes SM (1978) Effects of algal diet and temperature on the biochemical composition of the rotifer *Brachionus plicatilis*. Aquaculture 14:247–260

Silver MW, Bruland KW (1981) Differential feeding and fecal pellet composition of salps and pteropods and the possible origin of the deep-water flora and 'olive-green cells'. Mar Biol 62:263–273

Smayda TJ (1980) Phytoplankton species succession. In: Morris I (ed) The physiological ecology of phytoplankton, Blackwell Science, Oxford, p 493–570

StJohn MA, Lund T (1996) Lipid biomarkers: linking the utilization of frontal plankton biomass to enhanced condition of juvenile North Sea cod. Mar Ecol Prog Ser 131: 75–85

Steven DM, Glombitza R (1972) Oscillatory variation of phytoplankton populations in a tropical ocean. Nature 237: 105–107

Stihl A, Sommer U, Post AF (2001) Alkaline phosphatase activities among populations of the colony-forming, diazotrophic cyanobacterium *Trichodesmium* spp. (Cyanobacteria) in the Red Sea. J Phycol 62:310–317

Venrick EL (1990) Phytoplankton in an oligotrophic ocean: species structure and interannual variability. Ecology 71: 1547–1563

Venrick EL, Cummings SL, Kemper CA (1987) Picoplankton and the resulting bias in chlorophyll retained by traditional glass-fiber filters. Deep-Sea Res 34:1951–1956

Villareal TA (1995) Abundance and photosynthetic characteristics of *Trichodesmium* spp. along the Atlantic Barrier Reef at Carrie Bow Cay, Belize. PSZN I: Mar Ecol 16:259–271

Villareal TA, Carpenter EJ (1990) Diel buoyancy regulation in the marine diazotrophic cyanobacterium *Trichodesmium* spp. *thiebautii*. Limnol Oceanogr 35:1832–1837

Walsby AE (1978) The properties and buoyancy providing role of gas vacuoles in *Trichodesmium* spp. Ehrenberg. Br Phycol J 13:103–116

Wang Q, Li H, Post AF (2000) The nitrate assimilation genes of the marine diazotrophic cyanobacterium *Trichodesmium* sp. strain WH9601. J Bacteriol 182:1764–1767

Wolf-Vecht A, Paldor N, Brenner S (1992) Hydrographic indications of advection/convection in the Gulf of Eilat. Deep-Sea Res 39:1393–1401

Yahel G, Post AF, Fabricius K, Marie D, Vaulot D, Genin A (1998) Phytoplankton distribution and grazing near coral reefs. Limnol Oceanogr 43:551–563

Editorial responsibility: Gotthilf Hempel, Bremen, Germany

Submitted: May 3, 2001; Accepted: January 31, 2002
Proofs received from author(s): August 6, 2002

Vol. 239: 251–261, 2002 | MARINE ECOLOGY PROGRESS SERIES
Mar Ecol Prog Ser | Published August 23

Grazing during early spring in the Gulf of Aqaba and the northern Red Sea

Ulrich Sommer[1,*], Ulrike G. Berninger[1,2], Ruth Böttger-Schnack[3], Astrid Cornils[2], Wilhelm Hagen[3], Thomas Hansen[1], Tariq Al-Najjar[4], Anton F. Post[5], Sigrid B. Schnack-Schiel[2], Herwig Stibor[6], Dorothea Stübing[3], Stephen Wickham[5,7]

[1]Institut für Meereskunde an der Universität Kiel, Düsternbrooker Weg 20, 24105 Kiel, Germany
[2]Alfred-Wegener-Institut für Polar- und Meeresforschung, 27515 Bremerhaven, Germany
[3]Marine Zoologie, Universität Bremen (NW2), Postfach 33040, 28334 Bremen, Germany
[4]Marine Science Station, PO Box 195, Aqaba, Jordan
[5]Interuniversity Institute, PO Box 469, 88103 Eilat, Israel
[6]Zoologisches Institut, Ludwig-Maximilians-Universität, Karlsstraße 23-25, 80333 München, Germany
[7]Zoologisches Institut, Universität Köln, Weyertal 119, 50923 Köln, Germany

ABSTRACT: Zooplankton grazing on bacterio- and phytoplankton was studied in the Gulf of Aqaba and the Northern Red Sea during Meteor Cruise Me 44-2 in February-March 1999. Protozoan grazing on bacterioplankton and autotrophic ultraplankton was studied by the Landry dilution method. Microzooplankton grazing on phytoplankton >6 µm was studied by incubation experiments in the presence and absence of microzooplankton. Mesozooplankton grazing was studied by measuring per capita clearance rates of individual zooplankton with radioactively labelled food organisms and estimating *in situ* rates from abundance values. Protozoan grazing rates on heterotrophic bacteria and on algae <6 µm were high (bacteria: 0.7 to 1.1 d^{-1}, ultraphytoplankton: 0.7 to 1.3 d^{-1}), while grazing rates on *Synechococcus* spp. were surprisingly low and undetectable in some experiments. Mesozooplankton grazing was weak, cumulative grazing rates being ca. 2 orders of magnitude smaller than the grazing rates by protozoans. Among mesozooplankton, appendicularians specialised on smaller food items and calanoid copepods on larger ones.

KEY WORDS: Phytoplankton · Protozoa · Bacteria · Zooplankton · Grazing · Red Sea · Gulf of Aqaba

INTRODUCTION

Phytoplankton in the oligotrophic northern Red Sea and in the Gulf of Aqaba (Klinker et al. 1978, Reiss & Hottinger 1984) are characterised by a low biomass (<0.8 µg chlorophyll l^{-1}) dominated (>95%) by phytoplankton <8 µm (Lindell & Post 1995, Li et al. 1998, Yahel et al. 1998). Except for the early summer and fall summer bloom of the cyanobacterium *Trichodesmium* spp., algae measuring 8 to several 100 µm are scarce and contribute <10% of chlorophyll *a* (Yahel et al. 1998). Although not totally absent, they are usually countable in samples from plankton nets or by sedimentation of several 100 ml of water (Kimor & Golandsky 1977). Similar to phytoplankton, both protozoan and metazoan plankton are characterised by low biomass and low abundance. Nevertheless, all major functional and taxonomic groups of marine zooplankton are represented. However, neither total grazing pressure on phytoplankton nor the relative importance of different functional categories of zooplankton as grazers of different phytoplankton size-classes have been studied so far. The different size classes of phytoplankton and of zooplankton require different methods

*E-mail: usommer@ifm.uni-kiel.de

of grazing measurements. In this article, we present the synthesis of several simultaneously run, but independent, grazing studies performed during Meteor cruise Me 44-2 in the Gulf of Aqaba and the northern open Red Sea (15 February to 9 March 1999) together with data on zooplankton abundance and copepod lipid and gut contents as long-term (lipids) and short-term (gut contents) indicators of previous diet. This choice of season allowed comparison of plankton from a deeply mixed water column (Gulf of Aqaba, mixing depth >300 m) with plankton from a stratified water column (Red Sea, mixing depth <50 m at most stations). This contrast in the mixing regime is typical for this period, whereas a few weeks later summer stratification also begins in the Gulf of Aqaba (Wolf-Vecht et al. 1992, Genin et al. 1995).

MATERIALS AND METHODS

Phytoplankton size spectrum. Water samples were obtained from 10 l Go-Flo bottles on an CTD-rosette and passed through 100 µm mesh. Duplicate 1.5 ml samples were preserved in 1.8 ml cryotubes (Nunc) with 75 µl of 2.0% paraformaldehyde solution, quickly frozen, and stored in liquid nitrogen until flow cytometry was performed. Picoplankton were analysed on a FACScan flow cytometer (Becton Dickinson) modified to permit quantification of all groups including the dimly fluorescent surface populations of *Prochlorococcus* spp. (Li et al. 1993, Dusenberry & Frankel 1994); 10 µl of a 0.474 µm Fluoresbrite microsphere (Polysciences, Inc.) suspension were added as internal standard. Flow cytometry histograms were analysed with Cytowin software (Vaulot 1989).

Table 1. List of stations and positions of grazing experiments and mesozooplankton counts mentioned in this study. F: flow cytometry samples for picoplankton; M: microzooplankton grazing on nano- and microzooplankton according to Sommer (2000); P: grazing on picoplankton according to Landry et al. (1995); Z: mesozooplankton net hauls

Stn; Expt	Site	Date (dd.mm.yy)	North	East
118; F, M	Gulf of Aqaba	21.02.99	28.582′	34.651′
122; F	Gulf of Aqaba	22.02.99	29.492′	34.950′
123; P	Gulf of Aqaba	22.02.99	29.284′	34.817′
124; F	Gulf of Aqaba	22.02.99	29.083′	34.766′
126; F	Gulf of Aqaba	23.02.99	28.585′	34.650′
127; F	Gulf of Aqaba	23.02.99	28.334′	34.550′
130; F	Red Sea	24.02.99	27.418′	34.668′
132; F, M, P	Red Sea	24.02.99	27.298′	34.368′
134; F	Gulf of Aqaba	25.02.99	28.334′	34.550′
136; F	Gulf of Aqaba	25.02.99	28.834′	34.733′
138; F	Gulf of Aqaba	26.02.99	29.284′	34.817′
139; F	Gulf of Aqaba	26.02.99	29.492′	34.950′
145; F, M	Red Sea	27.02.99	27.654′	34.668′
147; F, P	Red Sea	28.02.99	27.183′	34.666′
148; F	Red Sea	28.02.99	27.397′	34.368′
152; M, Z	Gulf of Aqaba	02.03.99	28.334′	34.551′
156; Z	Red Sea	04.03.99	27.416′	34.083′
157; P	Gulf of Aqaba	05.03.99	29.491′	34.951

Zooplankton abundance. As standard devices for the quantitative collection of zooplankton, 2 multiple opening-closing nets were used: a smaller one (mouth opening 0.25 m^2) consisting of 5 nets of 55 µm mesh and a larger one (mouth opening 0.5 m^2) comprising 9 nets of 150 µm. Stratified vertical hauls covered the entire water column between the surface and the sea bottom. The filtered volume of the larger net was measured by a flowmeter, while the filtered volume of the smaller net was calculated on the basis of the vertical distance covered by the net's mouth area assuming 100% efficiency. All samples were fixed in a 4% formaldehyde seawater solution. For the present study, abundance data from 2 stations and the uppermost depth strata (0 to 50 and 50 to 100 m) were used. Samples from the 150 µm net were used for the counts of adults and late copepodids of calanoids and other large zooplankton, while samples from the 55 µm net were used for juveniles, small-bodied copepod taxa, and appendicularians.

Nano- and microzooplankton grazing on picoplankton. Microzooplankton grazing dominated by protozoa on autotrophic and heterotrophic picoplankton was studied by Landry et al.'s (1995) modification of the dilution method of Landry & Hasset (1982). This method is based on a dilution series of natural plankton suspension with filtered seawater. Net growth rates are calculated from cell counts at the beginning and at the end of the incubation period (in our case ca. 36 h). In more dilute samples, the encounter rates of predators with their prey is reduced, resulting in a higher net growth rate of the prey in comparison to less dilute treatments.

Water samples were collected at 5 different locations (Stns 123, 132, 147, 152, 157: Table 1). Particle-free water was prepared by filtration through a 0.2 µm cartridge filter. This water was mixed with unfiltered water to obtain dilution grades of 35, 50, 60, 80, 90, and 100% unfiltered water. Experiments were conducted in 2.5 l transparent polycarbonate bottles, incubated for 36 h in on-deck incubators cooled by a flow-through of surface water and exposed to ca. 30% of incident light. All experiments were run in duplicate bottles. Nutrients (12 µM N, 6 µM Si, 0.7 µM P) and vitamins were added to avoid nutrient limitation in the bottles. In 3 of the experiments, unenriched bottles were also incubated to estimate the extent of nutrient limitation. Samples were taken at the beginning and end of incubation for later microscopic counts. Samples for the enumeration of picoplankton and nanoplankton

were preserved in 1.25% glutaraldehyde and stored at 4°C; 15 ml of the fixed sample were filtered onto 0.2 µm Nuclepore filters and stained with the fluorochrome DAPI (1.0 µg l^{-1}). Heterotrophic pico- and nanoplankton and autotrophic ultraplankton (<8 µm) were counted using a blue filter set, whereby autotrophs were differentiated from heterotrophs on the basis of their red or orange autofluorescence. Samples of phytoplankton >8 µm were fixed in Lugol's iodine and counted under an inverted microscope.

Growth rates were calculated individually for each bottle. A linear regression of growth rate on the fraction of undiluted water yielded an estimate of the gross growth rate (μ; equivalent to the *y*-axis intercept) and of the grazing rate (γ; equivalent to the negative slope of the regression). Addition of nutrients in a parallel dilution series prevents nutrient limitation at lower dilutions. It yields an estimate of the maximal growth rate (μ_{max}) and, by comparison with the gross growth rate (μ) of the unenriched bottle, an assessment of the extent of nutrient limitation.

Microzooplankton grazing on nano- and microphytoplankton. Grazing rates on phytoplankton taxa >6 µm were obtained from shipboard experiments designed for the comparison of the relative importance of nutrient versus grazing control on medium-sized phytoplankton (Sommer 2000). Nutrient manipulations ranged from controls (no addition), over silicate enrichment (4 µM Si), to a full enrichment (4 µM Si, 4.5 µM N, 0.3 µM P) that ensured all phytoplankton were free of nutrient stress. Grazer manipulations consisted of sieving the sample through net-screens with mesh sizes of 100 µm (removal of adult metazoa, but not of protozoa and the smallest nauplii), 20 µm (removal of larger protozoa) and 10 µM (removal of medium-sized protozoa). Protozoa <10 µm were not removed because they usually feed on pico- but not on nanoplankton and their removal would also have removed all the target algae of this study.

The water samples for the experiments were taken from 10 m depth at 2 stations in the Gulf of Aqaba (Expt 1: Stn 118; Expt 4: Stn 152) and 2 stations in the open Red Sea (Expt 2: Stn 132; Expt 3: Stn 145). The manipulated water samples were incubated in 2 l polycarbonate bottles floating in a deck incubator. Each treatment was duplicated in separate bottles. The deck incubator was cooled by a flow-through of surface water (21 to 23°C) and shielded against direct sunlight by a Plexiglas cover which absorbed ca. 70% of incident radiation.

Subsamples (250 ml) from the incubation bottles were taken at the start of the experiments and after 2 and 5 d, and were preserved with Lugol's iodine for identification at the genus level and cell counts of the nano- and microplankton species. The scarcity of nano- and microphytoplankton (0.05 to 10 cells ml^{-1} in the initial samples) required the sedimentation of 200 ml samples prior to microscopic counting in an inverted microscope. If cell numbers were sufficient, 100 individuals were counted per taxon, thus giving 95% confidence limits of ca. ±20% (Lund et al. 1958). However, in many cases counting of the entire counting chamber resulted in ≪100 cells. The response of individual taxa to the experimental treatments was assessed by calculating net growth rates from the cell density data on Days 0 and 2: $r = \ln(N_2/N_0)/2$. Grazing rates (γ; d^{-1}) were calculated as the difference between net growth rates of the fully enriched treatments without microzooplankton removal and the fully enriched treatments sieved through 10 µm mesh (or 20 µm mesh in the case of phytoplankton taxa which did not pass the 10 µm screen). Data from the non-enriched bottles were not used, because nutrient excretion by zooplankton might have enhanced cell division rates relative to grazer-free treatments. It is assumed that microzooplankton grazing rates in the bottles do not respond to nutrient enrichment within 2 d and conform to the *in situ* rates (Sommer 2000). For the purpose of synthesis, the dependence of grazing rates on phytoplankton particle size was analysed by regression analysis. Particle size was defined as the greatest axial linear dimension (GALD). In the case of colonial or filamentous algae, colony or filament length were used instead of cell length.

Size-specific grazing rates of mesozooplankton. Grazing was measured by using radioactively labelled algae and bacteria of different sizes as tracers and freshly collected zooplankton individuals as grazers. The phytoplankton tracers were obtained from stock cultures. Sizes of the tracer algae (see Table 5) are characterised by the greatest axial linear dimension and the equivalent spherical diameter (ESD). All phytoplankton cultures were grown in 0.2 µm membrane-filtered Red Sea water with nutrients and trace metals added (von Stosch & Drebes 1964). Suspended heterotrophic bacteria were isolated by filtering seawater through 0.8 µm membrane filters. All cultures were kept at 22°C and an irradiance of about 100 µE cm^2 s^{-1}; 24 h prior to a grazing experiment, phytoplankton cultures were labelled with ^{14}C bicarbonate (250 µCi); bacteria were inoculated with radioactive glucose (25 µCi).

Zooplankton were collected by vertical plankton hauls (mesh size 100 µm). To keep gelatinous plankton intact, we replaced the original net beaker at the end of the net by a plastic bag. Zooplankton were separated into functional groups immediately after collection. For each taxonomic group used in a grazing experiment, 10 to 30 animals of the same size class were transferred to 1 l jars filled with <100 µm filtered

seawater to allow acclimation to experimental conditions. After approximately 4 h the animals were checked for viability and mobility to ensure that only intact individuals were introduced into our experimental set-up. Aliquots of equally-sized individuals were dried and analysed for carbon in a Fisons 1500 CN analyser.

Triplicate grazing trials were run with each size class of food organisms. Experiments were repeated 2 or 3 times. Radioactively labelled food organisms were added to 30 ml glass jars filled with Red Sea water filtered through a 100 µm mesh. Each glass jar contained between 1 and 3 experimental animals. Independent of the number of animals in the jar, a jar was always treated as 1 replicate. After a grazing period of 15 min, zooplankton were anaesthetised with carbonated water and collected on a 100 µm screen. Animals were thoroughly rinsed with GF/F-filtered seawater to remove adhering labelled cells. The animals were then pipetted into a scintillation vial. Tissue solubiliser was added (0.5 ml of Soluene 350), and digestion was accelerated by exposing the vial to 60°C for several hours. Additionally, Carbosorb was added to the vials to prevent loss of radioactive carbon. Passive adsorption of radioactive tracer on zooplankton was assessed using formalin-killed zooplankton which were introduced into the grazing experiments as controls. In order to determine the amount of particulate radioactivity in the grazing jars, 1 ml from each jar was filtered onto GF/F filters (algae) or 0.2 µm membrane filters (bacteria). Filters were exposed to vapours of concentrated HCl to remove non-incorporated radioactive bicarbonate.

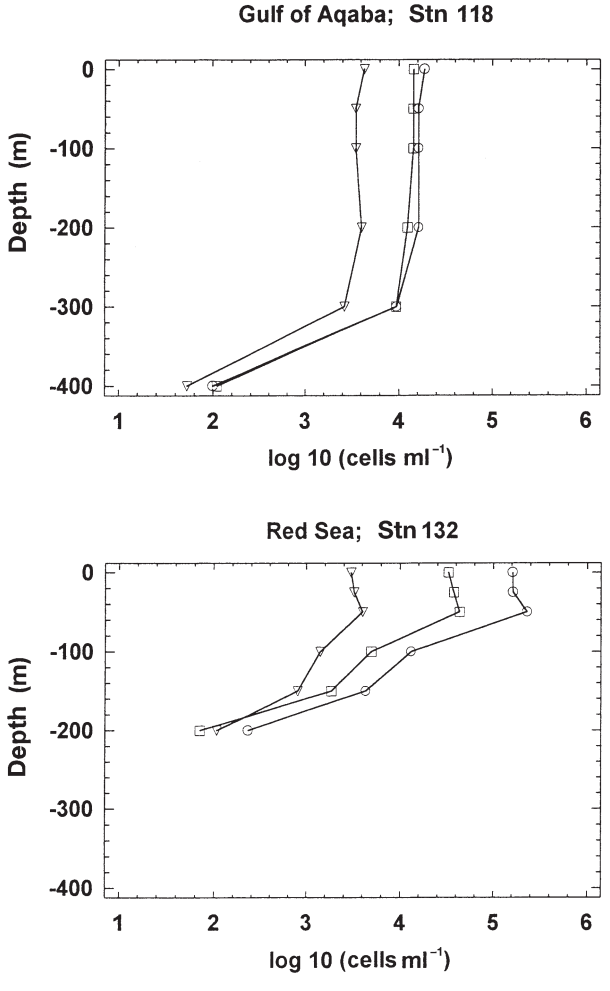

Fig. 1. Depth profiles of the 3 major picophytoplankton groups, *Prochlorococcus* spp. (○), *Synechococcus* spp. (□) and eukaryotes (▽) at Stns 118 (Gulf of Aqaba) and Stn 132 (northern Red Sea)

Radioactivity was measured by a liquid scintillation analyser (TRI CARB 2100 TR); Ultima Gold was used as a scintillation cocktail. Values of radioactivity (expressed in dpm) were corrected by subtracting passive adsorption of radioactive tracer by formalin-killed zooplankton. Individual clearance rates (ml ind.$^{-1}$ d^{-1}) for each tracer size class were computed using the equation provided by Haney (1971):

$$F = (\text{dpm ind.}^{-1}/\text{dpm ml}^{-1}\text{ grazing suspension}) \times (1440/t)$$

where F = clearance rate (ml ind.$^{-1}$ d^{-1}); grazing suspension = volume in which grazing occurred and to which specific tracer was added; and t = grazing time in minutes.

Lipid content and composition of copepods. Copepods, especially *Rhincalanus nasutus* CV and females, were collected at various stations in the Gulf of Aqaba and the northern Red Sea. The specimens were sampled by vertical multinet hauls from depths between 600 m to the surface. They were immediately transferred to a container with filtered seawater and sorted according to species and stages. The individuals were pooled for each sample (usually 40 to 50 specimens) and directly deep-frozen at –80°C or stored frozen in dichloromethane/methanol (2:1 by vol.) until analysis.

Lipids were extracted with dichloromethane/methanol (2:1 by vol.) after Folch et al. (1957) and Hagen (2000), and lipid classes were determined according to Fraser et al. (1985) by thin-layer chromatography/flame-ionisation detection (TLC-FID) with a Iatroscan MARK II. After transesterification of the lipids with 3% concentrated sulphuric acid in methanol, fatty acid methyl esters and free alcohols were simultaneously analysed in a gas chromatograph equipped with a DB-FFAP column. The gas chromatographic oven was temperature-programmed. The fatty acids and alcohols were identified with known standards. For analytical details refer to Kattner & Fricke (1986), Kattner et al. (1994), and Hagen (2000).

Table 2. Abundance (cells ml^{-1}; mean and minimum to maximum range) and biomass (biovolume based on mean cell size and mean abundances; μm^3 ml^{-1}) of small-sized phytoplankton groups in the Gulf of Aqaba and the Red Sea. Samples for fluorescence microscopy were the initial samples of the dilution experiments taken from Stns 123, 152, and 157 for the Gulf of Aqaba and from Stns 132 and 147 for the Red Sea. Sampling depth was 10 m, except for Stn 123 (50 m). Samples for flow-cytometry were taken from 10 m depth at Stns 118, 122, 124, 126, 127, 134, 136, 138, 139 (Gulf of Aqaba) and Stns 130, 132, 145, 147, 148 (Red Sea)

Phytoplankton group	Cell size (µm)	Vol. (μm^3)	Gulf of Aqaba		Red Sea	
			Abundance	Biomass	Abundance	Biomass
Estimated by flow cytometry						
Prochlorococcoccus spp.	0.6–0.8	0.18	18 100 5 100–48 000	3 240	204 000 150 000–260 000	36 720
Synechococcus spp.	0.9–1.2	0.70	16 500 8 200–30 800	11 550	29 100 15 400–35 000	20 370
Pico-eukaryotes	1.0–2.0	1.77	4 200 1 970–5 860	7 434	2 660 1 640–3 420	4 708
Estimated by fluorescence microscopy						
Synechococcus spp.	0.9–2.0	1.6	17 800 4 500–43 500	28 480	17 500 7 500–27 500	28 000
Phytoplankton <8 µm (without *Synechococcus* spp.)	0.6-4.0	6	3 990 580–7 180	23 940	1 530 860–2 200	9 180
Larger phytoplankton	>8	400[a]	2.42 1.26–3.80	968	2.47 2.13–2.81	988

[a]Based on thin, spindle-shaped *Rhizosolenia* spp., *Nitzschia* spp. and *Pseudonitzschia* spp., the dominant phytoplankton taxa >8 µm

RESULTS

Phytoplankton and bacterioplankton size-spectrum

Water-column conditions had a distinct effect on the abundance and composition of phytoplankton communities. Fig. 1 shows typical depth profiles for picoplankton abundance in the deeply mixed Gulf of Aqaba (Stn 118) and in the stratified northern Red Sea (Stn 132). Cells were distributed in a uniform way over 300 m at Stn 118, and *Synechococcus* spp. and *Prochlorococcus* spp. were present in equal abundance. However, at Stn 132 picoplankton depth distributions showed a distinct stratification, with highest cell numbers in the upper 60 m (Fig. 1). While picoeukaryote abundance at this site was about half that at Stn 118, *Synechococcus* spp. and *Prochlorococcus* spp. were more abundant by factors of 2 and 10 times, respectively.

A comparison of flow-cytometry analysis of samples at all sites taken at 10 m depth revealed considerable differences in the abundance of phototrophic picoplankton, with the smallest group (*Prochlorococcus* spp.) being 10 times more abundant in the stratified Red Sea, and picoplankton eukaryotes being 2 times more abundant in the deeply mixed waters of the Gulf of Aqaba (Table 2). Thus, the composition of phototrophic picophytoplankton in the Red Sea was similar to the composition in the Gulf of Aqaba during the period of summer stratification (Lindell & Post 1995). The ranges for the flow cytometer counts and for the microscopic counts indicate a pronounced spatial variability in both systems. Epifluorescence counts and inverted microscope counts were performed at fewer stations and, although they are probably less precise, they do permit an estimate of larger phytoplankton also. Phytoplankton >8 µm contributed ca. 0.01% to total cell number and ca. 2% to total biomass, as estimated from cell volumes.

The abundances of heterotrophic bacteria were not affected by the physical structure of the water masses. Numbers of heterotrophic bacteria were in the range to be expected for oligotrophic environments (5 to 5.5×10^5 ml^{-1} in the Red Sea and 3 to 5.3×10^5 ml^{-1} in the Gulf of Aqaba).

Zooplankton abundance

Copepods (including nauplii) were the most numerous group among the mesozooplankton in the Gulf of Aqaba and the northern Red Sea. Appendicularians ranked next in abundance in the upper strata, followed by chaetognaths, ostracods and gastropods, as usually found in the Red Sea (Böttger-Schnack 1995). Among the copepods, calanoids were most abundant, contributing about 40 to 50% of the total numbers (Fig. 2). Cyclopoids and poecilostomatoids ranked next, whereas harpacticoids were found in small numbers

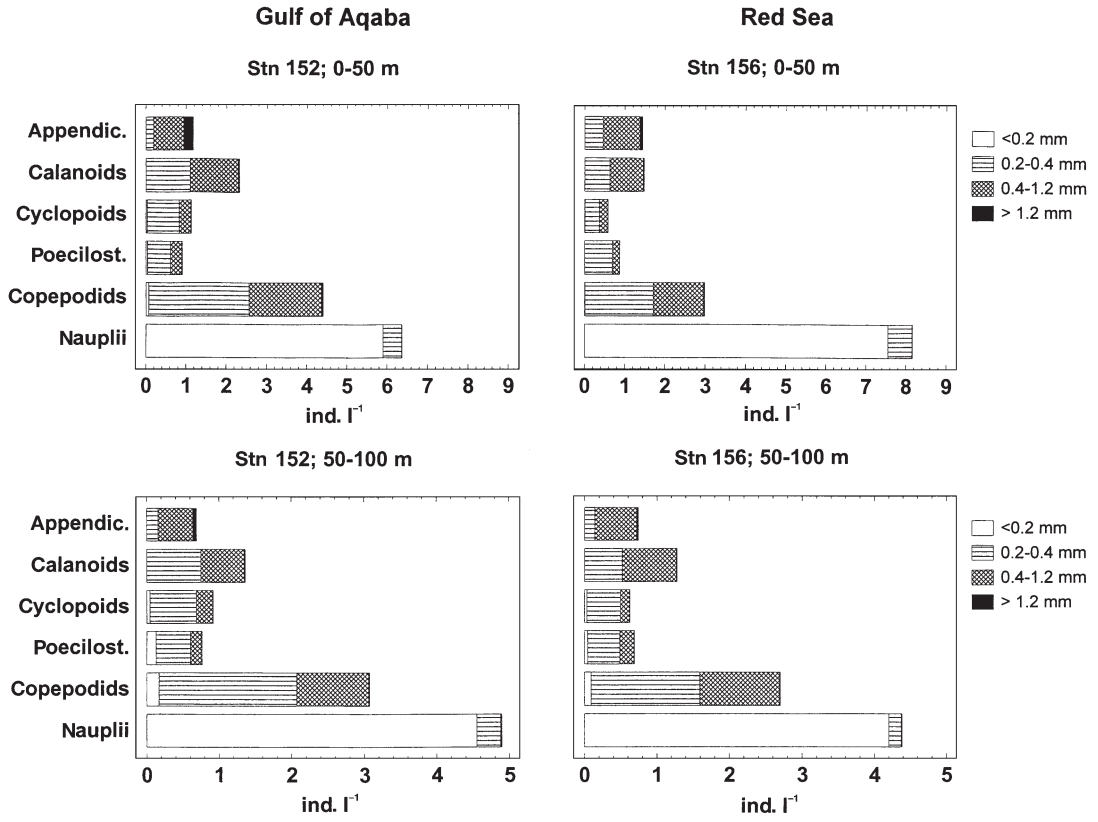

Fig. 2. Abundance of major mesozooplankton groups by size classes at Stn 152 (Gulf of Aqaba) and Stn 156 (northern Red Sea) Copepodids and nauplii were not sorted taxonomically. Appendic.: appendicularians; Poecilost.: poecilostomatoids

only. Most calanoid species belonged to the family Clausocalanidae (e.g. *Ctenocalanus vanus*, *Clausocalanus* spp.) and were of small size (about 1 to 2 mm). Larger calanoids such as *Rhincalanus nasutus* and *Pleuromamma indica* accounted for only a small portion of the calanoid abundance in the upper 100 m of the water column.

Table 3. Minimum to maximum ranges of greatest axial linear dimension of individual cells or chains/colonies (*) (GALD; µm) and microzooplankton grazing rates (γ; d^{-1}) on phyto plankton genera

Genus	GALD	γ
Small dinoflagellates	6.5–11	0.95–1.25
Pyramimonas	8–10	0.98–1.27
Rhodomonas	9.5–12.5	0.85–1.25
Emiliana	10–14	0.51–0.82
Navicula	12–18	0.78–1.10
Nitzschia	24–36	0.50–0.84
Thalassiosira	22–39	0.46–0.86
Gymnodinium	40–56	0.16–0.34
Rhizosolenia	50–102	0.30–0.64
Leptocylindrus	300–450*	0.05–0.45
Pseudonitzschia	330–470*	0.08–0.32

Nano- and microzooplankton grazing on picoplankton

Cell division rates (μ) of heterotrophic bacteria were moderately high (0.61 to 0.72 d^{-1} in the Red Sea and 0.86 to 1.30 d^{-1} in the Gulf of Aqaba) and were roughly balanced by grazing (γ = 0.73 to 0.89 d^{-1} in the Red Sea and 0.75 to 1.06 d^{-1} in the Gulf of Aqaba). There was no effect of nutrient addition on bacterial growth or grazing. The growth rates of bacteria in the dilution experiments were higher than those (<0.15 d^{-1}) obtained by *in situ* incorporation of ^{14}C-labelled leucine (Grossart & Simon 2002). This difference between the dilution method and tracer techniques has also been observed elsewhere, and has not yet been explained satisfactorily.

Neither *Synechococcus* spp. nor ultraphytoplankton showed a response to nutrient addition in either system. For *Synechococcus* spp., moderate growth and grazing rates could only be determined for 1 station in the Red Sea (Stn 147, μ = 0.64 d^{-1}; γ = 0.19 d^{-1}), while data scatter permitted no calculation for the other stations. Ultraphytoplankton responded to grazing pressure in both stations of the Red Sea (γ = 0.72 to 1.3 d^{-1}), but not in the Gulf of Aqaba.

Microzooplankton grazing on nano- and microphytoplankton

The grazer-removal experiments provided microzooplankton grazing rates on phytoplankton species ranging from ca. 6.5 to 225 µm particle length (GALD) and from 77 to 15 000 µm^3 cell volume. Grazing rates declined with increasing algal size, but were high throughout the entire range of phytoplankton sizes (Table 3; for further data see Sommer 2000). The best fit was obtained with linear regressions of the grazing rate (γ; d^{-1}) on log GALD (Table 4). Other size parameters (cell volume, ESD) provided poorer fits, but the trends were always similar. Grazing rates decreased with increasing size of algae. Differences between the experiments and the sites (Red Sea, Gulf of Aqaba) were analysed by ANOVA with log GALD as covariate. Both ANOVAs showed marginally insignificant effects of site (F-ratio = 3.136; p = 0.0868) and experiment (F-ratio = 2.448; p = 0.0845), but highly significant effects of log GALD (p < 0.0001). The small differences between the different experiments are plausible because of a very restricted range of microzooplankton abundances in the grazed treatments: nauplii 10 to 18 ind. l^{-1}; tintinnids 20 to 42 ind. l^{-1}; *Strombilidium* spp. 13 to 55 ind. l^{-1}; small unidentified ciliates 100 to 260 ind. l^{-1} (mean values for the grazer treatment; for further details see Sommer 2000).

Table 4. Regression of grazing rates by microzooplankton on greatest axial linear dimension (GALD) of phytoplankton (g = a.GALD^b). n: number of cases

Region; date	Stn	a	b	r^2	n	p
Southern Gulf; 21 Feb	118	1.99	−0.30	0.50	8	0.0325
Red Sea; 24 Feb	132	2.06	−0.30	0.78	8	0.0039
Red Sea; 27 Feb	145	3.88	−0.48	0.96	8	0.0001
Southern Gulf; 2 Mar	152	2.11	−0.40	0.76	8	0.0050
Pooled data		2.73	−0.41	0.69	32	<0.00001

Mesozooplankton grazing

Grazing by mesozooplankton fell into 2 categories of size preferences. Microphageous zooplankton have had the highest per capita clearance rates on bacteria (Appendicularia, Ostracoda) or on 3 µm algae (*Doliolum* spp.). Macrophageous zooplankton included all copepods studied and showed the highest per capita clearance rates for the largest (*Rhincalanus nasutus*) or second-largest (*Calanus* sp. and small calanoids) algal size category (Table 5). Animal sizes in the experiments were ca. 3.5 to 4 mm for *R. nasutus*, 3.5 mm for the appendicularians, 2.5 mm for *Doliolum* spp., 2.3 mm for *Calanus* sp., 1.5 mm for the ostracods, and 1.1 mm for the small calanoid copepods. Copepod lengths were measured from the front end of the head to the telson without taking the appendages into account; appendicularian lengths are trunk lengths without tail. The average carbon content of the different zooplankton groups was: small calanoids 4.36 ± 1.02 (SD) µgC ind.$^{-1}$; *Calanus* sp. 35.32 ± 3.78 µgC ind.$^{-1}$; Appendicularia 11.3 ± 2.3 µgC ind.$^{-1}$; *Rhincalanus* 73.3 ± 10.8 µgC ind.$^{-1}$; *Doliolum* 3.38 ± 0.94 µgC ind.$^{-1}$; Ostracods 25.87 ± 3.8 µgC ind.$^{-1}$.

Calculation of total community clearance rates (1 m^{-3} d^{-1}) from species-specific individual rates and species abundances could only be performed imperfectly, because of some mismatch between the animal taxa used in the grazing experiments and the most abundant groups (Fig. 2). Moreover, the majority of *in situ* zooplankton individuals were much smaller than the experimental individuals. Thus, assumptions about taxonomic/functional analogy and a size correction were needed. It was assumed that both the category 'calanoids' and the category 'copepodids' in Fig. 2 were best represented by the category 'small calanoids' in the grazing experiments. Phytoplankton grazing by adult cyclopoids and poecilostomatoids was considered negligible, because many of them are considered carnivorous, at least when small phytoplankton cells are dominant (Satour et al. 2000). Naupliar grazing was neglected as well in this calculation, because it was already included in microzooplankton grazing (see foregoing subsection). This means that appendicularians and small calanoids

Table 5. Clearance rate (ml ind.$^{-1}$ d^{-1}) of mesozooplankton on different-sized (GALD/ESD in µm) categories of food

Zooplankton	Bacteria (1/0.8 µm)	*Chlorella* spp. (3/2.7 µm)	Small pennate diatoms (15/8.259 µm)	*Thalassiosira* spp. (40/22 µm)	*Nitzschia* spp. (100/18 µm)
Appendicularia	126	113	107	15	3.8
Doliolium spp.	71	86	36	29	17
Ostracoda	19	7.6	7.6	3.8	0.95
Rhincalanus nasutus	0	5.5	10	21	91
Calanus sp.	0	1.2	7.8	39	29
Small calanoids	0	2	9	22	16.5

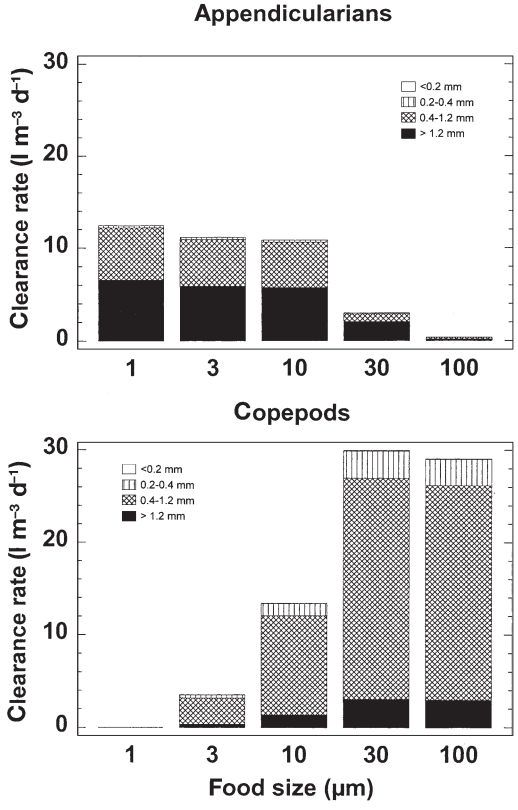

Fig. 3. Clearance rates of appendicularians and calanoid copepods on food particles of different size; cumulative plot of zooplankton size classes (open: <0.2 mm; vertically hatched: 0.2 to 0.4 mm, cross hatched: 0.4 to 1.2 mm, black: >1.2 mm

were considered the only significant mesozooplankton grazers.

Size correction was performed assuming that clearance rates scale with the square of linear body measurements because of the 2-dimensional nature of feeding structures, e.g. appendicularian filters. For the size class <0.2 mm, the calculated per capita clearance rate of 0.2 mm animals was used. For the size class 0.2 to 0.4 mm, the mean of the mean clearance rates of 0.2 and 0.4 mm animals was used. For the size class 0.4 to 1.2 mm, the mean of the clearance rates for 0.4 and 1.2 mm animals was used. For the >1.2 mm size class of small calanoids, the clearance rate of 1.2 mm animals was used, while for appendicularians >1.2 mm, the value for 2.65 mm animals was used (mean length of appendicularians >1.2 mm in the 100 µm net samples).

Based on the mean abundances of the stations and depth intervals in Fig. 2, appendicularian clearance rates of ca. 10 l m^{-3} d^{-1} were found for the smallest food particles and copepod clearance rates of ca. 30 l m^{-3} d^{-1} for large food particles (Fig. 3). This corresponds to instantaneous grazing rates (γ) of 0.01 and 0.03 d^{-1}, respectively.

Copepod lipid composition

The analyses of late copepodid stages (CV) and female *Rhincalanus nasutus* showed that the lipid contents of females and CV stages during the investigation period ranged around 30% of dry mass. For females (18 samples), the lipid content averaged 30.8 ± 4.9%; for the CV stages (5 samples) the mean was 30.3 ± 9.6%. Lipids were dominated by wax esters, which made up 87.3% of total lipids (10 samples). Other lipid classes comprised triacyglycerols (mean 3.2%), phospholipids (mean 9.1%) and cholesterol (0.3%). The principal fatty acids in the total lipid extract (8 samples) were 18:1(n-9) with 30.7%, 16:1(n-7) with 23.7%, 16:2 with 8.5% and 20:5(n-3) with 5.5% for females. These percentages were very similar to those of the CV stages (2 samples). The fatty alcohols consisted mainly of 2 shorter-chain components, 16:0 with 78.5% and 14:0 with 21% in the females, and 16:0 with 81.1% and 14:0 with 18.3% in the CV stages, respectively.

DISCUSSION

The summarised grazing data of zooplankton functional groups on phytoplankton functional groups are rough estimates only. Among other sources of error, experimentally obtained grazing-rate data from a few species of mesozooplankton only were extrapolated to functional groups, ignoring the small size classes. Moreover, stations from which the material for the different shipboard experiments was obtained and stations for the abundance samples did not always match because of logistic constraints. Nevertheless, the trends are sufficiently obvious to permit some clear semi-quantitative conclusions about overall grazing pressure and the relative importance of different zooplankton functional groups of zooplankton (Fig. 4).

A further methodological problem lies in the incubation time of the Landry et al. (1995)-type dilution experiments (36 h) that was needed to achieve a statistically significant response of the larger components of the microbial food web. A shorter incubation time (e.g. 6 h) would have reduced the bottle artifacts (e.g. wall growth), influencing bacterial growth rates, but incubation times <6 h would have missed any diel effects. Bacterial growth rates measured by the dilution technique were higher and clearly better in balance with grazing rates than the extremely low estimates obtained from leucine-uptake measurements (Grossart & Simon 2002). Calculating growth rates from the uptake of 1 substrate only involves some risky assumptions, which might not always apply.

The calculated grazing rates on bacteria and medium-sized phytoplankton were rather high, but

low or even undetectable for the picoplanktonic cyanobacteria *Synechococcus* spp. For heterotrophic bacteria and medium-sized algae, the system appears highly dynamic in spite of low nutrient levels and low phytoplankton biomass. In fact, calculated bacterial growth rates were in the middle of the range estimated for the same season in the slightly more eutrophic central Red Sea using metabolic inhibitors (0.34 to 2.3 d^{-1}: Weisse 1989). In order to balance grazing losses, a high production:biomass ratio of phytoplankton is required. This agrees with the high assimilation numbers measured during our cruise (C. Häse & M. Tilzer pers. comm.). High growth rates balanced by high loss rates at a low standing stock is the core of Goldman's (1984) 'spinning wheel' concept for the oligotrophic ocean. He even hypothesised maximal growth rates despite low nutrient concentrations (Goldman et al. 1979). Our dilution experiments have shown that phytoplankton dominated by pico- and small nanoalgae are indeed not limited by nutrients, while some nutrient limitation was found for stations with a higher contribution of large algae. This agrees too with the experiments by Sommer (2000), who found moderate but significant nutrient limitation for phytoplankton species >6 µm; nevertheless, even algae of this size are grazed at high rates. However, the period of deep mixing is the period with the weakest nutrient stress in the Gulf of Aqaba; stronger nutrient stress would be expected in the stratified period (Lindell & Post 1995).

The low growth and grazing rates of *Synechococcus* spp. do not fit into Goldman's (1984) concept and can only tentatively be explained from the available data. Low grazing rates are easiest explained by assuming that *Synechococcus* spp. are either avoided actively or is too large (0.9 to 1.2 µm) for ingestion by heterotrophic nanoflagellates and too small for ciliates. Indeed, heterotrophic flagellates were unusually small in the study area, and a preference for smaller food items (heterotrophic bacteria) might therefore be expected. A control of picoplanktonic cyanobacteria by heterotrophic nanopflagellates does not seem to be a universal rule in the oligotrophic ocean, but seems to vary between sites and seasons. Low grazing rates of flagellates on *Synechococcus* spp. were found by Dolan & Simek (1999) in the western Mediterranean Sea, while high rates were reported by (e.g.) Burkill et al. (1993) for the oligotrophic part of the Indian Ocean and by Sakka et al. (2000) for French Polynesia. But how can the low growth rates despite nutrient sufficiency be explained? Viral lysis is possible, but no proof is available, and it would probably have operated in the experimental bottles as well as *in situ*. Experimental artefacts such as artificial light inhibition are also possible, because algae were arrested at 30% surface irradiance instead of being circulated in the mixed water column. However, any explanation by artefacts would require an additional limiting factor *in situ*, since unrestricted growth and resultant blooms of autotrophic picoplankton were never observed.

Grazing by mesozooplankton is a negligible loss factor for any of their prey, be it bacteria, algae or protozoa. Mesozooplankton grazing rates are ca. 2 orders of magnitude lower than grazing rates by microzooplankton, and much smaller than the scatter of protozoan grazing rates or phytoplankton growth rates estimated. Admittedly, thus far, these estimates rest on many assumptions and abundance data for only 2 stations (data for more stations will become available in the future: R. Böttger-Schnack, S. B. Schnack-Schiel). However, no alternative way of calculating clearance rates and no conceivable level of mesozooplankton spatial variability would lead to estimates indicating that biomass loss due to mesozooplankton grazing is of equal importance to that due to protozoan grazing. It remains an open question to what extent a correction would be necessary it poecilostomatoid and cyclopoid copepods feed significantly on phytoplankton, contrary to our assumption.

Our results add to the well-established evidence that planktonic food webs of oligotrophic seas are dominated by the 'microbial loop' (picoplankton + bacteria + heterotrophic flagellates→ciliates→copepods) instead of the classic food chain (phytoplankton→copepods→

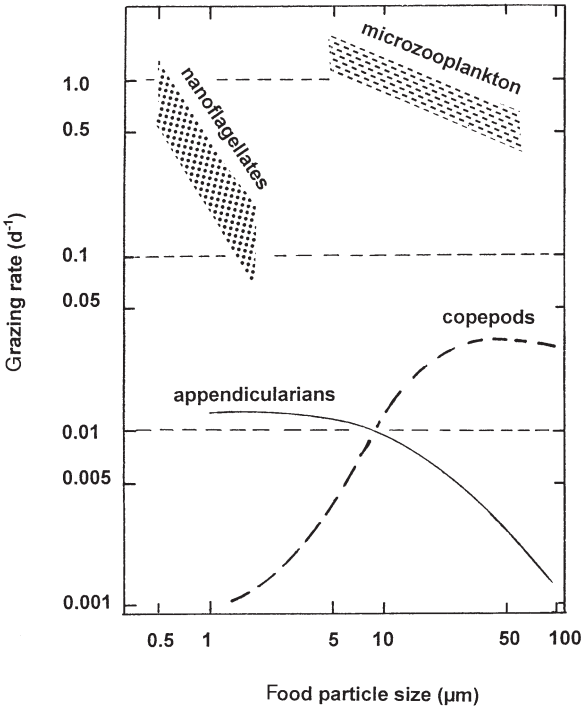

Fig. 4. Double logarithmic plot of the grazing rates of major functional groups of zooplankton on food particle size

fishes). The microbial loop has been proposed as a second major pathway of energy and carbon flow in the pelagic food web (Pomeroy 1974, Sieburth & Davis 1982, Azam et al. 1983). Because of the predominance of picophytoplankton in the oligotrophic ocean (Raven 1986, Stockner & Antia 1986) and the inability of copepods to feed on picoplankton, it is assumed that the microbial loop dominates over the classic food chain in oligotrophic systems (Sanders et al. 1992, Caron et al. 1995, 1999, Reckermann & Veldhuis 1997).

In addition, we have found that pelagic tunicates are more important grazers of pico- and smaller nanoplankton than are copepods within the size range of dominant phytoplankton in the Red Sea. Because of their high efficiency in capturing extremely small food particles, their high clearance rates, and their high intrinsic growth rates (Heron 1972, Deibel 1982a,b, Crocker et al. 1991, Bochdansky & Deibel 1997, Bone et al. 1997), it might be expected that tunicates could play an important role at least locally under suitable conditions. Therefore, we suggest that picoplankton feeding by tunicates should be considered a third major pathway in the pelagic food web.

The inability of copepods to feed on picoplankton and small (<5 µm) nanoplankton forces them to rely on protozoans as a major food source or on episodic blooms of larger algae. There was evidence of diatom-feeding by the strong signal of the fatty acid 16:1(n-7) (e.g. Graeve et al. 1994). This contrasts with a seasonal study of copepod gut contents at a station off Aqaba (Al-Najjar 2000), which did not find the diatom marker fucoxanthin, except in 1 sample of cyclopoid copepods on 7 March 1999 (7.26 ng ind.$^{-1}$). However, the 4 wk sampling regime of Al-Najjar's study was insufficient to detect episodic feeding events; lipid analysis would seem to provide more reliable information. Lipid composition is the result of dietary inputs over several weeks to months, depending on the life cycle of the species concerned.

In conclusion, phytoplankton grazing in the northern Red Sea and in the Gulf of Aqaba during the spring period is clearly dominated by microzooplankton as a result of the small size of the phytoplankton available. Appendicularians also feed on these algae, but are of less importance than microzooplankton. Copepods are the dominant mesozooplankton by number and biomass, but they occupy the third rather than the second trophic level.

Acknowledgements. Financial support by the DFG (Deutsche Forschungsgemeinschaft) and help by the crew of RV 'Meteor' are gratefully acknowledged. We express our thanks to Professor G. Hempel for the cruise leadership.

LITERATURE CITED

Al-Najjar T (2000) The seasonal dynamics and grazing control of phyto- and mesozooplankton in the northern Gulf of Aqaba. PhD thesis, Universität Bremen, Germany

Azam F, Fenchel T, Field JG, Meier-Reil LA, Thingstad F (1983) The ecological role of water column microbes in the sea. Mar Ecol Prog Ser 10:257–263

Bochdansky AB, Deibel D (1997) Functional feeding response and behavioral ecology of *Oikopleura vanhoeffeni* (Appendicularia, Tunicata). J Exp Mar Biol Ecol 233: 181–211

Bone Q, Braconnot JC, Carre C, Ryan KP (1997) On the filter-feeding of *Doliolum* (Tunicata: Thaliacea). J Exp Mar Biol Ecol 179:179–193

Böttger-Schnack R (1995) Summer distribution of micro- and small mesozooplankton in the Red Sea and Gulf of Aden, with special reference to non-calanoid copepods. Mar Ecol Prog Ser 118:81–102

Burkill PH, Leakey RJG, Owens NJP, Mantoura RFC (1993) *Synechococcus* and its importance to the microbial food-web in the northwestern Indian Ocean. Deep-Sea Res Part II 40:773–782

Caron DA, Cam HG, Kremer P, Lessard EJ and 6 others (1995) The contribution of microorganisms to particulate carbon and nitrogen in surface waters of the Sargasso Sea near Bermuda. Deep-Sea Res 42:943–972

Caron DA, Peele ER, Lim EL, Dennett MR (1999) Picoplankton and nanoplankton and their trophic coupling in surface waters of the Sargasso Sea south of Bermuda. Limnol Oceanogr 44:259–272

Crocker KM, Alldredge AL, Steinberg DK (1991) Feeding rates of the doliolid, *Dolioletta gegenbauri*, on diatoms and bacteria. J Plankton Res 13:77–82

Deibel D (1982a) Laboratory determined mortality, fecundity and growth rates of *Thalia democratica* Forskal and *Dolioletta gegenbauri* Uljanin (Tunicata, Thaliacea). J Plankton Res 4:143–153

Deibel D (1982b) Laboratory-measured grazing and ingestion rates of the salp, *Thalia democratica* Forksal and *Dolioletta gegenbauri* Uljanin (Tunicata, Thaliacea). J Plankton Res 4:189–201

Dolan JR, Simek K (1999) Diel periodicity in *Synechococcus* populations and grazing by heterotrophic nanoflagellates: analysis of food vacuole contents. Limnol Oceanogr 44: 1565–1570

Dusenberry JA, Frankel SL (1994) Increasing the sensitivity of FACScan flow cytometer to study oceanic picoplankton. Limnol Oceanogr 39:206–209

Folch J, Lees M, Sloane-Stanley GH (1957) A simple method for the isolation and purification of total lipids from animal tissue. J Biol Chem 226:497–509

Fraser AJ, Tocher DR, Sargent JR (1985) Thin-layer chromatography—flame ionization detection and the quantification of marine neutral lipids and phospholipids. J Exp Mar Biol Ecol 88:91–100

Genin A, Lazar B, Brenner S (1995) Vertical mixing and coral death in the Red Sea following the eruption of Mount Pinatubo. Nature 377:507–510

Goldman JC (1984) Oceanic nutrient cycles. In: Fasham MJ (ed) Flows of energy and materials in marine ecosystems: theory and practice. Plenum Press, London, p 137–170

Goldman JC, McCarthy JJ, Peavey DG (1979) Growth rate influence on the chemical composition of phytoplankton in oceanic waters. Nature 279:210–215

Graeve M, Kattner G, Hagen W (1994) Diet-induced changes in the fatty acid composition of Arctic herbivorous cope-

pods: experimental evidence of trophic markers. J Exp Mar Biol Ecol 182:97–110
Grossart HP, Simon M (2002) Bakterioplankton dynamics in the Gulf of Aqaba and in the northern Red Sea in early spring. Mar Ecol Prog Ser 239:263–276
Hagen W (2000) Lipids. In: Harris R, Wiebe P, Lenz J, Skjoldal HR, Huntley M (eds) ICES zooplankton methodology manual, Academic Press, San Diego, p 113–119
Haney JF (1971) An *in situ* method for the measurement of zooplankton grazing rates. Limnol Oceanogr 16:970–977
Heron AC (1972) Population ecology of a colonizing species: the pelagic tunicate *Thalia democratica*. Oecologia 10: 269–293
Kattner G, Fricke HSG (1986) Simple gas-liquid chromatographic method for the simultaneous determination of fatty acids and alcohols in wax esters of marine organisms. J Chromatogr 361:263–268
Kattner G, Graeve M, Hagen W (1994) Ontogenetic and seasonal changes in liquid and fatty acid/alcohol compositions of the dominant Antarctic copepods *Calanoides propinquus*, *Calanus acutus* and *Rhincalanus gigas*. Mar Biol 118:637–644
Kimor B, Golandsky B (1977) Microplankton of the Gulf of Elat: aspects of seasonal and bathymetric distribution. Mar Biol 42:55–67
Klinker J, Reiss Z, Kropach C, Levanon J, Harpaz H, Shapiro Y (1978) Nutrients and biomass distribution in the Gulf of Aqaba (Elat), Red Sea. Mar Biol 45:53–64
Landry MR, Hassett RP (1982) Estimating the grazing impact of marine micro-zooplankton. Mar Biol 67:283–288
Landry MR, Kirshtein J, Constantinou J (1995) A refined dilution technique for measuring the community grazing impact of microzooplankton, with experimental tests in the central equatorial Pacific. Mar Ecol Prog Ser 120: 53–63
Li H, Veldhuis MJW, Post AF (1998) Alkaline phosphatase activities among planktonic communities in the northern Red Sea. Mar Ecol Prog Ser 173:107–115
Li WKW, Zohary T, Jacobi YZ, Wood AM (1993) Ultraphytoplankton in the eastern Mediterranean Sea: towards deriving phytoplankton from biomass flow cytometric measurements of abundance, fluorescence and light scatter. Mar Ecol Prog Ser 102:79–87
Lindell D, Post AF (1995) Ultraphytoplankton succession is triggered by deep winter mixing in the Gulf of Aqaba (Eilat), Red Sea. Limnol Oceanogr 40:1130–1141
Lund JWG, Kipling C, LeCren ED (1958) The inverted microscope method of estimating algal numbers and the statistical basis of estimations by counting. Hydrobiologia 11: 143–170
Mackey MD, Mackey DJ, Higgins HW, Wright SW (1996) CHEMTAX—a program for estimating class abundance from chemical markers: application to HPLC measurements of phytoplankton. Mar Ecol Prog Ser 144: 265–283
Pomeroy LR (1974) The ocean foodweb, a changing paradigm. BioScience 24:499–504
Raven JA (1986) Physiological consequences of extremely small size for autotrophic organisms in the sea. Can Bull Fish Aquat Sci 214:1–70
Reckermann M, Veldhuis MJW (1997) Trophic interactions between picophytoplankton and micro- and nanozooplankton in the western Arabian Sea during the NE monsoon 1993. Aquat Microb Ecol 12:263–273
Reiss Z, Hottinger L (1984) The Gulf of Aqaba: ecological micropaleontology. Springer-Verlag, Berlin
Sakka A, Legendre L, Gosselin M, Delesalle B (2000) Structure of the oligotrophic planktonic food web under low grazing of heterotrophic bacteria: Takapoto Atoll, French Polynesia. Mar Ecol Prog Ser 197:1–17
Sanders RW, Caron DA, Berninger UG (1992) Relationship between bacteria and heterotrophic nanoplankton in marine and fresh waters: an inter-ecosystem comparison. Mar Ecol Prog Ser 86:1–14
Sautour B, Artigas LF, Delmas D, Herbland A, Laborde P (2000) Grazing impact of micro- and mesozooplankton during a spring situation in coastal waters off the Gironde estuary. J Plankton Res 22:531–552
Sieburth JM, Davis PG (1982) The role of heterotrophic nanoplankton in the grazing and nurturing of planktonic bacteria in the Sargasso and Caribbean Sea. Annu Inst Océanogr 58:285–296
Sommer U (1996) Plankton ecology: the past two decades of progress. Naturwissenschaften 83:293–301
Sommer U (2000) Scarcity of medium-sized phytoplankton in the Red Sea explained by strong bottom-up and weak top-down control. Mar Ecol Prog Ser 197:19–25
Stockner JG, Antia NJ (1986) Algal picoplankton from marine and freshwater ecosystems: a multidisciplinary perspective. Can J Fish Aquat Sci 43:2472–2503
Vaulot D (1989) CYTOPC: processing software for flow cytometric data. Signal Noise 2:8
Weisse T (1989) The microbial loop in the Red Sea: dynamics of pelagic bacteria and heterotrophic nanoflagellates. Mar Ecol Prog Ser 55:241–250
von Stosch HA, Drebes G (1964) Entwicklungsgeschichtliche Untersuchungen an zentrischen Diatomeen. IV. Helgol Wiss Meeresunters 11:209–257
Wolf-Vecht A, Paldor N, Brenner S (1992) Hydrographic indications of advection/convection effects in the Gulf of Eilat. Deep-Sea Res 39:1393–1401
Wright SW, Thomas DP, Marchant HJ, Higgins HW, Mackey MD, Mackey DJ (1996) Analysis of phytoplankton of the Australian sector of the Southern Ocean: comparison of microscopy and size fraction data with interpretations of pigment HPLC data using 'CHEMTAX' matrix factorisation program. Mar Ecol Prog Ser 144:285–298
Yahel G, Post AF, Fabricius K, Marie KD, Vaulot D, Genin A (1998) Phytoplankton distribution and grazing near coral reefs. Limnol Oceanogr 43:551–563

Editorial responsibility: Gotthilf Hempel, Bremen, Germany

Submitted: May 3, 2001; Accepted: January 31, 2002
Proofs received from author(s): July 9, 2002

Vol. 239: 263–276, 2002 | MARINE ECOLOGY PROGRESS SERIES
Mar Ecol Prog Ser | Published August 23

Bacterioplankton dynamics in the Gulf of Aqaba and the northern Red Sea in early spring

Hans-Peter Grossart*, Meinhard Simon

Institute for Chemistry and Biology of the Marine Environment, University of Oldenburg, 26111 Oldenburg, Germany

ABSTRACT: The northern Red Sea, with its northernmost extension the Gulf of Aqaba, is an oligotrophic marine ecosystem, for which the growth and substrate dynamics of the heterotrophic bacterioplankton have not yet been studied. In 1999, we carried out a comprehensive investigation of bacterioplankton growth dynamics in early spring (February/March), a time of year when the Gulf waters are deeply mixed, while permanent stratification prevails in the northern Red Sea. Most of the parameters measured yielded low values (bacterial numbers: 0.5 to 12.8×10^5 ml^{-1}; production: 0.9 to 56.8 ng C l^{-1} h^{-1}; growth rates: <0.01 to 0.15 d^{-1}; turnover rates of dissolved free amino acids, DFAA: 0.008 to 1.35 d^{-1}; glucose: 0.001 to 0.14 d^{-1}; and concentrations of dissolved free neutral monosaccharides: <2 to 86 nM). Glucose was the only monosaccharide detected in 93% of the samples. Concentrations of DFAA ranged from 13.2 to 176 nM, and those of dissolved combined amino acids and neutral monosaccharides from 0.42 to 3.69 µM and 0.05 to 3.31 µM, respectively. Uptake of glucose (as percent of bacterial production) in 93% of the samples was <50%, whereas that of DFAA was much higher, often exceeding 100% (the latter result may have been due to methodological biases). Most of the parameters measured were more variable and covered a wider range in the northern Red Sea than in the Gulf, where vertical patterns were more homogenous. Only concentrations of dissolved free neutral monosaccharides were systematically lower in the northern Red Sea. Bacterial production in this area was significantly correlated with turnover and uptake rates of DFAA, and with glucose turnover rates below 100 m. Aminopeptidase and β-glucosidase activities were fairly similar in both study areas, with means ranging from 19.4 to 29.9 nmol l^{-1} h^{-1}. Whereas aminopeptidase hydrolysis rates were in the same range as values found in other oceanic regions, β-glucosidase hydrolysis rates were much higher, possibly due to the persistence of active β-glucosidase in the dissolved phase, as has been reported for alkaline phosphatase in this area. Analysis of the data indicates that in the northern Red Sea bacterioplankton growth dynamics were mainly controlled by biological processes, whereas in the Gulf hydrographic processes were more important.

KEY WORDS: Bacteria · Bacterial production · Amino acids · Carbohydrates · Turnover rates · Aminopeptidase · Glucosidase · Gulf of Aqaba · Red Sea

INTRODUCTION

The microbial loop (Azam et al. 1983), including heterotrophic and autotrophic picoplankton and mixo- and heterotrophic nanoflagellates, has been shown to be most important in oligotrophic pelagic ecosystems such as the central oceanic gyres in tropical and subtropical regions, which are stratified and thus permanently nutrient-depleted. Most of the flow of energy and nutrient recycling (i.e. regenerated production) in these systems is mediated by trophic compartments of the microbial loop, whereas the participation of larger-sized compartments and thus export production is of relatively low significance (Eppley & Peterson 1979, Li et al. 1992, Buck et al. 1996). However, several studies have indicated that grazing of picoplankton by pelagic tunicates may be another sink, and may shortcut the flux of organic matter from the microbial loop to

*E-mail: hgrossart@icbm.de

higher trophic levels in oligotrophic marine ecosystems (Deibel 1982, Crocker et al. 1991, Acuña et al. 1996, Sommer et al. 2002). As one of the core components of the microbial loop, heterotrophic bacteria have been studied quite extensively in various stratified oceanic regions (Ducklow 1993, 1999, Kirchman et al. 1995, Rich et al. 1996, Goosen et al. 1997, Pedrós-Alió et al. 1999). Detailed simultaneous studies on bacterioplankton growth dynamics (including substrate availability, polymer hydrolysis and turnover and growth response) in these regions, however, are still rare (Christian & Karl 1995, Rich et al. 1996, Keil & Kirchman 1999).

The Red Sea, with its northernmost extension, the Gulf of Aqaba (165 km long × 15 km wide), is one of such highly oligotrophic regions in which autotrophic picoplankton and phytoplankton of <8 µm dominate the total phytoplankton biomass. Chlorophyll *a* (chl *a*) does not exceed 0.8 µg l^{-1} (Lindell & Post 1995) because of strong bottom-up control of phytoplankton growth (Sommer 2000). Whereas the Red Sea is permanently stratified, the Gulf of Aqaba, with a maximum depth of 1800 m, is characterized by deep winter mixing bringing high amounts of inorganic nutrients into the otherwise nutrient-depleted euphotic zone (Wolf-Vecht et al. 1992). Water exchange with the northern Red Sea occurs via the shallow (242 m) Strait of Tiran, with a near-surface inflow into the Gulf and an underlying outflow. Growth dynamics and the composition of the autotrophic picoplankton and bacteria grazed by heterotrophic nanoflagellates have been studied in this region (Weisse 1989, Lindell & Post 1995). Virtually nothing is known, however, about the substrate and growth dynamics of the heterotrophic bacterioplankton. In order to better evaluate and understand the significance of the microbial loop for pelagic trophodynamics in the Red Sea and the Gulf of Aqaba, it is essential to examine bacterioplankton trophodynamics in this area.

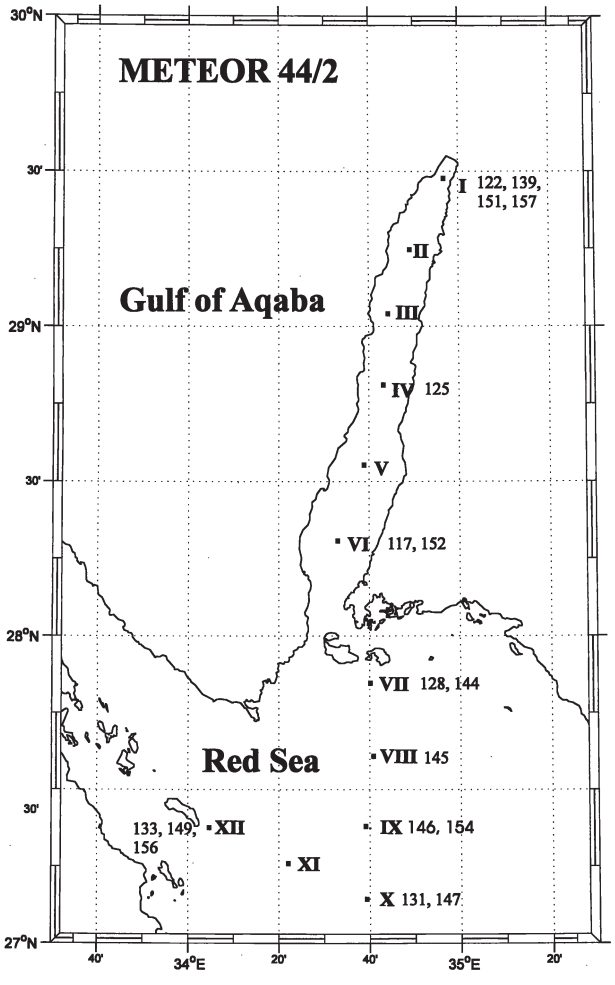

Fig. 1. Map of the study area. Numbers are sampling sites and station nos. as in Table 1

During Cruise M44/2 of RV 'Meteor' we studied substrate and growth dynamics of the heterotrophic bacterioplankton in the northern Red Sea and the Gulf of Aqaba in late February and early March 1999. This gave us the opportunity to compare the typical stratified situation of the northern Red Sea with the deeply mixed Gulf of Aqaba. Further, the simultaneous assessment of phytoplankton growth dynamics and grazing by proto-and metazooplankton enabled us to comprehensively evaluate the significance of the microbial loop during early spring in this region.

MATERIALS AND METHODS

The study was carried out during Cruise M44/2 of RV 'Meteor' between 21 February and 9 March 1999. For details of the hydrography and biology of the Gulf of Aqaba see Reiss & Hottinger (1984), Wolf-Vecht et al. (1992), and Lindell & Post (1995). During the cruise 12 sites were visited, but we sampled only 3 sites of a transect across the Gulf of Aqaba and 5 sites in the northern Red Sea (Fig. 1, Table 1). Several sites were visited at least twice. Water from various depths between the surface and 500 m was collected with 12 l Go-Flo bottles mounted on a CTD rosette from which subsamples were withdrawn into 1 l polyethylene (PE) flasks for further measurements.

Bacterial numbers. Samples for enumerating bacteria were fixed with 2% formalin. Enumeration was done by epifluorescence microscopy according to Porter & Feig (1980). Within 2 h of sampling, 2 to 5 ml were stained with DAPI (4,6-diamidinophenylindole) for 3 to 5 min, filtered through 0.2 µm black Nuclepore filters, and stored frozen at –20°C until enumeration in the laboratory 6 mo later. Bacterial numbers were determined at 1000× magnification with an epifluores-

cence microscope (Axioscope 2, Zeiss) and an image-analysis system (analysSIS, Soft Imaging System). At least 20 view fields were counted to minimize standard deviations (≤10%). We determined 20 size classes between ≤0.2 and 2.0 µm, but ≥85% of all measured bacteria were between 0.2 and 0.4 µm in size.

Bacterial production. Rates of bacterial biomass production were determined by the incorporation of ^{14}C-leucine (Kirchman et al. 1985, Simon & Azam 1989). Subsamples of 10 ml were withdrawn into clean polystyrene test tubes. Triplicates and a formalin-killed control were labelled with ^{14}C-leucine (10.8 GBq mmol^{-1}, Hartmann Analytic) at a final concentration of 10 nM. Incubation was in the dark at *in situ* temperature, and was stopped after 2.5 to 5 h by adding formalin (2% final concentration). After fixation, samples were filtered onto 0.45 µm nitrocellulose filters (Sartorius), rinsed with ice-cold particle-free seawater, and extracted with ice-cold 5% trichloroacetic acid (TCA) for 5 min. After rinsing the extracted filters twice with ice-cold 5% TCA, the filters were dissolved with ethylacetate and radioassayed by liquid scintillation counting. Biomass production was calculated from leucine incorporation rates using a conversion factor of 3.0 kg C (mol leucine)$^{-1}$ (Simon & Azam 1989). The coefficient of variation (CV, standard deviation/mean) of the triplicate measurements usually was <0.10.

Turnover rates of dissolved free amino acids (DFAA) and dissolved free monosaccharides (DFCHO). Turnover rates of a mixture of 16 ^{3}H-amino acids (Amersham, mean specific activity 1.97 GBq mat. C), and of ^{3}H-glucose (specific activity 429 GBq mmol^{-1}, Amersham) were measured basically in the same way as described for measurements of leucine incorporation (see foregoing subsection). Final concentrations of DFAA and added glucose were 0.5 nM, respectively. After stopping the incubation, samples were not extracted by ice-cold TCA, but were filtered directly onto 0.45 µm nitrocellulose filters, rinsed with particle-free seawater and radioassayed. The CV of the triplicate measurements usually was <0.10.

Hydrolytic enzyme activities: Aminopeptidase, α-, β-glucosidase, and chitinase activities of bacteria were measured using fluorogenic substrate analogs (Hoppe 1993). Incubations were performed with L-leucine-methyl coumarinylamide (Fluka) for determination of aminopeptidase activity, 4-methyl-umbelliferyl-α- and β-D-glucoside (Sigma) for α- and β-glucosidase activity, and 4-methyl-umbelliferyl-β-D-glucosaminide (Sigma) for chitinase activity. Hydrolysis was measured in 20 ml samples at 1 µM final concentration of the respective substrate analog. This concentration assured maximum hydrolysis rates at *in situ* temperature in the dark, as determined by saturation kinetics. All incubations were run for 2 h in triplicate and a control was killed with paraformaldehyde (4% final conc.). Fluorescence of all assays was measured in a filter fluorometer (TD 700, Turner Design) at 300 to 400 nm excitation and 410 to 610 nm emission. Hydrolytic enzyme activities were calculated after calibration with methyl-coumarinylamide and methyl-umbelliferyl, respectively.

Concentrations of dissolved amino acids and monosaccharides: Concentrations of DFAA were analyzed by high-performance liquid chromatography (HPLC) after ortho-phthaldialdehyde derivatization according to Lindroth & Mopper (1979) as modified by Simon & Rosenstock (1992). After prefiltration through a 0.2 µm tuffrin filter (Gelman Acrodisc) with low protein-binding capacitiy, samples were stored frozen at –20°C until analysis with a Thermo Separation Product HPLC system after 16 to 17 mo. Dissolved combined amino acids (DCAA) were analyzed as DFAA after hydrolysis with 6 N HCl at 100°C for 20 h. Concentrations of DFCHO were analyzed by HPLC and pulsed amperometric detection with a DIONEX instrument and a Carbopac PA 10 column according to Mopper et al. (1992) using 20 mM NaOH as eluent. After prefiltration, samples were stored frozen until analysis after 16 to 17 mo. Prior to analysis, samples were desalted by ion-exchange columns (Mopper et al. 1992, Borch & Kirchman 1997). Unavoidable losses

Table 1. Sites, station numbers, dates, and locations of Cruise 44/2 of RV 'Meteor' in the Gulf of Aqaba and northern Red Sea between 21 February and 9 March 1999. Station nos. correspond to those in Fig. 1

Region, Site	Stn No.	Date	Location N	Location E
Gulf of Aqaba				
I	122	22 Feb	29° 29.52′	34° 57.00′
	139	26 Feb	29° 29.52′	34° 57.00′
	151	01 Mar	29° 29.46′	34° 57.18′
	157	05 Mar	29° 29.46′	34° 57.06′
IV	125	23 Feb	28° 49.98′	34° 44.04′
VI	117	21 Feb	28° 20.22′	34° 33.06′
	152	02 Mar	28° 20.04′	34° 33.06′
Northern Red Sea				
VII	128	23 Feb	27° 53.04′	34° 40.02′
	144	27 Feb	27° 52.80′	34° 39.96′
VIII	145	27 Feb	27° 39.24′	34° 40.08′
IX	146	27 Feb	27° 24.96′	34° 39.96′
	154	03 Mar	27° 25.08′	34° 40.38′
X	131	24 Feb	27° 11.04′	34° 39.96′
	147	28 Feb	27° 10.98′	34° 39.96′
XII	133	24 Feb	27° 25.02′	34° 04.92′
	149	28 Feb	27° 25.02′	34° 05.04′
	156	04 Mar	27° 24.96′	34° 04.98′

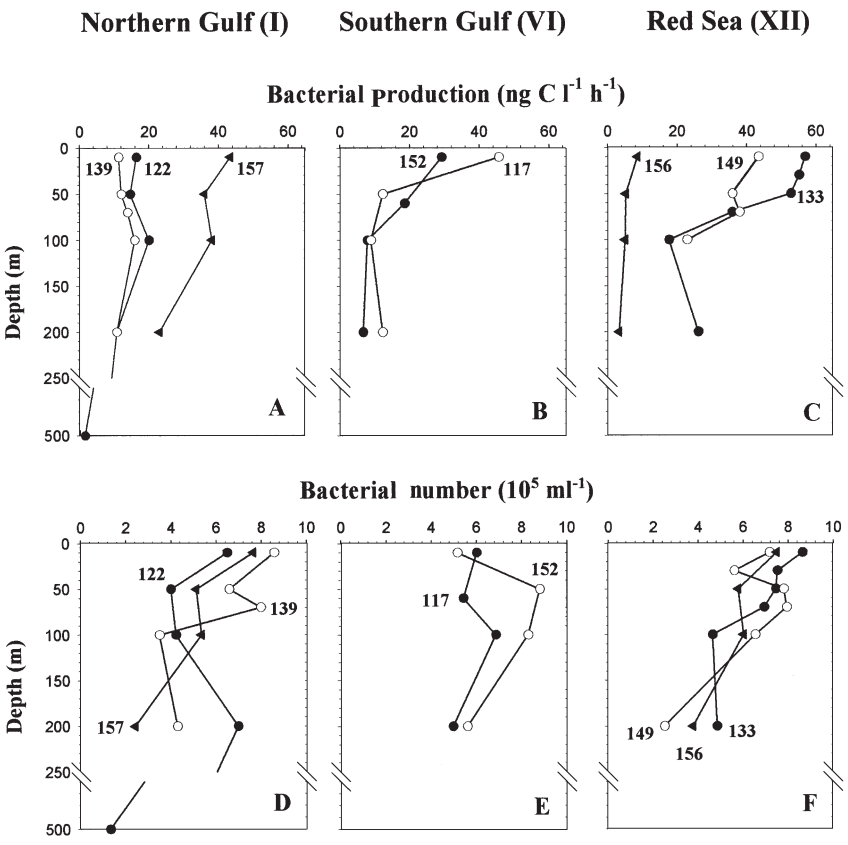

Fig. 2. Bacterial production (A–C) and bacterial numbers (D–F) in northern and southern Gulf of Aqaba and northern Red Sea. Sites, stations and sampling dates as in Table 1

of individual monosaccharides during desalting were corrected for by external standards. Dissolved combined neutral monosaccharides were analyzed as DFCHO after hydrolysis with 0.09 N HCl at 100°C for 20 h (Borch & Kirchman 1997). After hydrolysis, samples were desalted in the same way as those for the DFCHO analysis.

RESULTS

During our study period we encountered the typical hydrographic situation of winter and early spring, with temperatures of 20 to 23°C near the surface and in deep water layers. A strong northeasterly wind (8 to 14 m s^{-1}) prevailed until 27 February. The Gulf exhibited a mixing regime, with an increasing mixing depth towards its northern end near Aqaba, where it reached 300 m in the first few days of our investigation. During an intense convection event on 26 February, the mixing depth increased to 550 m in the northern Gulf. Thereafter it stabilized around 400 m (Plähn et al. 2000). The northern Red Sea was stratified throughout the investigation period, with an increasing stability towards the southern stations. As long as the northeasterly wind prevailed, the mixed layer in the northern Red Sea remained well-mixed in the upper 50 to 100 m and allowed an input of nutrients from deeper layers by turbulent diffusion, as indicated by the vertical distribution of inorganic nutrients such as phosphate (M. Badran unpubl. data). When the wind ceased after 28 February, the upper 100 m became well-stratified with a mixed layer of <50 m, such that the nutrient input from deeper layers ceased. The different stratification regimes were also reflected in the different vertical and horizontal distributions of chl *a*. In the northern Gulf the vertical distribution of chl *a* was homogenous and low (≤0.25 µg chl *a* l^{-1}), whereas towards the southern part of the Gulf and the northern Red Sea, elevated concentrations of up to 0.43 µg chl *a* l^{-1} occurred in the mixed layer (N. Stambler unpubl. data).

Bacterioplankton growth dynamics

Bacterioplankton biomass production exhibited pronounced differences in the Gulf of Aqaba and the

northern Red Sea and thus was consistent with the distribution of chl *a*. At the northernmost site in the Gulf (Site I), bacterial production remained below 43.4 ng C l^{-1} h^{-1} in the mixed layer and did not show pronounced vertical variations (Fig. 2A). During the intense mixing event on 26 February (Stn 139), the lowest values occurred. During the first 10 d, bacterial production decreased in the upper 200 m, but exhibited highest values at our last visit to this station on 5 March (Stn 157). In the southern Gulf at Site VI, rates of bacterial production continuously decreased with increasing depth in the upper 100 m (Fig. 2B). The values at this site were rather similar to bacterial production rates and vertical patterns in the upper 100 m at Site VII (26.4 to 39.6 ng C l^{-1} h^{-1}, Stn 128), the northernmost location in the Red Sea (Fig. 1). At Site VI, the upper 200 m already showed signatures of the northern Red Sea, as indicated by salinity values, and thus suggested an influence of the inflowing Red Sea, surface water on bacterial production at this site. In the northern Red Sea, bacterial production rates in the first week of the investigation were much higher than in the northern Gulf. At Site XII (Stn 133) the highest rates of bacterial production were recorded, reaching 56.8 ng C l^{-1} h^{-1} (Fig. 2C). In contrast to the Gulf, rates of bacterial production decreased substantially in the northern Red Sea in the second week, except at Site XII, where bacterial production rates strongly decreased only on 4 March (Stn 156). Despite the spatio-temporal differences, mean values of bacterial production in both study areas were similar (Table 2).

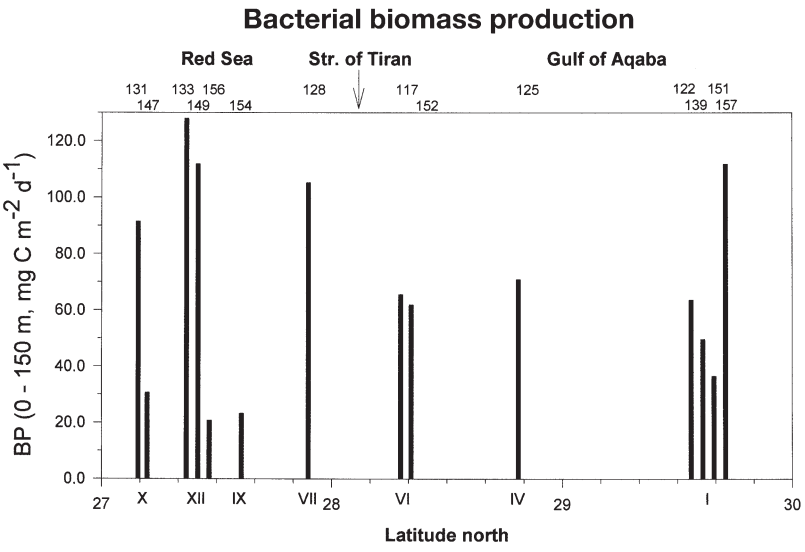

Fig. 3. Bacterial biomass production (BP) integrated over the upper 150 in the Gulf of Aqaba and northern Red Sea. Sites and dates (bottom abscissa) and station nos. (top abscissa) as in Table 1

In order to assess bacterial production (m^{-2} d^{-1}) we integrated bacterial production rates over the upper 150 m and converted hourly rates to daily rates by multiplication with a factor of 24. Rates ranged from 20.8 to 128 mg C m^{-2} d^{-1}. Highest values (exceeding 90 mg C m^{-2} d^{-1}) occurred in the northern Red Sea until 28 February and in the Gulf at Site I on March 5 (Fig. 3). On our first visit to the northern Red Sea on 23 and 24 February, rates were substantially higher than in the Gulf. When we revisited the northern Red Sea thereafter, rates were much reduced, except at Site XII (Stn 149). While rates at Site VI in the southern Gulf were fairly similar on 21 February and 2 March, rates at Site I in the Gulf increased 3-fold between 1 and 5 March.

Bacterial numbers ranged between 0.9 and 12.8 × 10^5 ml^{-1} and did not exhibit pronounced differences between the Gulf and the northern Red Sea. Horizontal variability in the Gulf was higher than in the northern Red Sea, where numbers, however, consistently decreased with increasing depth (Fig. 2D–F). Bacterial numbers did not show any significant correlation with bacterial production.

Bacterial growth rates were calculated from bacterial production rates and cell numbers, assuming expo-

Table 2. Mean (±SD) bacterial production (BP), concentrations of dissolved free (DFAA) and combined (DCAA) amino acids and dissolved free neutral (DFCHO) and dissolved combined fee neutral (DCCHO) monosaccharides, turnover rates of DFAA and glucose, uptake of DFAA and DFCHO as percentage of BP, aminopeptidase and β-glucosidase hydrolysis rates in Gulf of Aqaba and northern Red Sea

Parameter	Gulf of Aqaba	Northern Red Sea
Bacterial production (ng C l^{-1} h^{-1})	17.3 ± 10.6	21.3 ± 17.6
DFAA (nM)	47.9 ± 24.0	69.3 ± 38.1
DCAA (µM)	1.44 ± 0.85	1.37 ± 0.78
DFCHO (nM)	18.0 ± 22.4	3.3 ± 6.0
DCCHO (µM)	0.57 ± 0.60	0.66 ± 0.48
DFAA turnover rate (d^{-1})	0.38 ± 0.32	0.45 ± 0.36
Glucose turnover rate (d^{-1})	0.045 ± 0.029	0.049 ± 0.032
DFAA uptake (% BP)	242.9 ± 216.5	361.7 ± 282.4
DFCHO uptake (% BP)	19.5 ± 32.5	3.1 ± 5.7
Aminopeptidase (nmol l^{-1} h^{-1})	23.2 ± 21.9	29.9 ± 28.2
β-glucosidase (nmol l^{-1} h^{-1})	19.4 ± 24.9	22.7 ± 16.6

nential growth. Rates ranged between <0.01 and 0.15 d^{-1}, and thus were rather low. Their vertical and spatial distribution followed that of bacterial production at all stations except Stn 157. While in the northern Gulf values increased towards the end of our study period, they decreased in the northern Red Sea.

Turnover of amino acids and monosaccharides

Turnover rates of DFAA ranged between <0.05 and 1.35 d^{-1} (Fig. 4A–C), with a mean of 0.38 and 0.45 d^{-1} in the Gulf and the northern Red Sea, respectively (Table 2). At Site I in the northern Gulf, temporal patterns followed that of bacterial production, with high values at the beginning and the end of our investigation period. In the northern Red Sea, at Site XII lowest DFAA turnover rates were measured on our last visit (Stn 156). Comparing all data, there was a trend of reduced DFAA turnover rates in the northern Red Sea below 100 m (0 to 100 m: mean of 0.53 ± 0.36; >100 m: mean of 0.13 ± 0.12). In the Gulf this trend was less pronounced (0 to 100 m: mean of 0.41 ± 0.33; >100 m: mean of 0.30 ± 0.29). Bacterial production rates were significantly correlated with DFAA turnover rates in the northern Red Sea ($r^2 = 0.55$, $p < 0.05$) but not in the Gulf. Correlations were closer below 100 m ($r^2 = 0.71$) than above ($r^2 = 0.46$).

Turnover rates of glucose ranged between <0.005 and 0.14 d^{-1} (Fig. 4D–F), with a mean of 0.045 and 0.049 d^{-1} in the Gulf and the northern Red Sea, respectively (Table 2), and thus were 1 order of magnitude lower than those of DFAA. Vertical and spatial patterns in general followed that of DFAA (Fig. 4D–C) turnover rates (Fig. 4D–F), as demonstrated by the highly significant correlation between both parameters ($r^2 = 0.66$, $p < 0.05$). Bacterial production rates were significantly correlated to glucose turnover rates in the northern Red Sea below 100 m ($r^2 = 0.55$, $p < 0.05$), but not above 100 m and not in the Gulf.

Concentrations of DFAA ranged between 13 and 176 nM (Fig. 5A-C), with means in the Gulf and the northern Red Sea of 47.9 and 69.3 nM, respectively (Table 2). In the Gulf, the vertical distribution was more homogenous than in the northern Red Sea. Highest concentrations in the northern Gulf occurred during the convection event on 26 February (Stn 139). Thereafter, concentrations decreased again, showing an inverse trend to the temporal patterns of bacterial production (Fig. 2A). Particularly high values of 70 to

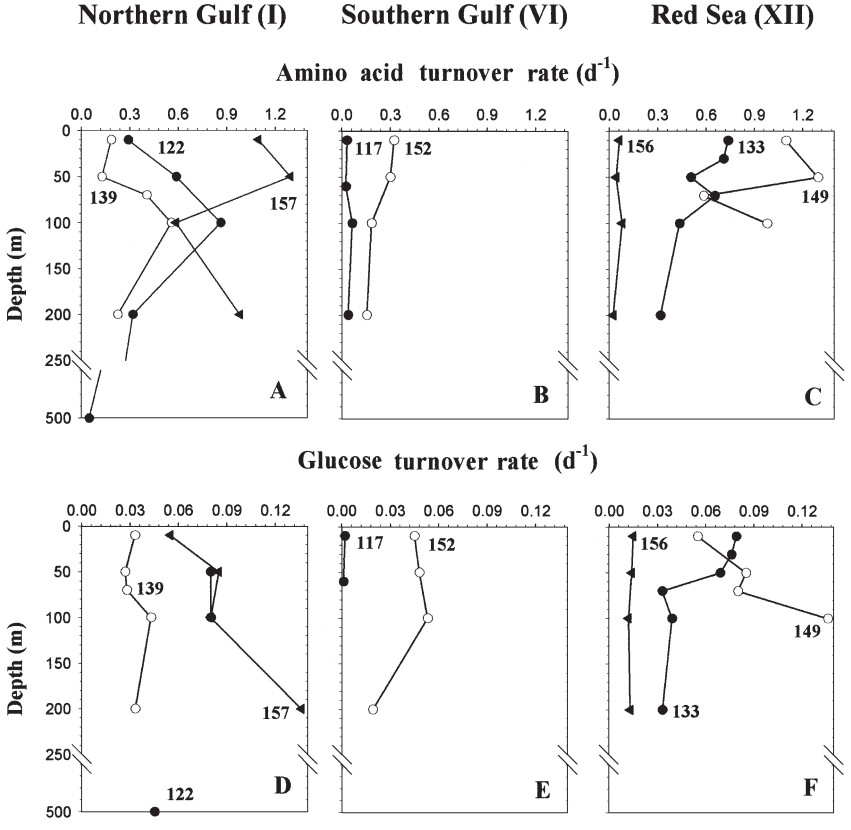

Fig. 4. Amino acid turnover rate (A–C) and glucose turnover rate (D–F) in the northern and southern Gulf of Aqaba and northern Red Sea. Sites, stations and sampling dates as in Table 1

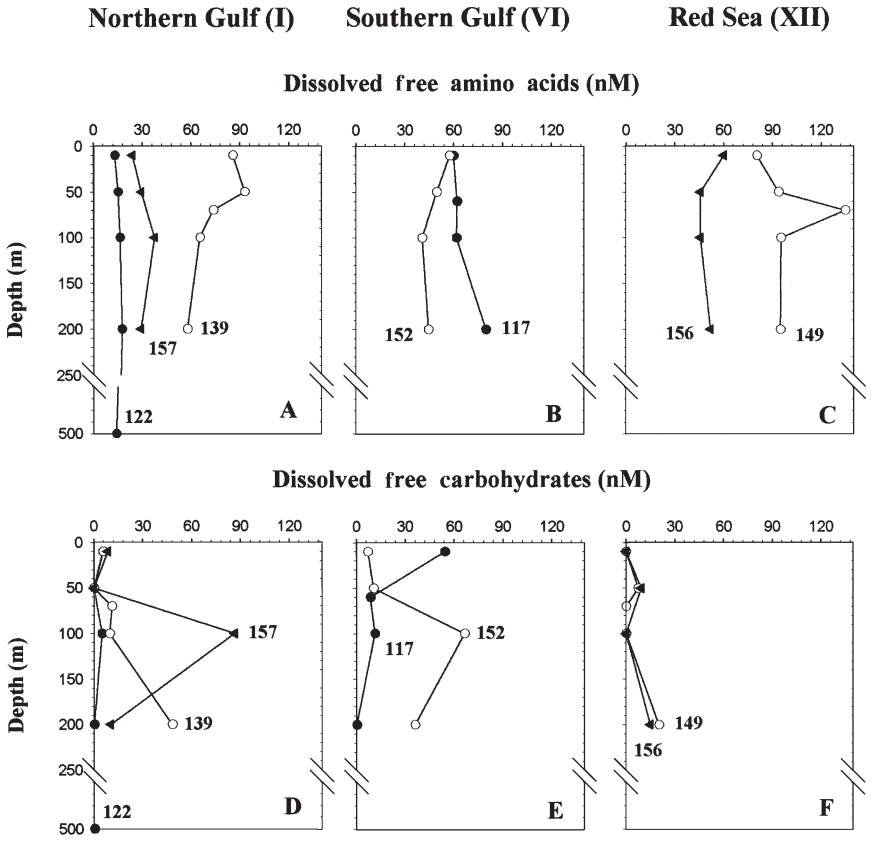

Fig. 5. Dissolved free amino acids (A–C) and dissolved free neutral monosaccharides (D–F) in the northern and southern Gulf of Aqaba and northern Red Sea. Sites, stations and sampling dates as in Table 1

130 nM were recorded in the upper 200 m at Site VII. There was no consistent covariation of DFAA concentrations with any other bacterioplankton-related parameter measured. Glycine+threonine and alanine, followed by aspartate, phenylalanine and valine were the dominant single amino acids in all profiles except Stn 147 and 149, where these amino acids constituted nearly similar amounts.

Concentrations of DFCHO were lower than those of DFAA except in 4 cases. They ranged from below the detection limit (2 nM) to 86 nM and remained <60 nM in 95% of the cases (Fig. 5D–F). In most profiles, the vertical distribution of DFCHO concentrations remained fairly constant, but in some cases, such as at Site I (Stns 139, 151, 157), Site VI (Stn 152) and at Site IX (Stn 154), elevated concentrations occurred at 100 m depth and below. Concentrations of DFCHO in the Red Sea were usually lower than in the Gulf, and were less variable (Table 2). Glucose was the only monosaccharide in 54 of the 58 samples analyzed. In 4 samples galactose and fructose were also detected, but their concentrations did not exceed that of glucose.

Concentrations of DCAA ranged from 0.4 to 3.69 µM (amino acid equivalents: Fig. 6A–C), with means of 1.44 and 1.37 µM in the Gulf and the northern Red Sea, respectively (Table 2). Vertical distributions of DCAA exhibited some variation, with a tendency of increasing concentrations with increasing depth in the Gulf. In the northern Red Sea, only in 2 cases were elevated concentrations recorded at 100 m or below. Alanine, serine, glycince+threonine, valine, aspartate, and glutamate were the dominant amino acids in the DCAA pool (Table 3), but their concentrations exhibited some inconsistent variations among the various stations and depths. In both study areas DCAA dominated total dissolved amino acids by >94%. Concentrations of dissolved combined neutral monosacchorides (DCCHO) ranged from 0.05 to 3.3 µM (monosaccharide equivalents: Fig. 6D–F), with means of 0.57 and 0.66 µM in the Gulf and the northern Red Sea, respectively (Table 2). Vertical patterns of DCCHO concentrations in general remained fairly homogenous, even though in some cases peaks occurred at individual depths. Only in 1 profile, at Site I in the Gulf (Stn 151) and at a few single depths in the northern Red Sea, were concentrations of DCCHO higher than those of DCAA. Glucose was the dominant monosaccharide in all profiles except Stns 117 and 125, and comprised 30 to

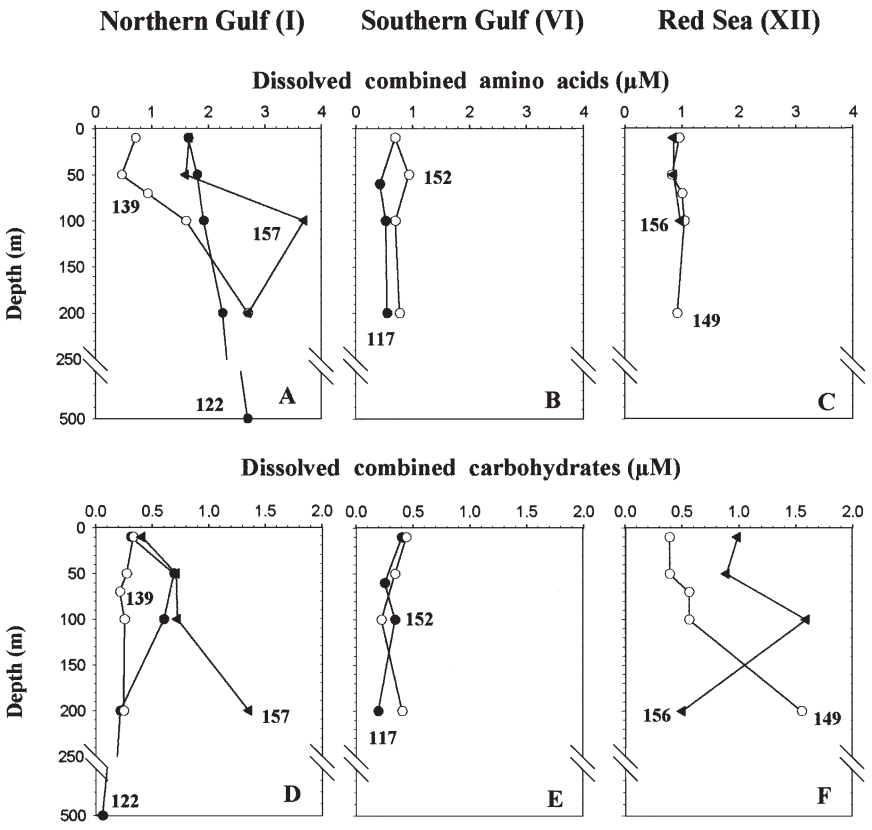

Fig. 6. Dissolved combined amino acids (A–C) and dissolved combined neutral monosaccharides (D–F) in the northern and southern Gulf of Aqaba and northern Red Sea. Sites, stations and sampling dates as in Table 1

75 mol% (mean of 47 and 51 mol%) in the Gulf and the northern Red Sea, respectively (Table 4). Further monosaccharides in the DCCHO pool were galactose, mannose, rhamnose, arabinose, and fucose, which were present in much lower concentrations than glucose. In the profiles of Stns 117 and 125, all the listed monosaccharides were present in fairly equal concentrations, and at some depths, mannose even dominated. DCCHO always dominated the total pool of dissolved neutral monosaccharides by >96%.

Uptake rates of DFAA were calculated from the turnover rates and the concentrations, and expressed in C units, assuming 50 g C per mol amino acid. They were significantly correlated to bacterial production rates in the northern Red Sea ($r^2 = 0.69$, $p < 0.05$), but not in the Gulf. Here we only report uptake rates as percentage of bacterial production. Uptake rates ranged from 20 to >100% of bacterial production, with means of 243 and 362% in the Gulf and the northern Red Sea, respectively (Table 2). Uptake rates of DFCHO were calculated from turnover rates of glucose and concentrations of DFCHO and on the basis of 72 g C per mol monosaccharide. Uptake rates ranged from <5 to >100% of bacterial production, with means of 19.5 and 3.1% in the Gulf and the northern Red Sea, respectively (Table 2).

Aminopeptidase hydrolysis rates ranged from <2 to 210 nmol l^{-1} h^{-1} (Fig. 7A–C), with means of 23.2 and 29.9 nmol l^{-1} h^{-1} in the Gulf and the northern Red Sea, respectively (Table 2). Highest rates were measured in the northern Red Sea at Site VII (Stn 144) and at Site XII (Stn 149) at 50 m. At all stations, aminopeptidase hydrolysis rates exhibited some vertical variabilities, but no general systematic trend or covariation with other parameters occurred. At Site I in the Gulf, rates increased during the first 10 d of our investigation period at 50 m and below, and remained high until the end of our study. In the northern Red Sea, highest rates always occurred in the upper 50 m. Aminopeptidase hydrolysis rates per bacterium ranged from <0.05 to 49.2 amol $cell^{-1}$ h^{-1}. In the northern Red Sea, cell-specific aminopeptidase hydrolysis rates were on average 2.3-fold higher than in the Gulf.

β-glucosidase hydrolysis rates ranged from <2 to 105.2 nmol l^{-1} h^{-1} (Fig. 7D–F), with means of 19.4 and 22.7 nmol l^{-1} h^{-1} in the Gulf and the northern Red Sea, respectively (Table 2). Highest rates occurred in the Gulf, but values exceeding 40 nmol l^{-1} h^{-1} occurred also in the northern Red Sea. In the Gulf at Site I enhanced rates occurred at Stn 139 and 151, simultaneously with reduced rates of bacterial production. As for amino-

peptidase, the vertical and spatial patterns did not covary systematically with those of any other measured parameter. β-Glucosidase hydrolysis rates per bacterium ranged from <0.1 to 43.8 amol cell^{-1} h^{-1}. In the northern Red Sea, cell-specific β-glucosidase hydrolysis rates were on average 2.6-fold higher than in the Gulf. α-glucosidase hydrolysis rates ranged from <1 to 35 nmol l^{-1} h^{-1}, and 80% of the values were below 20 nmol l^{-1} h^{-1} (data not shown). Spatio-temporal patterns did not covary systematically with those of β-glucosidase. Hydrolysis rates of β-glucosidase, however, were higher than that of α-glucosidase in 89% of the measured values. The ratio of aminopetidase/β-glucosidase varied greatly (from <0.1 to 23.5), but 92% of the values were <10. Mean values in the Gulf and the northern Red Sea were 4.6 ± 6.2 and 2.1 ± 2.6, respectively.

Table 3. Composition (mol. %) of dissolved combined amino acids (DCAA) in the Gulf of Aqaba (Stns 122, 139, 151, 157, 125, 117, 152) and northern Red Sea (Stns 128, 154, 131, 147, 149, 156) between 10 and 200 m depth

DCAA	Depth (m)				Mean
	10	50	100	200	
Gulf of Aquaba					
Aspartate	8.52	9.86	9.90	7.84	9.03
Glutamate	8.76	8.48	7.42	7.19	7.96
Serine	22.38	16.62	19.23	19.08	19.33
Histidine	1.55	2.29	2.41	2.81	2.27
Glycine/threonine	12.88	12.82	12.62	9.99	12.08
Arginine	2.00	2.81	2.22	2.38	2.35
Alanine	15.48	16.04	15.54	17.74	16.20
Tyrosine	5.61	4.08	4.14	5.06	4.72
Methionine	2.61	3.83	2.97	3.11	3.13
Valine	11.73	13.12	14.72	13.12	13.17
Phenylalanine	3.74	3.08	2.96	4.53	3.58
Isoleucine	1.53	2.05	1.60	2.53	1.93
Leucine	2.88	4.13	3.69	3.74	3.61
Northern Red Sea					
Aspartate	8.50	8.63	9.22	8.55	8.72
Glutamate	7.77	7.89	8.30	8.27	8.06
Serine	19.72	16.20	15.99	13.87	16.45
Histidine	1.58	2.05	2.06	2.47	2.04
Glycine/threonine	13.66	13.64	14.01	12.65	13.49
Arginine	2.59	3.08	2.62	2.36	2.67
Alanine	17.27	15.88	16.19	18.56	16.98
Tyrosine	6.09	6.57	5.55	6.21	6.10
Methionine	2.85	2.76	3.13	2.47	2.80
Valine	11.87	14.05	13.07	13.30	13.07
Phenylalanine	3.56	4.12	4.17	5.05	4.22
Isoleucine	1.50	1.69	2.01	1.96	1.79
Leucine	2.86	3.15	3.49	3.70	3.30

DISCUSSION

This is the first comprehensive report on bacterioplankton growth and substrate dynamics in the oligotrophic Gulf of Aqaba and the Red Sea. The data were collected during early spring, when the Gulf exhibits a deep and increasing mixing regime towards its northern end compared to the stratified northern Red Sea. Many of our measured parameters (most clearly the rates of bacterial production) reflected the vertical mixing and stratification regimes in the 2 areas, which also showed some temporal variations. In the stratified northern Red Sea, the range of most parameters related to bacterioplankton growth and substrate dynamics was higher than in the deeply mixed Gulf, covering the lowest as well as (often) the highest values. Further, data from the Gulf were not correlated amongst each other, whereas in the northern Red Sea highly significant correlations existed. This suggests that in the Gulf hydrographic properties, i.e. vertical mixing, were more important in controlling bacterioplankton growth dynamics, whereas in the northern Red Sea biological and, in particular, microbial processes were more important.

Bacterioplankton growth and substrate dynamics in the oligotrophic

Table 4. Composition (mol. %) of dissolved combined neutral monosaccharides (DCCHO) in the Gulf of Aqaba (Stns 122, 139, 151, 157, 125, 117, 152) and northern Red Sea (Stns 128, 154, 131, 147, 149, 156) between 10 and 200 m depth

DCCHO	Depth (m)				Mean
	10	50	100	200	
Gulf of Aquaba					
Fucose	5.46	6.26	6.56	5.94	6.06
Rhamnose	7.48	4.78	7.48	7.07	6.70
Arabinose	5.70	4.74	6.58	6.31	5.84
Galactose	18.90	20.29	21.36	19.82	20.09
Glucose	43.18	51.34	44.77	50.82	47.53
Mannose	19.11	12.57	13.78	10.04	13.88
Northern Red Sea					
Fucose	5.36	4.32	5.04	3.36	4.52
Rhamnose	5.85	6.43	0	6.17	4.61
Arabinose	6.41	5.86	7.24	6.53	6.51
Galactose	18.93	18.12	0	15.89	13.23
Glucose	52.08	55.23	46.12	51.35	51.20
Mannose	10.87	8.97	18.82	16.69	13.84

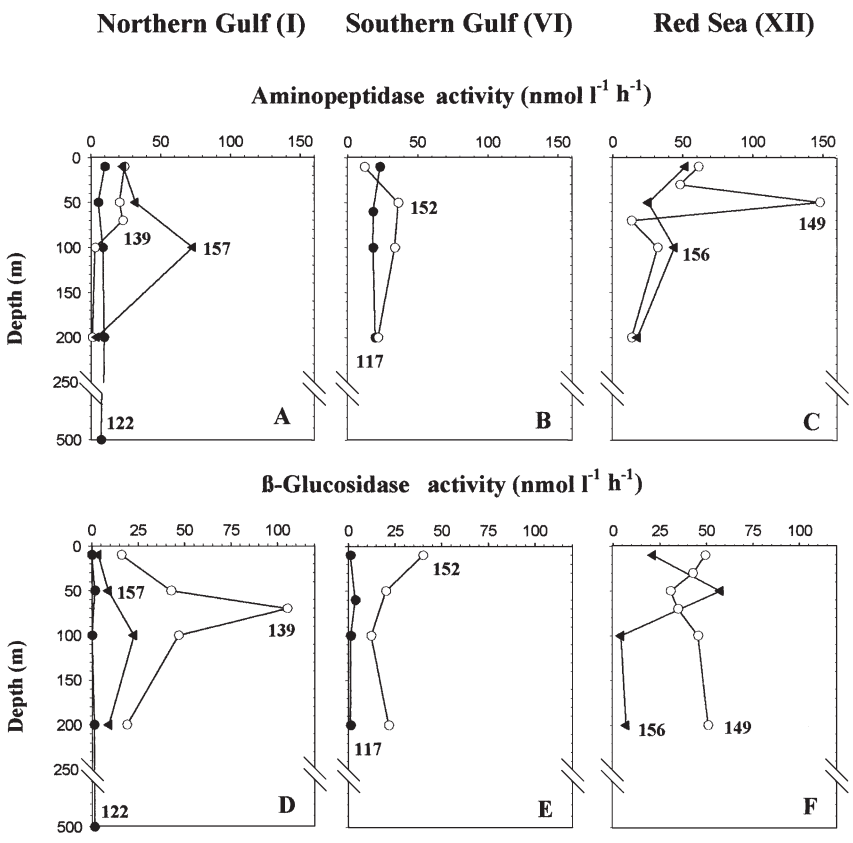

Fig. 7. Aminopeptidase activity (A–C) and β-glucosidase activity (D–F) in the northern and southern Gulf of Aqaba and northern Red Sea. Sites, stations and sampling dates as in Table 1

Gulf of Aqaba and the northern Red Sea are typical of other oceanic regions of similar trophic state. Our integrated bacterial production rates ranged from 21 and 127 mg C m^{-2} d^{-1}, and were in the range of values measured in the Sargasso Sea (11 to 36 mg C m^{-2} d^{-1}: Carlson et al. 1996; 117 mg C m^{-2} d^{-1}: Rivkin & Anderson 1997), the Caribbean Sea (124 mg C m^{-2} d^{-1}: Rivkin & Anderson 1997), the western Indian Ocean (36 to 231 mg C m^{-2} d^{-1}: Goosen et al. 1997), and the equatorial Pacific (72 to 180 mg C m^{-2} d^{-1}: Kirchman et al. 1995). In summer, chl *a* increases 2 to 3 times in the stratified northern Gulf compared to early spring, when we conducted our study (Lindell & Post 1995). Hence, bacterial production rates presumably are also higher in summer, but still in the ranges occurring in other oligotrophic regions. Bacterioplankton growth rates in our study were low (<0.15 d^{-1}) and also well in the range of values reported for other oligotrophic oceanic regions such as the Sargasso Sea, Caribbean Sea, Gulf of Mexico, equatorial and subtropical north Pacific, and the NW Mediterranean Sea (Rivkin & Anderson 1997, Ducklow 1999, Pedrós-Alió et al. 1999).

The ratio of bacterial production to primary production in oligotrophic oceanic regions does not differ from that in other regions, but may vary substantially depending on the season and the given regional situation (Ducklow 1999). During our cruise, for which primary production data are also available (C. Häse et al. unpubl. data) this ratio also varied greatly (from 0.04 to 1.58) and did not reflect systematic differences between the 2 areas. Highest ratios (1.58 and 0.34) were recorded at Sites X (Stn 131) and I (Stn 139), i.e. at stations with the lowest primary production and with high bacterial production rates. The lowest ratios (≤0.08) were recorded at Sites I (Stn 157), IX (Stn 154) and XII (Stn 156) towards the end of the study period, when primary production was 4- to 10-fold higher. Whereas at Site I in the Gulf bacterial production increased parallel to but much less steeply than primary production, bacterial production rates in the northern Red Sea decreased, thus emphasizing further the different hydrographic and trophic conditions in the 2 study areas.

The significance of the microbial loop in the trophodynamics in the Gulf of Aqaba and the northern Red Sea has been demonstrated by the dominance of autotrophic picoplankton and eukaryotic algae <8 µm in the phytoplankton (Lindell & Post 1995). Our data,

together with data on primary production (C. Häse et al. unpubl. data) provide further evidence of the importance of the microbial loop in this oligotrophic ecosystem. Simultaneous studies on the grazing impact of various zooplankton groups showed that heterotrophic nanoflagellates (HNF) were the major consumers of the heterotrophic bacterioplankton, even though appendicularians were shown to consume up to 10% of the bacterioplankton production (Sommer et al. 2002). The bacterioplankton grazing rates by HNF measured by Sommer et al. by the dilution technique were balanced by bacterial growth rates, which were higher than ours by a factor of 6 to 9. The dilution technique requires long (i.e. 24 to 36 h) incubation times, and thus may lead to enhanced bacterial growth due to containment effects. Hence, ambient HNF grazing rates may be lower and closer to the bacterial growth rates we measured. The bacterial grazing rates by appendicularians reported by Sommer et al. (2002) were measured in short-term (15 min) incubations using radiolabeled bacteria, and thus presumably resulted in more realistic values than HNF grazing rates. Hence, the significance of appendicularians as bacterioplankton grazers may even be greater than assumed by Sommer et al. (2002). Under conditions of low concentrations of nanoplankton but relatively enhanced concentrations of picoplankton such as in oligotrophic oceanic regions, appendicularians can be very important consumers of picoplankton (Crocker et al. 1991, Acuña et al. 1996).

During the last 10 to 15 yr, many studies in various pelagic environments have shown that dissolved amino acids and neutral monosaccharides are the most important substrates for bacterioplankton growth (e.g. Kirchman 1990, Keil & Kirchman 1993, 1999, Münster 1993, Kirchman et al. 1994, Rich et al. 1996, 1997, Weiss & Simon 1999, Rosenstock & Simon 2001). Most evidence stems from measurements of turnover and uptake rates of DFAA, dissolved proteins and DFCHO, together with bacterioplankton production. Our study provides further information from an oligotrophic environment not yet studied in this respect. In contrast to most other studies, we collected simultaneous data on concentrations of DFAA, DCAA, DFCHO and DCCHO, turnover rates of DFAA and glucose, and aminopeptidase and glucosidase activities. This comprehensive data set enables us to estimate the relative significance of dissolved amino acids and monosaccharides for bacterioplankton growth simultaneously; this has rarely been done before.

The concentrations of DFAA we measured varied greatly but did not show any consistent covariation with other parameters measured. Compared to values available from other oligo- and mesotrophic oceanic regions they appear to be rather high. Carlucci et al. (1984) and Williams (1986) in the Southern California Bight found concentrations of 3 to 80 nM, which are nearly in the same range as concentrations reported from the subarctic Pacific (5 to 89 nM: Simon 1991). In the Sargasso Sea concentrations of <20 nM were reported by Suttle et al. (1991) and Keil & Kirchman (1999). The only region for which consistently higher values (48 to 233 nM) were reported is the Arctic Ocean (Rich et al. 1997). Because our concentrations appear rather high and the ratio DFAA uptake rates over bacterial production often exceeded 100% (Table 2), we cannot exclude the possibility that our samples became contaminated, possibly during prefiltration. Concentrations of DCAA also varied greatly without any clear-cut relationships to other parameters measured. Only a few comparable data from other oceanic regions such as the Southern California Bight and the Sargasso Sea are available, and these are below 0.75 µM (Williams 1986, Keil & Kirchman 1999).

Nearly all concentrations of DFCHO we found were lower than those of DFAA, and were largely dominated by glucose. In the Gulf, concentrations were substantially higher than in the northern Red Sea, where they were often close to the detection limit. The desalting procedure, in addition to ions, removes monosaccharides, e.g. glucose by 37% (Borch & Kirchman 1997). Therefore, samples with low DFCHO concentrations are affected most strongly by the desalting procedure, which may result in an underestimate of DFCHO concentrations. We do not know if our analyses, in particular those in the northern Red Sea, were affected by this methodological bias. Hence, our DFCHO concentrations are conservative. Comparable data on DFCHO concentrations measured by HPLC from oceanic environments are only available for the equatorial Pacific and the Arctic Ocean. In both these regions, higher concentrations were reported, with means ranging from 28 to 137 nM in the equatorial Pacific (Rich et al. 1996) and from 42 to 90 nM in the Arctic Ocean (Rich et al. 1997). As in our study, glucose dominated the DFCHO pool in these areas, in the Arctic Ocean to a higher extent (75% of total DFCHO) than in the equatorial Pacific (24 to 36%). Because identical methods for the desalting and HPLC analysis were used in all studies, we assume that the data from the various oceanic regions exhibit true differences.

Except for 2 depth profiles between 2 and 4000 m from the equatorial Pacific with a total of 9 isolated values (Skoog & Benner 1997) our DCCHO concentrations are the only ones available from an oceanic environment that have been analyzed by HPLC after HCl hydrolysis. Our data are well in the range of those from the equatorial Pacific in the upper 400 m. The distribution (mol%) of galactose and mannose in both data sets are also in the same range, but we found higher

concentrations of glucose and lower concentrations of rhamnose and fucose than Skoog & Benner in the equatorial Pacific. DCCHO concentrations analyzed by the MBTH (3-methyl-2-benzothiazolinone hydrazone hydrochloride) method after HCl hydrolysis in the equatorial Pacific, the Gulf of Mexico and the North Atlantic (Pakulski & Benner 1994) were higher than our values. Hydrolysis with sulphuric acid yields even higher DCCHO concentrations than with HCl, mobilizing more recalcitrant carbohydrates to the detection as monosaccharides (Pakulski & Benner 1994). This additional fraction of DCCHO, however, presumably is less involved in the biological cycling and not hydrolyzed enzymatically as rapidly as the HCl-hydrolyzable fraction (see below). In most cases, DCCHO concentrations were lower than DCAA concentrations. This is in contrast to the few other reports on simultaneous measurements of concentrations of DCCHO and DCAA from pelagic environments (Williams 1986, Simon et al. 2000), and may be a further indication that our DCAA analyses yielded too high concentrations because of contaminated samples.

Turnover rates of DFAA were closely correlated to those of glucose, but consistently higher. This notion, together with the concentrations and the estimated uptake rates of DFAA and DFCHO, indicates that DFAA were more important than DFCHO as bacterial substrates, irrespective of the possible contamination of the DFAA samples. In support of this, DFAA turnover rates were much better correlated to bacterial production rates, in particular in the northern Red Sea, than DFCHO turnover rates. Our DFAA turnover rates were much lower than values reported for the Sargasso Sea, which ranged from 3 to 8 d^{-1} (Keil & Kirchman 1999), but in the same range as values reported from the Arctic Ocean (0.237 to 0.454 d^{-1}: Rich et al. 1997). In contrast, our DFCHO turnover rates were about 1 order of magnitude lower than values determined in the equatorial Pacific and the Arctic Ocean by Rich et al. (1996, 1997). We do not know whether these differences are due to principal differences in the relative cycling of amino acids and carbohydrates in these ecosystems or whether they reflect seasonal variations. Weiss & Simon (1999) found in the mixed layer of a mesotrophic lake, that from spring to early summer, DFAA turnover rates were much faster than those of DFCHO, whereas in late summer and fall no difference occurred. Hence, we assume that the differences between turnover rates of DFAA and DFCHO in our study area compared to the other oceanic environments reflect seasonal rather than principal regional differences.

Our DFAA uptake rates (which measured net uptake and not the respired fraction) were surprisingly high, often exceeding 100% of bacterial production, presumably due to contaminated DFAA samples (see above). Also Rich et al. (1997), for the Arctic Ocean, reported DFAA uptake rates often greatly exceeding bacterial production. In studies of other oceanic environments, the ratio of DFAA uptake over bacterial production ranges between <20 and ~60% (e.g. Simon 1991, Kirchman et al. 1994, Keil & Kirchman 1999), and presumably is more realistic than the high values we estimated. Nevertheless, these studies, together with ours, emphasize the significance of DFAA as bacterial substrates in oceanic environments. Our uptake rates of DFCHO constituted a lower but still significant fraction of bacterial production. They may have been too low because of a possible underestimate of DFCHO concentrations (see above). The only 2 other studies which determined the significance of DFCHO for bacterial production in oceanic environments found that glucose alone accounted for a higher fraction of bacterial production than ours, ranging from 12 to 122% of bacterial production (Rich et al. 1996, 1997). Only in the Arctic Ocean did Rich et al. (1997) also simultaneously determine the uptake of glucose and DFAA, and found that DFAA were 2 to 9 times more important as a bacterial substrates than glucose, emphasizing further the relatively higher significance of DFAA compared to DFCHO.

Uptake of DFAA and DFCHO accounts for a significant fraction of the carbon demand for bacterial production, but other substrates may be utilized as well. Keil & Kirchman (1993, 1999) and Rosenstock & Simon (2001) showed that dissolved proteins are another important substrate for bacterioplankton growth, and can explain percentages of bacterial production exceeding that achieved on DFAA or DFCHO. Polymeric substrates such as proteins and polysaccharides need to be hydrolyzed prior to bacterial uptake as oligo- or monomers, hence hydrolysis rates of aminopeptidase and glucosidases reflect the potential of bacteria to exploit these polymers as substrates. Our results show that potential hydrolysis rates of aminopeptidase and β-glucosidase, measured at saturating substrate concentrations, were fairly similar, without pronounced differences between the 2 study areas. Whereas the aminopeptidase hydrolysis rates we measured are in the same range as in the few other studies of oceanic environments (Rosso & Azam 1987, Christian & Karl 1995, Hoppe & Ullrich 1999) our β-glucosidase hydrolysis rates were higher than values for the Indian Ocean (Hoppe & Ullrich 1999), or for the subtropical Pacific and the Gerlache Strait in the Southern Ocean (Christian & Karl 1995). They were in the same range as values reported for the equatorial Pacific (Christian & Karl 1995). This suggests that in our study area and the equatorial Pacific, bacteria have a higher potential to exploit DCCHO, which may result in

reduced concentrations of its available fraction. This suggestion is consistent with the relatively low concentrations of HCl-hydrolyzable DCCHO found in our study area and the equatorial Pacific (Pakulski & Benner 1994). Pakulski & Benner found much higher concentrations of HCl-hydrolyzable DCCHO in the Gerlache Strait, where β-glucosidase activities are low. Similar conclusions of inverse relationships between high hydrolytic activities of β-glucosidase as well as aminopeptidase and their substrates were drawn from data on limnetic systems (Simon et al. 2000).

It is intriguing that we found such high activities of β-glucosidase even though turnover rates of glucose, the major hydrolysis product, were rather low. Provided that this finding was not due to methodological biases, (for which we do not have any indication), it suggests that the low DFCHO turnover and uptake was not a response to the high β-glucosidase activity measured. A possible explanation for this puzzling discrepancy is that β-glucosidase activities were not associated with bacterial cells, but persisted in a dissolved and active state despite low DCCHO concentrations. Li et al. (1998) found alkaline phosphatase activities persisted for several months in the Gulf of Aqaba in the dissolved state and constituted 42 to 74% of the total activity. If this were also true for the high β-glucosidase activities measured in the present study, they would not be directly linked to the ambient rather low bacterial requirements for carbohydrates.

In summary, our results give further evidence of the highly oligotrophic status of the Gulf of Aqaba and northern Red Sea. Bacterioplankton growth and substrate dynamics in the stratified northern Red Sea were more variable and appeared to be more driven by biological processes, whereas at the well-mixed northernmost station in the Gulf hydrographic properties appeared to be more important. Our comprehensive findings are comparable to those of the few other studies of oceanic regions with similar trophic regimes. They emphasize the importance of amino acids as substrates for bacterioplankton growth, whereas carbohydrates appear to be less important. On the other hand, the high β-glucosidase activities we found suggest that, at times, carbohydrates may be more important for bacterioplankton growth. In order to better understand the relative significance of amino acids and carbohydrates in the trophodynamics of bacterioplankton growth in such nutrient-depleted oceanic systems, more comprehensive data sets are needed.

Acknowledgements. We would like to thank the crew of RV 'Meteor' for their excellent support on shipboard. We are most grateful to N. Selje, who assisted in nearly all experimental work on board, day and night, and to Birgit Kürzel for the carbohydrate analyses. We appreciate the cooperation of M. Badran, C. Häse, and N. Stambler in making available unpublished data on inorganic nutrients, primary production, and chlorophyll *a*, respectively. This work was supported by grants from the Deutsche Forschungsgemeinschaft awarded to G. Hempel and M.S.

LITERATURE CITED

Acuña JL, Deibel D, Morris CC (1996) Particle capture mechanism of the pelagic tunicate *Oikopleura vanhoeffeni*. Limnol Oceanogr 41:1800–1814

Azam F, Fenchel T, Field JG, Gray JS, Meyer-Reil LA, Thingstad F (1983) The ecological role of water-column microbes in the sea. Mar Ecol Prog Ser 10:257–263

Borch NH, Kirchman DL (1997) Concentration and composition of dissolved combined neutral sugars (polysaccharides) in seawater determined by HPLC-PAD. Mar Chem 57:85–95

Buck KR, Chavez FP, Campbell L (1996) Basin-wide distributions of living carbon components and the inverted trophic pyramid of the central gyre of the North Atlantic Ocean, summer 1993. Aquat Microb Ecol 10:283–298

Carlson C, Ducklow HW, Sleeter TD (1996) Stocks and dynamics of bacterioplankton in the northwestern Sargasso Sea. Deep-Sea Res Part II 43:491–516

Carlucci AF, Craven DB, Henrichs SM (1984) Diel production and microheterotrophic utilization of dissolved free amino acids in waters off southern California. Appl Environ Microbiol 48:165–170

Christian JR, Karl DM (1995) Bacterial ectoenzymes in marine waters: activity ratios and temperature responses in three oceanographic provinces. Limnol Oceanogr 40:1042–1049

Crocker KM, Alldredge AL, Steinberg DK (1991) Feeding rates of the doliolid, *Dolioletta gegenbauri*, on diatoms and bacteria. J Plankton Res 13:77–82

Deibel D (1982) Laboratory-measured grazing and ingestion rates of the salp, *Thalia democratica* Forksal and *Dolioletta gegenbauri* Uljanin (Tunicata, Thaliacea). J Plankton Res 4:189–201

Ducklow HW (1993) Bacterioplankton distributions and production in the northwestern Indian Ocean and Gulf of Oman. September 1986. Deep-Sea Res 40:753–771

Ducklow HW (1999) The bacterial component of the oceanic euphotic zone. FEMS Microbiol Ecol 30:1–10

Eppley RW, Peterson BJ (1979) Particulate organic matter flux and planktonic new production in the deep ocean. Nature 282:677–680

Goosen NK, van Rijswijk P, DeBie M, Peene J, Kromkamp J (1997) Bacterioplankton abundance and production and nanozooplankton abundance in Kenyan coastal waters (Western Indian Ocean). Deep-Sea Res Part II 44: 1235–1250

Hoppe HG (1993) Use of fluorogenic model substrates for extracellular enzyme activity (EEA) measurements of bacteria. In: Kemp PF, Sherr BF, Sherr EB, Cole JJ (eds) Handbook of methods in aquatic microbial ecology. Lewis Publishers, Boca Raton, FL, p 423–432

Hoppe HG, Ullrich S (1999) Profiles of ectoenzymes in the Indian Ocean: phenomena of phosphatase activity in the mesopelagic zone. Aquat Microb Ecol 19:139–148

Keil RG, Kirchman DL (1993) Dissolved combined amino acids: chemical forms and utilization by marine bacteria. Limnol Oceanogr 38:1256–1270

Keil RG, Kirchman DL (1999) Utilization of dissolved protein and amino acids in the northern Sargasso Sea. Aquat Microb Ecol 18:293–300

Kirchman DL (1990) Limitation of bacterial growth by dissolved organic matter in the subarctic Pacific. Mar Ecol Prog Ser 62:47–54

Kirchman DL, K'nees E, Hodson RE (1985) Leucine incorporation and its potential as a measure of protein synthesis by bacteria in natural systems. Appl Environ Microbiol 49: 599–607

Kirchman DL, Ducklow HW, McCarthy JJ, Garside C (1994) Biomass and nitrogen uptake by heterotrophic bacteria during the spring phytoplankton bloom in the North Atlantic Ocean. Deep-Sea Res Part I 41:879–895

Kirchman DL, Rich JH, Barber RT (1995) Biomass and biomass production of heterotrophic bacteria along 140° W in the equatorial Pacific: effect of temperature on the microbial loop. Deep-Sea Res Part II 42:603–619

Li H, Veldhuis MJW, Post AF (1998) Alkaline phosphatase activities among planktonic communities in the northern Red Sea. Mar Ecol Prog Ser 173:107–115

Li WKW, Dickie PM, Irwin BD, Wood AM (1992) Biomass of bacteria, cyanobacteria, prochlorophytes, and photosynthetic eukaryotes in the Sargasso Sea. Deep-Sea Res 39: 501–519

Lindell D, Post AF (1995) Ultraphytoplankton succession is triggered by deep winter mixing in the Gulf of Aqaba (Eilat), Red Sea. Limnol Oceanogr 40:1130–1141

Lindroth P, Mopper K (1979) High performance liquid chromatographic determinations of subpicomole amounts of amino acids by precolumn fluorescence derivatization with o-phthaldialdehyde. Anal Chem 51:1667–1674

Mopper K, Schultz CA, Chevolot L, Germain C, Revuelta R, Dawson R (1992) Determinations of sugars in unconcentrated seawater and other natural waters by liquid chromatography and pulsed amperometric detection. Environ Sci Technol 26:133–138

Münster U (1993) Concentrations and fluxes of organic carbon substrates in the aquatic environment. Antonie Leeuwenhoek 63:243–274

Pakulski JD, Benner R (1994) Abundance and distribution of carbohydrates in the ocean. Limnol Oceanogr 39:930–940

Pedrós-Alió C, Calderón-Paz JI, Guixa-Boixereu N, Estrada M, Gasol JM (1999) Bacterioplankton and phytoplankton biomass and production during summer stratification in the northwestern Mediterranean Sea. Deep-Sea Part I 46: 985–1019

Plähn O, Badran M, El-Deek M, Sangok Y, Badewien T, Elbrächter M, Manasreh R, Walter M (2000) Physical and chemical oceanography: hydrography and tracer measurements. In: Pätzold J, Halbach PE, Hempel G, Weikert H (eds) Meteor Bericht 00–3: Östliches Mittelmeer–Nördliches Rotes Meer 1999, Cruise No. 44, Hamburg, p 59–62

Porter KG, Feig YS (1980) The use of DAPI for identifying and counting aquatic microflora. Limnol Oceanogr 25:943–948

Reiss Z, Hottinger L (1984) The Gulf of Aqaba: ecological micropaleontology. Springer-Verlag, Berlin

Rich JH, Ducklow HW, Kirchman DL (1996) Concentrations and uptake of neutral monosaccharides along 140° W in the equatorial Pacific: contribution of glucose to heterotrophic bacterial activity and the DOM-flux. Limnol Oceanogr 41:595–604

Rich JH, Gosselin M, Sherr EB, Sherr BF, Kirchman DL (1997) High bacterial production, uptake and concentration of dissolved organic matter in the Central Arctic Ocean. Deep-Sea Res II 44:1645–1663

Rivkin RB, Anderson MR (1997) Inorganic nutrient limitation of oceanic bacterioplankton. Limnol Oceanogr 42: 730–740

Rosenstock B, Simon M (2001) Sources and sinks of dissolved free amino acids and protein in a large and deep mesotrophic lake. Limnol Oceanogr 46:644–654

Rosso AL, Azam F (1987) Proteolytic activity in coastal oceanic waters: depth distribution and relationship to bacterial populations. Mar Ecol Prog Ser 41:231–240

Simon M (1991) Isotope dilution of intracellular amino acids as a tracer of carbon and nitrogen sources of marine planktonic bacteria. Mar Ecol Prog Ser 74:295–301

Simon M, Azam F (1989) Protein content and protein synthesis rates of planktonic marine bacteria. Mar Ecol Prog Ser 51:201–213

Simon M, Rosenstock B (1992) Carbon and nitrogen sources of planktonic bacteria in Lake Constance studied by the composition and isotope dilution of intracellular amino acids. Limnol Oceanogr 37:1496–1511

Simon M, Jontofsohn M, Parparov A, Berman T (2000) Turnover of combined amino acids and carbohydrates on organic aggregates and in the bulk water in Lake Kinneret and other pelagic ecosystems. Arch Hydrobiol Spec Issue Adv Limnol 55:365–377

Skoog A, Benner R (1997) Aldoses in various size fractions of marine organic matter: implications for carbon cycling. Limnol Oceangr 42:1803–1813

Sommer U (2000) Scarcity of medium-sized phytoplankton in the Red Sea explained by strong bottom-up and weak top-down control. Mar Ecol Prog Ser 197:19–25

Sommer U, Berninger UG, Böttger-Schnack R, Schnack-Schiel SB and 8 others (2002) Grazing during early spring in the Gulf of Aqaba and the northern Red Sea. Mar Ecol Prog Ser 239:251–261

Suttle CA, Chan AM, Fuhrman JA (1991) Dissolved free amino acids in the Sargasso Sea: uptake and respiration rates, turnover times, and concentrations. Mar Ecol Prog Ser 70:189–199

Weiss M, Simon M (1999) Consumption of labile dissolved organic matter by limnetic bacterioplankton: the relative significance of amino acids and carbohydrates. Aquat Microb Ecol 17:1–12

Weisse T (1989) The microbial loop in the Red Sea: dynamics of pelagic bacteria and heterotrophic nanoflagellates. Mar Ecol Prog Ser 55:241–250

Williams PM (1986) Chemistry of the dissolved and particulate phases in the water column. In: Eppley RW (ed) Lecture notes on coastal and estuarine studies, Springer-Verlag, Berlin, Heidelberg, New York, Tokyo, p 51–83

Wolf-Vecht A, Paldor N, Brenner S (1992) Hydrographic indications of advection/convection effects in the Gulf of Eilat. Deep-Sea Res 39:1393–1401

Editorial responsibility: Gotthilf Hempel, Bremen, Germany

Submitted: May 3, 2001; Accepted: January 31, 2002
Proofs received from author(s): July 18, 2002

Vol. 239: 277–285, 2002 | MARINE ECOLOGY PROGRESS SERIES
Mar Ecol Prog Ser | Published August 23

Effect of reef framework and bottom sediment on nutrient enrichment in a coral reef of the Gulf of Aqaba, Red Sea

Mohammed Rasheed[1, 2,*], Mohammad I. Badran[2], Claudio Richter[3], Markus Huettel[1]

[1]Max Planck Institute for Marine Microbiology, Celsiusstraße, 28359 Bremen, Germany
[2]Marine Science Station, University of Jordan and Yarmouk University, Aqaba, Jordan
[3]Centre for Tropical Marine Ecology ZMT, Fahrenheitstraße 6, 28359 Bremen, Germany

ABSTRACT: Inorganic nutrients and chlorophyll *a* concentrations were measured bi-weekly in a transect across a coral reef in the Gulf of Aqaba over a period of 1 yr. The nutrient and chlorophyll concentrations were compared to those in adjacent offshore waters (400 m depth). In reef and offshore waters, nutrient (ammonium, nitrite, nitrate, phosphate and silicate) and chlorophyll *a* data showed seasonal changes, with high concentrations in winter and low concentrations in summer. However, throughout the summer, nutrient concentrations in the coral reef waters significantly exceeded those in the offshore waters, while this difference was less pronounced in winter. This difference was caused by nutrient release from regenerative spaces in the reef framework and coral sand. In the reef framework water (i.e. cavity water), nutrient concentrations were 1.2- to 2.3-fold higher than those in the surrounding waters, corresponding to fluxes of 14.5 mmol m^{-2} d^{-1} for ammonium, 7.7 mmol m^{-2} d^{-1} for nitrate, 0.9 mmol m^{-2} d^{-1} for nitrite, and 1.3 mmol m^{-2} d^{-1} for phosphate. In the less permeable reef sediments, nutrient concentrations exceeded those of the free-stream waters by factors of 15 to 80. Here, the calculated diffusive fluxes were 0.06 mmol m^{-2} d^{-1} for ammonium, 0.03 mmol m^{-2} d^{-1} for nitrate, 0.01 mmol m^{-2} d^{-1} for nitrite, 0.01 mmol m^{-2} d^{-1} for phosphate, and 0.07 mmol m^{-2} d^{-1} for silicate. Our results highlight the importance of the reef framework and coral sand for the trapping and mineralization of particulate organic matter and the regeneration of nutrients in oligotrophic coral reef waters.

KEY WORDS: Nutrients · Coral reef · Seasonality · Porewater · Reef framework · Coral sand

INTRODUCTION

Although most coral reefs grow in oligotrophic waters (Furnas 1992), they belong to the most productive coastal marine ecosystems (Sorokin 1993). The exchange of substances between reef, open water, land and atmosphere is small relative to their concentrations and turnover within the coral reefs. The high biomass and productivity of coral reefs is explained by the tight internal recycling of matter (Wiebe et al. 1975, Andrews & Müller 1983, Risk & Müller 1983). Gross primary production in coral reef waters has been shown to be 1 to 2 orders of magnitude higher than in the surrounding oligotrophic water (d'Elia & Wiebe 1990, Adey 1998). Reef-related physical and biological processes mediate intensive exchange of dissolved and particulate matter between the coral reef and the water in the reef environment. Coral sands and reef framework may play important roles in this exchange process.

In most reef ecosystems, corals occupy roughly half the surface area, and sands cover the other half. Due to the porous structure of the coral sand, its permeability is relatively high and the porosity of the reef sediment can reach 50%. Pore water analyses in these cal-

*E-mail: my_rasheed@yahoo.com

careous sediments revealed elevated nutrient concentrations relative to the overlying bottom water (Holm 1978, Smith et al. 1981, Arenas & de la Lanza 1983, Entsch et al. 1983, Nixon & Pilson 1983, Williams 1984, Williams et al. 1985, Furnas et al. 1993, Szmant & Forrester 1996).

Beneath the living surface of the coral reefs, coral skeletal remains and other calcareous biogenic materials form a highly permeable framework, where the volume of coral reef cavities may reach up to half the bulk volume (Ginsburg 1983). These framework cavities are inhabited by a wide variety of organisms (Kobluk & van Soest 1989). Organic matter trapped within the framework or imported by the reef fauna is consumed by the organisms that colonize the cavities and that return ammonia and phosphate to the framework water (Ferrer & Szmant 1988). Nutrient concentrations in reef cavities, therefore, exceed those of waters surrounding the reef (Risk & Müller 1983, Ayukai 1993, Richter et al. 2001).

Because of their large specific surface areas, coral sands and reef framework may have an important biocatalytic function and may act as nutrient buffers in reef ecosystems exposed to seasonal nutrient changes. Seasonal variability of the nutrient supply in coral reef environments has received little attention due to the perception that seasonal fluctuations are less pronounced in tropical climates. Nonetheless, high-latitude reefs, such as those of the Gulf of Aqaba, undergo strong seasonal variations in primary productivity (Kinsey 1977) that are unexpected on the basis of temperature and light fluctuations alone.

Our understanding of the relationship between reef productivity and nutrient availability is limited, despite the importance of nutrients for the growth and health of corals (Ward 1990, Torrance 1991, Hallock et al. 1993, Atkinson et al. 1995). In this study, we investigated the seasonal changes of chlorophyll *a* and nutrients in the water column and in a fringing reef ecosystem of the Gulf of Aqaba, and we measured coral framework and sediment pore-water nutrient concentrations in order to assess the importance of framework and sediment in the nutrient balance of the coral reef.

MATERIALS AND METHODS

The study was conducted in a well-developed coral reef located in the northern Gulf of Aqaba in a marine reserve close to the Marine Science Station in Aqaba. Water samples were collected concurrently from the reef site and an offshore site 3 km from the Marine Science Station (Fig. 1A). Along the reef transect, surface and bottom water (ca. 50 cm above the sediment) were sampled biweekly at stations 5, 10, 20, and 30 m from the bottom (Fig. 1B). At the stations at 20 and 30 m water depth, additional samples were taken at 10 m depth intervals. The offshore reference station was sampled at water depths of 0.5 and 25 m. The bottom-water samples were collected by divers, while all other samples were collected with Niskin bottles. All samples were kept on ice until analysis. In the laboratory, 1 l of each sample was filtered through a pre-rinsed 0.45 µm cellulose-membrane filter and analyzed for ammonium, nitrite, nitrate, phosphate and silicate concentrations according to Strickland & Parsons (1972). The material on the membrane filter was used for the determination of chlorophyll *a* based on the method published by Arar & Collins (1992), using a Turner Designs, TD-700 fluorometer.

In June and December 1998, water samples from coral reef cavities and free-flowing reef waters were simultaneously taken at hourly intervals over a period of 24 h (Fig. 1B). Water was collected using a multichannel peristaltic pump mounted on a boat, using

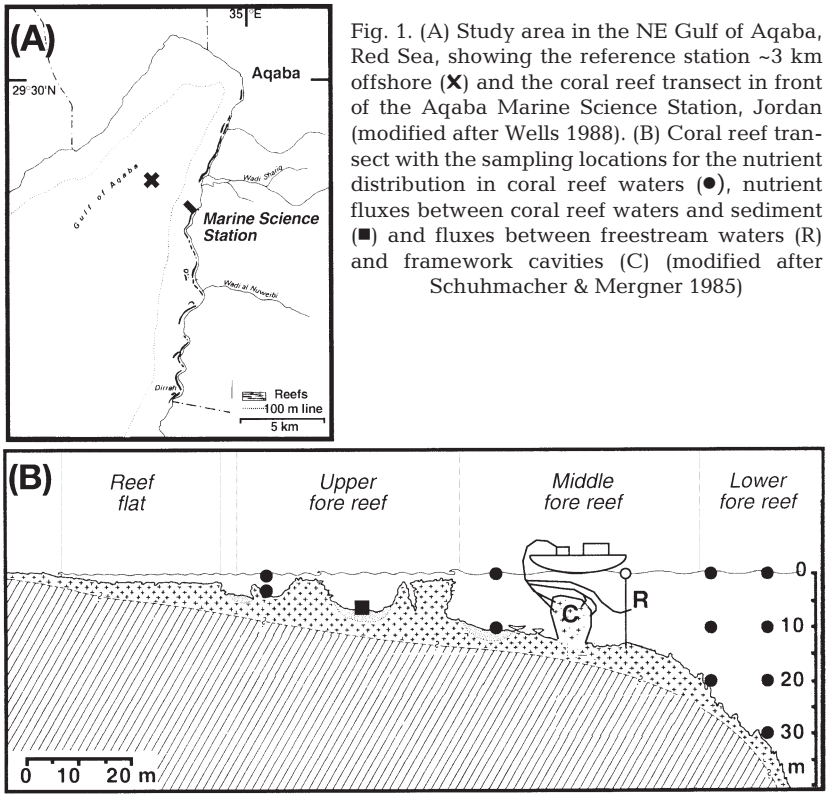

Fig. 1. (A) Study area in the NE Gulf of Aqaba, Red Sea, showing the reference station ~3 km offshore (✖) and the coral reef transect in front of the Aqaba Marine Science Station, Jordan (modified after Wells 1988). (B) Coral reef transect with the sampling locations for the nutrient distribution in coral reef waters (●), nutrient fluxes between coral reef waters and sediment (■) and fluxes between freestream waters (R) and framework cavities (C) (modified after Schuhmacher & Mergner 1985)

Table 1. Annual average (SD) nutrient (µM) and chlorophyll *a* (µg l^{-1}) concentrations in offshore and coral reef waters during summer (n= 70) and winter (n = 28)

Variable	Reef water		Offshore water	
	Summer	Winter	Summer	Winter
Inorganic nitrogen	0.35 (0.09)	0.65 (0.08)	0.13 (0.03)	0.58 (0.05)
Phosphate	0.06 (0.01)	0.09 (0.01)	0.02 (0.01)	0.07 (0.01)
Silicate	1.05 (0.14)	1.78 (0.10)	0.70 (0.01)	1.43 (0.03)
Chlorophyll *a*	0.19 (0.02)	0.23 (0.03)	0.14 (0.02)	0.23 (0.02)

10 m long, 5 mm diameter silicone tubing inserted into 8 randomly selected cavities within a 4 m diameter coral pinnacle located at a depth of 3 to 6 m. Tubes were fixed axially into ~6 cm wide, ~30 cm deep cavities using elastic plastic rods. Tubes were inserted two-thirds of the way into the cavities, i.e. at ~20 cm distance from the entrance. Free-flowing water was collected with 2 tubes fixed on moorings 3 m upstream from the pinnacle; 100 ml samples were drawn at 50 ml min^{-1} and taken to the laboratory for subsequent analysis of nutrients. Between samplings, the flow was reversed, using double-distilled water at rates of 2 ml min^{-1} to avoid fouling of the tubing. With an average volume of the sampled cavities of ~3 l and a water residence time of less than 5 min, we found no dilution effect of the freshwater on salinity in the cavities. Nutrient fluxes between coral reef cavities and free-flowing waters were calculated according to the formula

$$F = \Delta N \times V_c / T$$

where ΔN is the concentration difference between the cavity and free-flowing reference (mmol m^{-3}), V_c is the volume of cavities per unit area of reef (m^3 m^{-2}), and T is the residence time of water in the cavities. For the upper 0.2 m of framework investigated, V_c was 0.07 m (Richter et al. 2001). A conservative estimate for T is 300 s (Richter & Wunsch 1999).

From June 1999 until March 2000, interstitial water of the coral reef sediments were sampled at a 5 m-deep reef site (Fig. 1B) using a method similar to that described by Hesselein (1976). The sediments in this site consist mainly of carbonate sands, with a medium grain size of 500 µm, an average porosity of 47%, a permeabilty of 143×10^{-12} m^2, an organic content of 0.5%, and a calcium carbonate content of 80%; 50 ml of the filtered pore water was diluted to 250 ml with distilled deionized water for nutrient analyses. The pore-water nutrient concentrations were compared to those of the bottom water overlying the sediment. Minimum fluxes of NH_4^+, NO_2^-, NO_3^-, PO_4^{-3} and $Si(OH)_4$ from the sediment were calculated according to Fick's first law of diffusion:

$$F = ø \times D \times dC / dz$$

where F is the flux (mmol m^{-2} d^{-1}), ø is sediment porosity, D is the coefficient of diffusion (m^2 d^{-1}), and dC / dz is the concentration gradient at the sediment-water interface (mmol m^{-4}). Diffusion coefficients for ammonium, nitrate, nitrite and phosphate were taken from Li & Gregory (1974) for a water temperature of 25°C and corrected for a tortuosity using a porosity of 0.47 and the tortuosity-porosity relationship reported by Beekman (1990). The value for silicate was taken from Lerman (1979) and Callender & Hammond (1982) and corrected for tortuosity. The calculated diffusion coefficients were 8.85, 6.66, 6.70, 2.97 and 5.89×10^{-5} m^{-2} d^{-1} for ammonium, nitrate, nitrite, phosphate and silicate respectively.

To assess whether nutrients were significantly different in coral reef waters from those in the offshore waters, ANOVA (5% significance level) was performed based on a calculation of the differences in the average of concentrations between coral reef waters and offshore waters in summer and winter.

RESULTS

In order to compare nutrient concentrations of reef and offshore waters, surface and 25 m samples of the offshore waters were averaged and plotted with the average of the coral reef waters from various depths against time (Fig. 2). Nutrient and chlorophyll *a* concentrations in reef and offshore waters showed seasonal changes, with high concentrations in winter and low concentrations in summer. The concentrations began to increase in October. Nutrient and chlorophyll *a* concentrations in the reef waters exceeded those in the offshore waters (Fig. 2, Table 1), particularly in summer, when inorganic nitrogen and phosphate concentrations exceeded offshore values by up to 3 times. The pattern was less consistent during win-

Table 2. Mean differences in nutrient (µM) and chlorophyll *a* (µg l^{-1}) concentrations between reef and offshore waters in summer and winter. p-values were obtained from ANOVA at significance level of 5%. *Significant difference

Variable	Summer		Winter	
	Mean difference	p	Mean difference	p
Inorganic nitrogen	0.22	<0.0001*	0.07	0.4761
Phosphate	0.04	<0.0001*	0.02	0.0057*
Silicate	0.35	0.0015*	0.35	0.0178*
Chlorophyll *a*	0.05	0.0316*	0.00	0.7394

ter, when gradient reversals occurred, both for inorganic nitrogen (e.g. nitrate, February through April: Fig. 2) and chlorophyll *a* (January through March: Fig. 2). As a result, moderate cross-shore differences were found only for phosphate and silicate in winter, as opposed to strong and highly significant differences for all parameters in summer (Table 2).

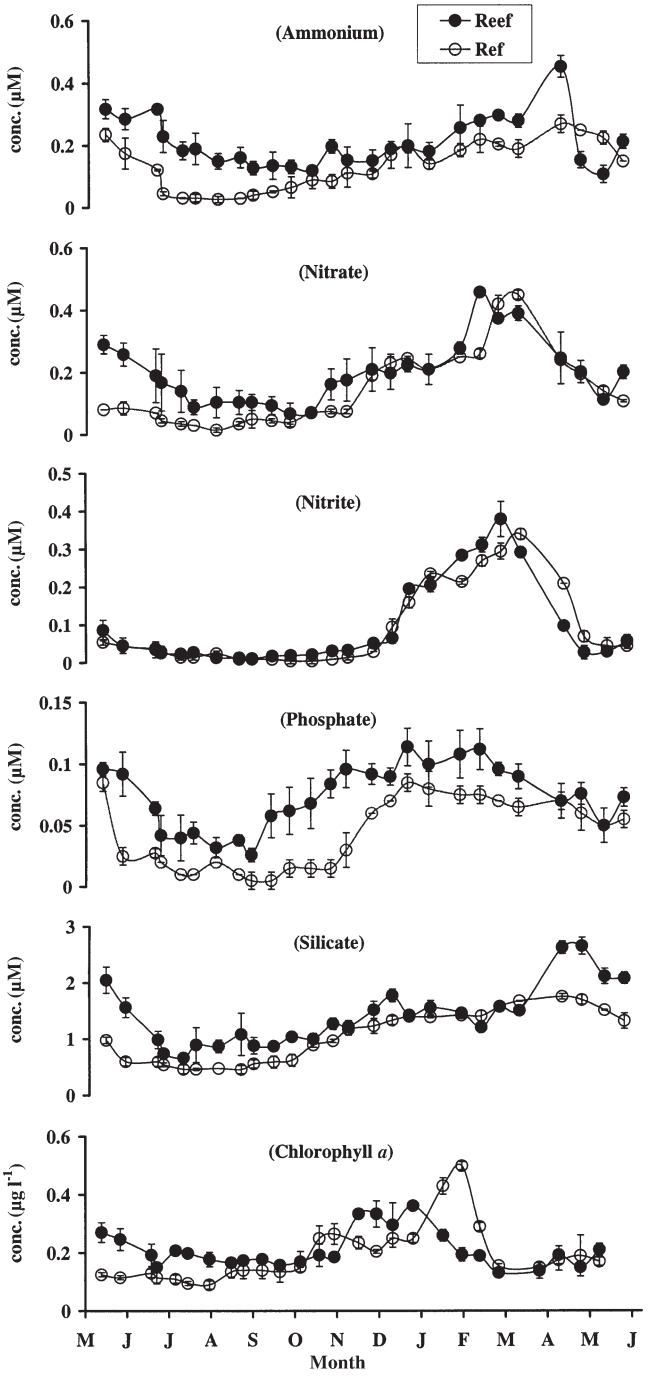

Fig. 2. Nutrient and chlorophyll *a* concentrations in coral reef (Reef) and offshore reference (Ref) waters during the period May 1997 to May 1998

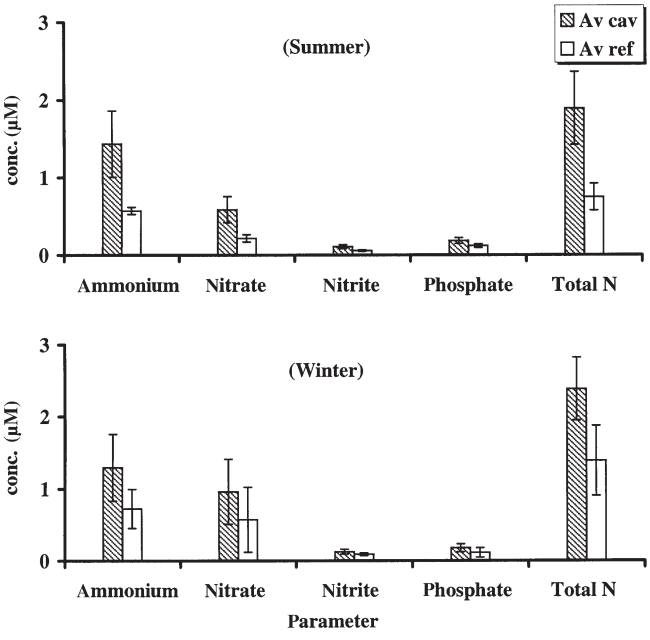

Fig. 3. Average nutrient concentrations in the framework of the coral reef (Av cav) and surrounding waters (Av ref)

Within the reef framework, nutrient concentrations were higher than in the freestream waters (Fig. 3) in approximately 90% of the cases. Much higher nutrient concentrations were found in sediment pore waters compared to concentrations in the water above the sediment (factors of 21 to 80 in summer and 15 to 74 in winter: Fig. 4).

DISCUSSION

This study shows, for the first time, clear seasonal changes in nutrient and chlorophyll *a* in reef and offshore waters, as well as differences in these parameters between the two. Enhancement of nutrient concentrations in reef water was found particularly during summer. Higher nutrient concentrations were found in the sediment pore water and in the reef framework than in the surrounding water. This steep concentration gradient would result in fluxes of these nutrients to the surrounding water.

Seasonal pattern of nutrients in coral reef waters

According to Furnas et al. (1990), Hatcher & Hatcher (1981), and Ayukai (1993), it is difficult to detect seasonal variations in reef-water nutrient concentrations

by sampling at 1 mo or longer intervals because of the strong short-term variations in the reef waters. Our results demonstrate temporal and spatial changes in the nutrient concentrations in the coastal environment of the northern Gulf of Aqaba, whereas no significant difference in current speed and direction between summer and winter were found (M. Rasheed et al. unpubl. data). We have shown that the coral reef ecosystem in the Gulf of Aqaba is subjected to seasonal changes, with elevated concentrations of all measured nutrients in fall and winter. The main 2 reasons which could cause these seasonal changes are (1) deep-water column-mixing during winter increasing the nutrient concentrations in the coastal waters and boosting phytoplankton growth (Venrick et al. 1973, Souvermezoglou et al. 1989, Lindell & Post 1995), and (2) water-column stratification and increased light intensities during summer, which result in a depletion of the inorganic nutrients by enhanced primary production (Olson 1981, Souvermezoglou et al. 1989).

Comparison between nutrient and chlorophyll *a* values in reef and offshore waters

In our study we found spatial differences in nutrient concentrations between reef water and offshore water adjacent to the reef. During the summer months, when the offshore water was nutrient-depleted, concentrations of nutrients and chlorophyll *a* in the reef water were higher than in the offshore water. During winter, strong vertical mixing reduced the differences in nutrient and chlorophyll *a* concentrations between reef and offshore waters. Vertical mixing moved deep water, rich in nutrients, up into the water column (Venrick et al. 1973, Klinker et al. 1978, Levanon-Spanier et al. 1979, Olson 1981, Al-Najjar 2000), while horizontal mixing caused nutrient equilibration between reef and offshore waters. Nitrogen enrichment of coral reef waters has been reported by several authors (Meyer & Shultz 1985, Blanchot et al. 1989, Tribble et al. 1990, Bell 1991), and the reef in the Gulf of Aqaba showed similar trends (Badran & Foster 1998). Enhanced primary productivity during winter months in the Gulf of Aqaba was recorded by Levanon-Spanier et al. (1979).

Possible reasons for higher nutrient concentrations in reef waters

Increased nutrient concentrations in reef waters can originate from anthropogenic sources such as nutrient-rich groundwater input (d'Elia et al. 1981, Lewis 1985), sewage discharge (Johannes 1975) and terrestrial runoff (Marsh 1977). However, these sources are negligible in our study area because the reef is an environmentally protected zone and there is no groundwater input (no salinity change was recorded in the study area) and very little rainfall throughout the year. The higher silicate concentrations could be attributable partly to an influx of atmospheric silicate-rich desert dust (Alfuqaha unpubl. data). We suggest that the higher nutrient concentrations in the reef are caused by the efficient trapping and decomposition of suspended particles by the reef framework, coral sands and reef biota, as well as nitrogen fixation by organisms living in the reef environment.

Framework

Our study has shown that the concentrations of nutrients in the framework water were higher than those in the free-flowing water (Fig. 3), which would cause nutrient fluxes from the framework to the surrounding water. The average fluxes in summer and winter from the framework reached approximately 14.5 mmol

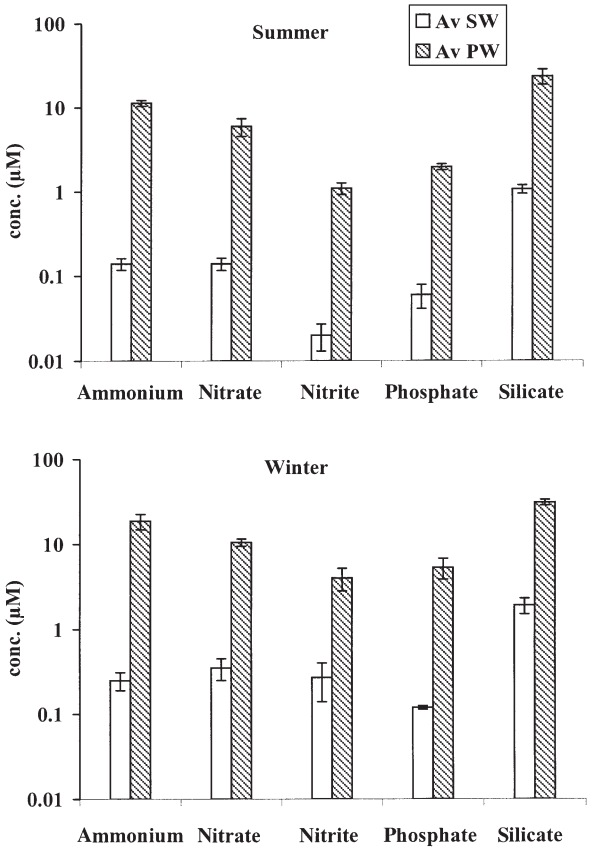

Fig. 4. Average nutrient concentrations during summer and winter (June 1999 to March 2000) in pore water (Av PW) and sediment water interface (Av SW) of the coral reef

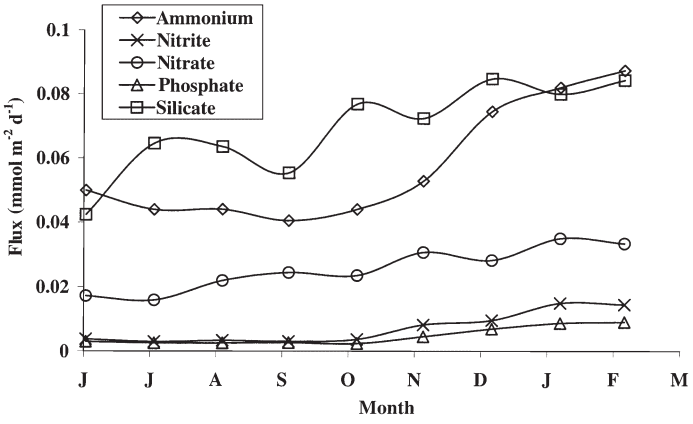

Fig. 5. Calculated nutrient fluxes from the sediment to the water column during the period June 1999 to March 2000

m^{-2} d^{-1} for ammonium, 7.7 mmol m^{-2} d^{-1} for nitrate, 0.9 mmol m^{-2} d^{-1} for nitrite, and 1.3 mmol m^{-2} d^{-1} for phosphate. These fluxes may have added more nutrients to the reef water, particularly during summer, when the concentrations were low (Fig. 2). Three mechanisms may be responsible for the higher nutrient concentrations in the framework: (1) decomposition of organic matter enclosed in the framework carbonates that had been overgrown by corals (e.g. coral tissue, boring organisms, coralline algae), (2) suspended particulate matter, including small phytoplankton and bacteria that had been efficiently trapped by the abundant suspension feeders living within the reef framework (Gast et al. 1998, Richter & Wunsch 1999, Richter et al. 2001), and (3) remineralization of faeces from migrating invertebrates and fishes, which forage on and above the reef and use cavities as a temporary shelter (Bray et al. 1981, Meyer et al. 1983). Similar findings were reported by Ferrer & Szmant (1988) and Tribble et al. (1988), who measured increased nutrient concentrations in the cavities of the reef of Belize Barrier Reef and Kaneohe Bay respectively, and a net flux of nutrients from the reef framework to the surrounding water. These findings indicate that the reef framework is an important site for organic matter mineralization in the reef (Andrews & Müller 1983, Szmant-Froelich 1983, Sansone 1985, Buddemeier & Oberdorfer 1986, Tribble et al. 1986, 1988) and suggest that the framework may act as a temporal nutrient source in the reef environment.

Coral sands

We measured increased nutrient concentrations in the pore water of the sediment relative to the overlying water during summer and winter (Fig. 4). This steep concentration gradient would result in a net flux of nutrients from the pore water to the overlying water (Fig. 5). Fluxes of ammonia, nitrite, nitrate and phosphate increased during the winter months (December to March: Fig. 5). The average fluxes over the whole year were 0.06 mmol m^{-2} d^{-1} for ammonium, 0.03 mmol m^{-2} d^{-1} for nitrate, 0.01 mmol m^{-2} d^{-1} for nitrite, 0.01 mmol m^{-2} d^{-1} for phosphate, and 0.07 mmol m^{-2} d^{-1} for silicate. However, the calculated fluxes only represent the diffusive fluxes from the sediment, as the calculation we used (Fick's law of diffusion) does not include fluxes caused by bioturbation and advective pore-water exchange (Clavero et al. 2000). Laboratory core incubation resulted in silicate fluxes which exceeded the calculated silicate flux by a factor of 20 (Rasheed et al. unpubl. data), suggesting that both bioturbation and advective pore-water exchange probably added to the flux.

This indicates that the coarse-grained carbonate reef sediments may act as a biocatalytic converter, similar to the porous framework. We suggest that organic matter filtered from the water column when bottom currents interact with the permeable sediment (Huettel et al. 1996, Huettel & Rusch 2000) is decomposed in the sedimentary microbial food chain. The products of the mineralization, the nutrients, are then released into the pore water and overlying water column. Increased nutrient concentrations in the pore water of reef sediments were also reported by Capone et al. (1992) for the Great Barrier Reef, Szmant & Forrester (1996) for the Florida Coral Reef, and Ciceri et al. (1999) for the northern lagoon of Venice. Nutrient release from reef pore waters to the water column was reported by several authors (e.g. Fuentes & Espino 1990, Bertuzzi et al. 1996, Charpy-Roubaud et al. 1996, Ciceri et al. 1999). The flux of ammonium in our study (0.06 mmol m^{-2} d^{-1}) was lower than the fluxes reported by Charpy-Rouband et al. (1996) (0.16 mmol m^{-2} d^{-1}) and Bertuzzi et al. (1996) (0.3 mmol m^{-2} d^{-1}). However, phosphate flux in our study was higher compared to the previous 2 studies (0.010, 0.004, and 0.001 respectively). The differences in the flux values resulted from different nutrient concentrations in the water column and in the pore water, which might be attributable to the differences in the organic matter loading and different chemical and physical properties of the study areas (Shum & Sundby 1996, Hulthe et al. 1998). Charpy-Roubaud et al. (1996) found that aerobic bacteria that live in coral sediment could mineralize organic compounds to mineral end-products. In most tropical shallow marine environments like the Gulf of Aqaba, the highest metabolic activity is associated with the benthos (Zieman 1982, d'Elia & Wiebe 1990).

Reef biota

Corals, mollusks, polychaetes, echinoderms and a variety of other reef-dwelling organisms can efficiently filter and digest organic particles from water in the reef and thereby also increase the concentration of nutrients in the reef water relative to the offshore water (Hatcher & Hatcher 1981, Andrews & Müller 1983, Tribble et al. 1988, Larned 1999).

Nitrogen fixation

Nitrogen fixation in the different habitats within the reef has been reported in several studies (e.g. Wiebe et al. 1975, Goldner 1980, Wilkinson et al. 1984). According to Crossland & Barnes (1976), corals themselves do not have the ability to fix nitrogen, but endolithic organisms in the coral skeleton do. Shashar et al. (1994) reported a fixation rate of 0.6 to 1.0 mmol N_2 m^{-2} d^{-1} in the Gulf of Aqaba and reported that 70% of the fixation occurred in the sand-covered lagoon.

CONCLUSIONS

Our study has shown seasonal changes in the nutrient concentrations in the reef and a nutrient gradient between reef water and offshore water during summer. In winter, high nutrient concentrations in the coastal zone in the Gulf of Aqaba caused by enhanced water-column mixing remove this gradient. In summer, particle trapping and biocatalytic conversion of dissolved and particulate material in framework and reef sands increase the nutrient concentrations in the reef water relative to the offshore water. This nutrient availability during summer permits a higher primary productivity in the reef environment during this period in comparison to the offshore water, as indicated by the chlorophyll *a* data. We conclude that the decomposition activity and buffer capacity of the coral sands and reef framework play an important role in the support of primary productivity in the coral reef ecosystem during phases of nutrient depletion in the water column. During the fall and winter months, sands and framework accumulate nutrients (due to sorption and binding processes) and particulate organic matter. This organic matter is decomposed in the pore space of the sand and reef framework, and the resulting nutrients may be gradually released during the summer months.

Acknowledgements. This work forms part of the Red Sea Programme and has been funded by the German Federal Ministry of Education and Research (BMBF grant no. 03F0245A). Thanks are due to the director and the staff members of the Marine Science Station for their support during this study. Thanks are also due to Khalid Al-Tarabeen for his assistance in the laboratory and to Tariq Al-Salman, Riyad Manasreh, Saber Al-Rousan, Britta Munkes, Iris Kötter and Mark Wunsch for their help in the field.

LITERATURE CITED

Adey WH (1998) Coral reefs: algal structured and mediated ecosystems in shallow, turbulent, alkaline waters. J Phycol 34:393–406

Al-Najjar T (2000) The seasonal dynamics and grazing control of phyto- and mesozooplankton in the northern Gulf of Aqaba. PhD thesis, Bremen University

Andrews JC, Müller HR (1983) Space-time variability of nutrients in a lagoonal patch reef. Limnol Oceanogr 28: 215–227

Arar EJ, Collins GB (1992) In vitro determination of chlorophyll *a* and pheophytin *a* in marine and freshwater phytoplankton by fluorescence. Environmental Monitoring System Laboratory Office of Research and Development, US Environmental Protection Agency, Cincinnati, OH

Arenas FV, de la Lanz EG (1983) Annual phosphorus budget of a coastal lagoon in the northwest of Mexico. Ecol Bull 35:431–440

Atkinson MJ, Carlson B, Crow GL (1995) Coral growth in high-nutrient, low-pH seawater: a case study of corals cultured at the Waikiki Aquarium, Hawaii. Coral Reefs 14: 215–223

Ayukai T (1993) Temporal variability of the nutrient environment on Davies Reef in the Central Great Barrier Reef, Australia. Pac Sci 47:171–179

Badran MI, Foster P (1998) Environmental quality of the Jordanian coastal waters of the Gulf of Aqaba, Red Sea. Aquat Ecosyst Health Manag 1:75–89

Beekman JW (1990) Mathematical description of heterogeneous materials. Chem Eng Sci 45:2603–2610

Bell PRF (1991) Status of eutrophication in the Great Barrier Reef lagoon. Mar Pollut Bull 23:89–93

Bertuzzi A, Faganeli J, Brambati A (1996) Annual variation of benthic nutrient fluxes in shallow coastal waters (Gulf of Trieste, northern Adriatic Sea). PSZN I: Mar Ecol 17: 261–278

Blanchot J, Charpy L, Le Borgne R (1989) Size composition of particulate organic matter in the lagoon of Tikehau atoll (Tuamotu archipelago). Mar Biol 102:329–339

Bray RN, Miller AC, Geesey GG (1981) The fish connection: a trophic link between planktonic and rocky reef communities? Science 214:204–205

Buddemeier RW, Oberdorfer JA (1986) Internal hydrology and geochemistry of coral reefs and atoll islands: key to diagenetic variations. In: Schroeder JH, Purser BH (eds) Reef diagenesis. Springer-Verlag, Berlin, p 91–111

Callender E, Hammond DE (1982) Nutrient exchange across the sediment-water interface in the Potomac River estuary. Estuar Coast Shelf Sci 15:395–413

Capone DG, Dunham SE, Horrigan SG, Duguay LE (1992) Microbial nitrogen transformations in unconsolidated coral reef sediments. Mar Ecol Prog Ser 80:75–88

Charpy-Roubaud C, Charpy L, Sarazin G (1996) Diffusional nutrient fluxes at the sediment-water interface and organic matter mineralization in an atoll lagoon (Tikehau, Tuamotu Archipelago, French Polynesia). Mar Ecol Prog Ser 132:181–190

Ciceri G, Ceradina S, Zitelli A (1999) Nutrient benthic fluxes

and pore-water profiles in a shallow brackish marsh of the lagoon of Venice. Ann di Chim 89:359–375
Clavero V, Izquierdo JJ, Fernandez JA, Niell FX (2000) Seasonal fluxes of phosphate and ammonium across the sediment-water interface in a shallow small estuary (Palmones River, southern Spain). Mar Ecol Prog Ser 198:51–60
Crossland CJ, Barnes DJ (1976) Acetylene reduction by coral skeleton. Limnol Oceanogr 21:153–156
d'Elia CF, Wiebe WJ (1990) Biogeochemical nutrient cycles in coral reef ecosystems. In: Dubinsky Z (ed) Coral reefs. Elsevier Science Publishers, Amsterdam, p 49–74
d'Elia CF, Webb KL, Porter JW (1981) Nitrate-rich groundwater input to Discovery Bay, Jamaica: a significant source of N to local coral reefs? Bull Mar Sci 31:903–910
Entsch B, Boto KG, Sim RG, Wellington JT (1983) Phosphorus and nitrogen in coral reef sediment. Limnol Oceanogr 28: 465–476
Ferrer LM, Szmant AM (1988) Nutrient regeneration by the endolithic community in coral skeletons. Proc 6th Int Coral Reef Symp 3:1–4
Fuentes VA de le G, Espino L (1990) Metabolism as determinant of nutrient exchange in organic-rich sediments of a coastal lagoon. Cienc Mar 16:45–62
Furnas MJ (1992) The behavior of nutrients in tropical aquatic ecosystems. In: Connell DW, Hawker DW (eds) Land use patterns and nutrient loadings of the Great Barrier Reef Region. James Cook University, Townsville, p 162–179
Furnas MJ, Mitchell AW, Gilmartin M, Revelante N (1990) Phytoplankton biomass and primary production in semi-enclosed reef lagoons of the central Great Barrier Reef, Australia. Coral Reefs 9:1–10
Furnas MJ, Mitchell AW, Skuza M (1993) Nitrogen and phosphorus budgets for the Great Barrier Reef. Final Report to the Great Barrier Reef Marine Park Authority, Aust Inst Mar Sci, Townsville
Gast GJ, Wiegmann S, Wieringa E, van Duyl FC, Bak RPM (1998) Bacteria in coral reef water types: removal of cells, stimulation of growth and mineralization. Mar Ecol Prog Ser 167:37–45
Ginsburg RN (1983) Geological and biological roles of cavities in coral reefs. In: Barnes DJ (ed) Perspectives on coral reefs. Aust Inst Mar Sci, Townsville, p 148–153
Goldner LL (1980) Nitrogen fixation (acetylene reduction) in shallow water Bahamian environments. Bull Mar Sci 30: 444–453
Hallock P, Müller FE, Halas JC (1993) Coral reef decline. Natl Geogr Res Explor 9:358–378
Hatcher RAI, Hatcher BG (1981) Seasonal and spatial variation in dissolved inorganic nitrogen in One Tree Reef lagoon. Proc 4th Int Coral Reef Symp 1:419–424
Hesselein RH (1976) An *in situ* sampler for close internal pore-water studies. Limnol Oceanogr 21:912–924
Holm NG (1978) Phosphorus exchange through the sediment-water interface. Mechanism studies of dynamic processes in the Baltic Sea. Contrib Microb Geochem Dep Geol Univ Stockh 3:149
Huettel M, Rusch A (2000) Transport and degradation of phytoplankton in permeable sediment. Limnol Oceanogr 45:534–549
Huettel M, Ziebis W, Forster S (1996) Flow-induced uptake of particulate matter in permeable sediments. Limnol Oceanogr 41:309–322
Hulthe G, Hulth S, Hall POJ (1998) Effect of oxygen on degradation rate of refractory and labile organic matter in continental margin sediments. Geochim Cosmochim Acta 62: 1319–1328
Johannes RE (1975) Pollution and degradation of coral reef communities. Elsevier Oceanogr Ser 12:13–15
Kinsey DW (1977) Seasonality and zonation in coral reef productivity and calcification. Proc 3rd Int Coral Reef Symp 2: 383–388
Klinker J, Reiss Z, Kropach C, Levanon I, Harpaz H, Shapiro Y (1978) Nutrients and biomass distribution in the Gulf of Aqaba (Eilat), Red Sea. Mar Biol 45:53–64
Kobluk DR, van Soest RWM (1989) Cavity-dwelling sponges in a southern Caribbean coral reef and their paleontological implications. Bull Mar Sci 44:1207–1235
Larned ST (1998) Nitrogen- versus phosphorus-limited growth and sources of nutrients for coral reef macroalgae. Mar Biol 132:409–421
Lerman A (1979) Geochemical processes, water and sediment environment. John Wiley & Sons, New York
Levanon-Spanier I, Padan E, Reisis Z (1979) Primary production in a desert-enclosed sea—the Gulf of Eilat (Aqaba), Red Sea. Deep-Sea Res 26:673–685
Lewis JB (1985) Groundwater discharge onto coral reefs, Barbados (West Indies). Proc 5th Int Coral Reef Symp 6: 477–481
Li YH, Gregory S (1974) Diffusion of ions in sea water and in deep sea sediment. Geochim Cosmochim Acta 38: 703–714
Lindell D, Post AF (1995) Ultraphytoplankton succession is triggered by deep winter mixing in the Gulf of Aqaba (Eilat), Red Sea. Limnol Oceanogr 40:1130–1141
Marsh JA (1977) Terrestrial inputs of nitrogen and phosphorus on fringing reefs of Guam. Proc 3rd Int Coral Reef Symp 1:331–336
Meyer JL, Schultz ET (1985) Tissue condition and growth rate of corals associated with schooling fish. Limnol Oceanogr 30:157–166
Meyer JL, Schultz ET, Helfman GS (1983) Fish schools: an asset to corals. Science 220:1047–1049
Nixon SW, Pilson MEQ (1983) Nitrogen in estuarine and coastal marine ecosystems. In: Carpenter ED, Carpenter DG (eds) Nitrogen in the marine environment. Academic Press, New York, p 565–648
Olson RJ (1981) Differential photoinhibition of marine nitrifying bacteria: a possible mechanism for the formation of the primary nitrite maximum. J Mar Res 39:227–238
Richter C, Wunsch M (1999) Cavity-dwelling suspension feeders in coral reefs—a new link in reef trophodynamics. Mar Ecol Prog Ser 188:105–116
Richter C, Wunsch M, Rasheed M, Koetter I, Badran MI (2001) Endoscopic exploration of Red Sea coral reefs reveals dense populations of cavity dwelling sponges. Nature 413: 726–730
Risk MJ, Müller HR (1983) Pore water in coral heads: evidence for nutrient regeneration. Limnol Oceanogr 28: 1004–1008
Sansone FJ (1985) Methane in the reef flat pore-waters of Davies Reef, Great Barrier Reef (Australia). Proc 5th Int Coral Reef Symp 3:415–419
Schuhmacher H , Mergner H (1985) Quantitative Analyse von Korallengemeinschaften des Sanganeb-Atolls (mittleres Rotes Meer). 2. Vergleich mit einem Riffareal bei Aqaba (nördliches Rotes Meer) am Nordrande des indopazifischen Riffgürtels. Helgol Wiss Meeresunters 39:419–440
Shashar N, Feldstein T, Cohen Y, Loya Y (1994) Nitrogen fixation (acetylene reduction) on a coral reef. Coral Reefs 13:171–174
Shum KT, Sundby B (1996) Organic matter processing in continental shelf sediments—the subtidal pump revisited. Mar Chem 53:81–87

Smith SV, Kimmerer WJ, Laws EA, Brock RE, Walsh TW (1981) Kaneohe Bay sewage diversion experiment: perspectives on ecosystem responses to nutritional perturbation. Pacific Sci 35:279–402

Sorokin YI (1993) Coral reef ecology. Springer-Verlag, Berlin

Souvermezoglou E, Metzl N, Poisson A (1989) Red Sea budgets of salinity, nutrients and carbon calculated in the Strait of Bab-El-Mandab during the summer and winter seasons. J Mar Res 47:441–456

Strickland JDH, Parsons TR (1972) A practical handbook of seawater analysis, 2nd edn. Bull Fish Res Board Can 167:310

Szmant-Froelich A (1983) Functional aspects of nutrient cycling in coral reefs. NOAA Symp Ser Undersea Res 1:133–139

Szmant AM, Forrester A (1996) Water column sediment nitrogen and phosphorus distribution patterns in the Florida Keys, USA. Coral Reefs 15:21–41

Torrance DC (1991) Deep ecology: rescuing Florida's reef. Nat Conserv July–Aug, p 9–17

Tribble GW, Sansone FJ, Andrews CC, Smith SV (1986) Organic geochemistry of reef interstitial water. EOS Trans Am Geophys Un 67:997

Tribble GW, Sansone FJ, Li YH, Smith SV, Buddemeier RW (1988) Material fluxes from a reef framework. Proc 6th Int Coral Reef Symp 2:577–582

Tribble GW, Sansone FJ, Smith SV (1990) Stoichiometric modeling of carbon diagenesis within a coral reef framework. Geochim Cosmochim Acta 54:2439–2449

Venrick El, McGowan JA, Mantyla AW (1973) Deep maximua of photosynthetic chlorophyll *a* in the Pacific Ocean. Fish Bull 71:41–52

Ward F (1990) Florida's coral reefs are imperiled. Natl Geogr 178:114–132

Wells SM (1988) Coral reefs of the world, Vol 2. Indian Ocean, Red Sea and Gulf. The IUCN Conservation Monitoring Center, Cambridge, UK

Wiebe WJ, Johannes RE, Webb KL (1975) Nitrogen fixation in a coral reef community. Science 188:257–259

Wilkinson CR, Williams DMcB, Sammarco PW, Hogg RW, Trott LA (1984) Rates of nitrogen fixation on coral reefs across the continental shelf of the central Great Barrier Reef. Mar Biol 80:255–262

Williams SL (1984) Uptake of sediment ammonium and translocation in the marine green alga *Caulerpa cupressoides*. Limnol Oceanogr 29:374–379

Williams SL, Gill IP, Yarish SM (1985) Nitrogen cycle in back reef sediments. Proc 5th Int Coral Reef Symp 3:389–394

Zieman JC (1982) The ecology of the seagrasses of south Florida: a community profile. US Fish Wildl Serv FWS/OBS-82/25 123

Editorial responsibility: Gotthilf Hempel, Bremen, Germany

Submitted: May 3, 2001; Accepted: January 31, 2002
Proofs received from author(s): July 8, 2002

Vol. 239: 287–299, 2002 | MARINE ECOLOGY PROGRESS SERIES
Mar Ecol Prog Ser | Published August 23

Changes in trophic community structure of shore fishes at an industrial site in the Gulf of Aqaba, Red Sea

M. A. Khalaf[1], M. Kochzius[2,*]

[1]Marine Science Station, PO Box 195, Aqaba, Jordan
[2]Centre for Tropical Marine Ecology—ZMT, Fahrenheitstrasse 6, 28359 Bremen, Germany

ABSTRACT: The semi-enclosed Gulf of Aqaba is under high pressure by urban and industrial pollution, shipping and port activities as well as tourism. Off the Jordanian Red Sea coast, the trophic community structure of shore fishes was determined on coral reefs in front of an industrial area (disturbed), in a marine reserve and site without industry or port activities (undisturbed), as well as in a seagrass-dominated bay. Planktivores were the most abundant feeding guild on coral reefs as well as in the seagrass-dominated bay. The relative abundance of feeding guilds other than planktivores seems to be strongly influenced by the benthic habitat. Multivariate analysis clearly separated disturbed from undisturbed sites, whereas univariate measures, such as species richness, diversity and evenness did not reveal any negative impact of disturbance. The disturbance of the coral reefs led to changes in the fish community through the reduction of total fish abundance by 50%, increased total abundance of herbivorous and detritivorous fishes, decreased total abundance of invertebrate- and fish-feeders, and increased relative abundance of planktivorous fishes.

KEY WORDS: Trophic community structure · Pollution · Shore fishes · Coral reef · Seagrass meadow · Red Sea

INTRODUCTION

The semi-enclosed Gulf of Aqaba is under high pressure by urban and industrial pollution (Mergner 1981, Walker & Ormond 1982, Abu-Hilal 1987, Abu-Hilal & Badran 1990, Abelson et al. 1999), shipping and port activities (Fishelson 1973, Loya 1975, Abu-Hilal 1985, Badran & Foster 1998) as well as tourism (Riegl & Velimirov 1991, Hawkins & Roberts 1994). The Jordanian coastline has a length of about 27 km with a discontinuous series of fringing reefs of 13 km length, interrupted by bays which are mostly covered with seagrass meadows (UNEP/IUCN 1988). During the last 25 yr, 30 to 40% of the Jordanian coastline has been altered from a pristine natural environment to a heavily used port and industrial area (Abu-Hilal 1997). In 2001, Aqaba was declared a Special Economic Zone, and therefore rapid increase in port and industrial activities is to be expected.

Industry and port activities are expected to disturb the coastal ecosystem, which will lead to changes in the fish community. On the one hand, degradation of coral reefs leads to coral death, loss of the complex habitat structure and decrease of associated invertebrates, on the other hand, algal growth is enhanced due to open substrate caused by coral decease and, in some cases, eutrophication. Fishes that depend on corals or associated invertebrates as a source of food are likely to be reduced, whereas planktivores, herbivores and detritivores can increase in relative abundance so long as the dead corals still provide shelter.

*Corresponding author. Present address: Biotechnology and Molekular Genetics, UFT-FB2, University of Bremen, Leobener Strasse, 28359 Bremen, Germany.
E-mail: kochzius@uni-bremen.de

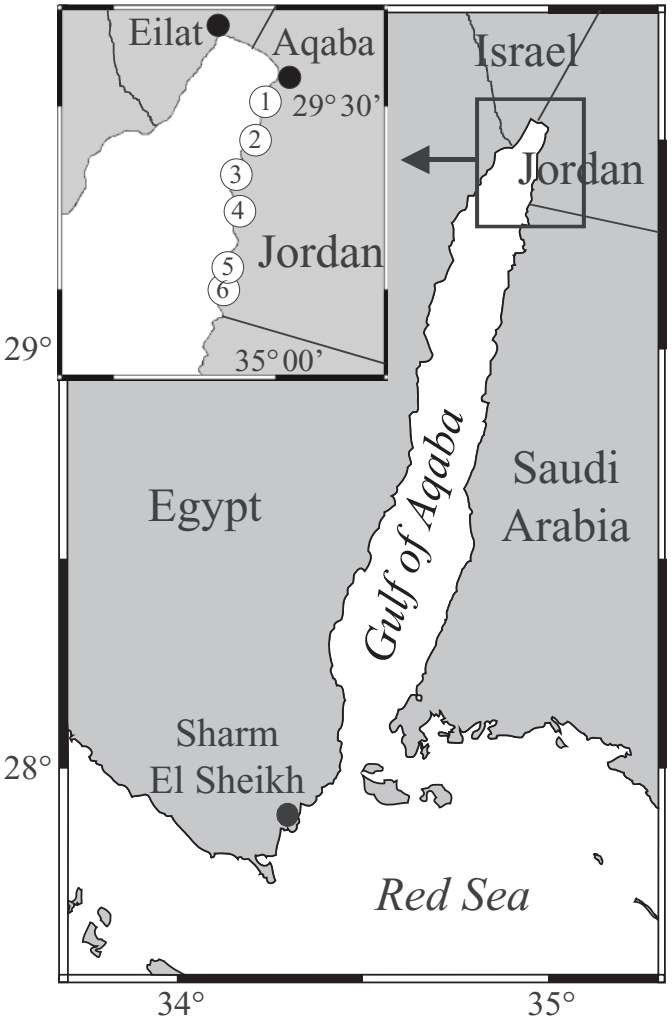

Fig. 1. Gulf of Aqaba, showing study sites along Jordanian coast. 1: cement jetty (29° 28.990′ N, 34° 59.010′ E); 2: Marine Science Station (29° 27.250′ N, 34° 58.359′ E; distance from Site 1. = 3.4 km); 3: tourist camp (N 29° 26.351′ N, 34° 58.272′ E; distance from Site 2 = 1.6 km); 4: Al-Mamlah Bay (29° 24.345′ N, 34° 58.549′ E; distance from Site 3 = 3.7 km); 5, 6: Jordan Fertiliser Industries and Jordan Fertiliser Industries jetty (29° 22.134′ N, 34° 57.667′ E; distance from Site 4 = 4.1 km)

Investigations of the impact of coral mining (Shepherd et al. 1992) and coral bleaching (Lindahl et al. 2001) on fish communities have shown that univariate measures, such as species richness and diversity, are not appropriate to reveal changes in the fish community. Therefore, we investigated the trophic community structure of fishes on disturbed as well as undisturbed coral reefs, and in a seagrass-dominated bay along the Jordanian coast. The disturbed reefs are located in front of an industrial area and port, whereas the undisturbed reefs are situated in a marine reserve and at sites with no industry or port activity.

MATERIALS AND METHODS

Study sites. Our investigation of the general trophic community structure of shore fishes in the Gulf of Aqaba is based on 5 coral reefs and the seagrass-dominated Al-Mamlah Bay at the Jordanian coast (Fig. 1). The degree of human-induced disturbance differs greatly along the coastline. The sites regarded as undisturbed are completely closed for human activities (marine reserve) or utilised for small-scale fishing as well as recreational activities. At the disturbed sites, the fringing reef in front of the Jordan Fertiliser Industries (JFI) is under pressure due to port activity, solid waste disposal, spillage during loading and unloading of ships (e.g. sulphur, ammonia), as well as disposal of waste oil from trucks (Gladstone et al. 1999) (see Table 1). In the past, parts of the reef flat were filled in for a parking place and the JFI jetty (Mahasneh & Meinesz 1984). A study on coral diseases revealed a 10-fold higher number of infected coral colonies at the JFI than in the marine reserve (Al-Moghrabi 2001). Values of phosphate concentrations (Badran & Foster 1998), heavy metals (Abu Hilal & Badran 1990), and algal cover (M.A.K. pers. obs.) are higher at the disturbed JFI than in the marine reserve at the Marine Science Station (MSS). Phosphate concentrations at JFI reach the threshold value of 0.1 to 0.2 µM, a level proposed as indicating polluted (Bell 1992). The distance between the disturbed and undisturbed sites is around 8 km.

Visual census. The fish communities in shallow-water habitats along the Jordanian coast were surveyed by the visual census technique using SCUBA, as described by English et al. (1994). Transects of 50 m length and 5 m width (250 m^2) were marked along lines at 6 sites parallel to the shore (Fig. 1, Table 2). At each site, visual censuses were conducted along 3 transects on the shallow reef slope (6 m) and deep reef slope (12 m), respectively. The distance between the transects at each site was 10 to 20 m. After laying the transect line, an observer would wait 5 to 10 min to allow fishes to resume their normal behaviour. Subsequently the diver swam 50 to 60 min along the transect and recorded all fishes encountered 2.5 m on each site of the line and 5 m above the transect. Differences in the skill and technique of the observers are a source of imprecision and/or bias (Thompson & Mapstone 1997). Therefore, the first author (M.A.K.) identified and recorded all fishes of about 30 mm total length or larger on a plastic slate. The visual census technique is widely applied and accepted for ecological fish studies on coral reefs (English et al. 1994). However, all our conclusions are restricted to diurnally active and non-cryptic species (Brock 1982). At 5 sites (cement jetty, Marine Science Station, tourist camp, Jordan Fertiliser

Table 1. Human-induced disturbance on coral reefs along Jordanian Red Sea coast, Gulf of Aqaba

Site	State	Human impact	Activities
Cement jetty	Undisturbed	Medium	Some fishing (hook and line)
Marine Science Station	Undisturbed	Very low	Marine reserve; occasionally illegal fishing
Tourist camp	Undisturbed	Low	Swimming and snorkeling
Jordan Fertiliser Industries	Disturbed	Very high	High port activity; solid waste; phosphate and trace metal pollution, sedimentation
Jordan Fertiliser Industries jetty	Disturbed	Very high	Very high port activity; solid waste; phosphate and trace metal pollution; accidental discharge of sulphur and ammonia, sedimentation

Industries and Jordan Fertiliser Industries jetty) 3 censuses were conducted at each depth in November 1999 and March 2000. In 1997 and 1998, 39 censuses were conducted at Al-Mamlah Bay at 6 m depth and 43 census at 12 m depth (Table 2). A total of 212 349 fishes were counted, representing 198 species belonging to 121 genera and 43 families. Affiliation of species with trophic groups is based on Khalaf & Disi (1997) and on field observations (Table 3).

Statistical analysis. Community indices such as fish abundance, species richness (number of species), Shannon-Wiener diversity (H'; ln basis), and Pielou's evenness (J') were compared among sites and depths using 1-way ANOVA. Homogeneity of variances was tested with the F-test and, if necessary, data were $\log(1+x)$-transformed to obtain homogeneity of variances. If transformation of the data did not lead to homogeneity of variances, no statistical test was conducted. The F-test was performed with a spreadsheet analysis programme, and 1-way ANOVA was carried out with STATISTICA 5.1 (StatSoft 1997).

Multivariate analysis of the data such as cluster analysis, MDS (multi-dimensional scaling), ANOSIM (analysis of similarities) significance test, as well as SIMPER (similarity percentages) were performed with PRIMER 5 software (Primer-E 2000). Hierarchical clustering and MDS was based on Bray–Curtis similarities. In contrast to species with very low abundance, highly abundant species can disturb an analysis. Therefore, when necessary, data were standardised (see Fig. 4A,B).

MDS is a 3-dimensional ordination of samples brought down to a 2-dimensional plot. The quality of the MDS plot is indicated by its stress value: values <0.2 give a potentially useful 2-dimensional picture, stress <0.1 corresponds to a good ordination, and stress <0.05 is an excellent representation.

The ANOSIM significance test compares similarities of species compositions between samples and can give evidence of differences. Global R indicates the degree of similarity between the tested groups, with values between –1 and 1. If all replicates within sites are more similar to each other than any replicate from different sites, the value of R is 1, values close to zero indicate that the similarity between sites is very high. A 1-way layout of ANOSIM was performed with the original data, no transformation or standardisation was conducted.

SIMPER is an analytical tool used to reveal the average Bray-Curtis dissimilarity between groups of samples. The aim of the analysis in our study was to calculate the contribution of each feeding guild to the differences between sites (Clarke & Warwick 1994).

RESULTS

Fish community parameters (Fig. 2)

Species richness showed no difference between disturbed and undisturbed coral reefs. Diversity (H') and evenness (J') were higher at the disturbed sites, whereas fish abundance on disturbed reefs was 51.4 % lower than on undisturbed reefs.

Relative species richness and relative abundance of trophic groups (Table 4)

In terms of number of species belonging to different feeding guilds, predators on invertebrates (25.3 %)

Table 2. Sampling sites along Jordanian Red Sea coast, Gulf of Aqaba

Site	n	6 m	n	12 m
Cement jetty	3	Nov 1999	3	Nov 1999
Marine Science Station	3	Nov 1999	3	Nov 1999
Tourist camp	3	Nov 1999	3	Nov 1999
Al-Mamlah Bay	39	Apr 1997–Aug 1999	43	Apr 1997–Aug 1999
Jordan Fertiliser Industries	3	Apr 2000	3	Apr 2000
Jordan Fertiliser Industries jetty	3	Apr 2000	3	Mar 2000

Table 3. Affiliation of fishes from Jordanian Red Sea coast with trophic groups based on Khalaf & Disi (1997) and on field observations. C: corallivore; D: detritivore; H: herbivore (feeds on macroalgae; Scaridae: H/C), IF: invertebrate-feeder; IFF: invertebrate- and fish-feeder; O: omnivore; Pi: piscivore; Pl: planktivore

Species	Trophic Group
Torpedinidae	
Torpedo panthera	IFF
Muraenidae	
Gymnothorax nudivomer	IFF
Siderea sp.	Pi
S. grisea	Pi
Synodontidae	
Saurida gracilis	Pi
Synodus sp.	Pi
S. variegatus	Pi
Atherinidae	
Atherinomorus lacunosus	Pl
Holocentridae	
Myripristis murdjan	Pl
Neoniphon sammara	Pl
Sargocentron caudimaculatum	Pl
S. diadema	Pl
Fistulariidae	
Fistularia commersonii	IFF
Centriscidae	
Aeoliscus punctulatus	Pl
Syngnathidae	
Corythoichthys flavofasciatus	IF
C. nigripectus	IF
C. schultzi	IF
Trachyrhamphus bicoarctatus	Pl
Scorpaenidae	
Dendrochirus brachypterus	IF
Inimicus filamentosus	
Pterois miles	IFF
P. radiata	IF
Scorpaenidae	
Scorpaenopsis sp.	IFF
S. barbata	IFF
Synanceia verrucosa	Pi
Serranidae	
Anthias taeniatus	Pl
Cephalopholis hemistiktos	IFF
C. miniata	IFF
Epinephelus fasciatus	IFF
Grammistes sexlineatus	IFF
Pseudanthias squamipinnis	Pl
Variola louti	IFF

Species	Trophic Group
Carangidae	
Carangoides fulvoguttatus	IFF
Decapterus macrosoma	Pl
Gnathanodon speciosus	IFF
Caesionidae	
Caesio lunaris	Pl
C. suevicus	Pl
C. varilineata	Pl
Nemipteridae	
Scolopsis ghanam	IF
Gerreidae	
Gerres oyena	IF
Haemulidae	
Diagramma pictum	IFF
Lethrinidae	
Lethrinus sp.	IF
Monotaxis grandoculis	IF
Sparidae	
Diplodus noct	O
Mullidae	
Mulloidichthys flavolineatus	IFF
Parupeneus cyclostomus	IFF
P. forsskali	IFF
P. macronema	IFF
P. rubescens	IFF
Pempheridae	
Pempheris vanicolensis	IFF
Chaetodontidae	
Chaetodon auriga	O
C. austriacus	C
C. fasciatus	O
C. melannotus	C
C. paucifasciatus	O
C. trifascialis	C
Heniochus diphreutes	Pl
H. intermedius	O
Pomacanthidae	
Apolemichthys xanthotis	O
Centropyge multispinis	H
Genicanthus caudovittatus	Pl
Pomacanthus imperator	IF
Pygoplites diacanthus	IF

Species	Trophic Group
Pomacentridae	
P. trilineatus	
Mugilidae	
Crenimugil crenilabis	D
Labridae	
Anampses caeruleopunctatus	IF
A. lineatus	IF
A. meleagrides	IF
A. twistii	IF
Bodianus anthioides	IF
B. axillaris	IF
B. diana	IF
Cheilinus sp.	O
C. lunulatus	O
C. mentalis	O
C. trilobatus	O
Cheilio inermis	O
Cirrhilabrus rubriventralis	Pl
Coris aygula	IF
C. caudimacula	IF
C. gaimard gaimard	IF
C. variegata	IF
Gomphosus caeruleus klunzingeri	IF
Halichoeres marginatus	IF
Halichoeres scapularis	IF
Hemigymnus fasciatus	IF
Hologymnosus annulatus	IFF
Labroides dimidiatus	IF
Larabicus quadrilineatus	C
Macropharyngodon bipartitus	IF
Novaculichthys macrolepidotus	IF
Oxycheilinus digrammus	IF
Paracheilinus octotaenia	Pl
Pseudocheilinus evanidus	Pl
P. hexataenia	Pl
Pteragogus cryptus	
P. pelycus	
Stethojulis albovittata	IF
S. interrupta	IF
Thalassoma lunare	IFF
T. rueppellii	IFF
Thalassothia cirrhosa	IFF
Xyrichtys pavo	IF

Species	Trophic Group
Scaridae	
Ecsenius aroni	IF
E. frontalis	IF
E. gravieri	IF
Exallias brevis	C
Meiacanthus nigrolineatus	IF
Plagiotremus tapeinosoma	Pi
Plagiotremus townsendi	Pi
Gobiidae	
Amblyeleotris steinitzi	IF
A. sungami	IF
Amblygobius albimaculatus	IF
Bryaninops natans	Pl
Fusigobius longispinus	IF
Gnatholepis anjerensis	IF
Gobiodon citrinus	
Istigobius decoratus	IF
Lotilia graciliosa	IF
Valenciennea puellaris	IF
Acanthuridae	
Acanthurus nigrofuscus	H
A. sohal	H
Ctenochaetus striatus	D
Naso unicornis	H
Zebrasoma veliferum	O
Z. xanthurum	O
Siganidae	
Siganus argenteus	H
S. luridus	H
S. rivulatus	H
Scombridae	
Euthynnus affinis	IFF
Bothidae	
Bothus pantherinus	IF
Samaridae	
Samaris cristatus	
Soleidae	
Pardachirus marmoratus	IF
Balistidae	
Balistapus undulatus	O
Pseudobalistes fuscus	O
Sufflamen albicaudatus	IF

Table 3. Continued

Species	Trophic Group	Species	Trophic Group	Species	Trophic Group	Species	Trophic Group
Monacanthidae		*C. novemstriatus*	Pl	*Calotomus viridescens*	H	*Cantherhines pardalis*	O
Aluterus scriptus	O	*Abudefduf vaigiensis*	O	*Chlorurus gibbus*	H	*Pervagor randalli*	O
Pseudochromidae		*Amblyglyphidodon flavilatus*	Pl	*C. sordidus*	H	**Ostraciidae**	
Pseudochromis flavivertex	O	*A. leucogaster*	Pl	*Hipposcarus harid*	C	*Pseudomonacanthus pusillus*	
P. fridmani	O	*Amphiprion bicinctus*	Pl	*Leptoscarus vaigiensis*	H	*Ostraccion cubicus*	O
P. olivaceus	O	*Chromis dimidiata*	Pl	*Scarus ferrugineus*	H	*O. cyanurus*	O
P. springeri	O	*C. pelloura*	Pl	*S. fuscopurpureus*	H	*Tetrosomus gibbosus*	O
Priacanthidae		*C. pembae*	Pl	*S. ghobban*	H	**Tetraodontidae**	
Priacanthus hamrur	Pl	*C. ternatensis*	Pl	*S. niger*	H	*Arothron diadematus*	O
Apogonidae		*C. viridis*	Pl	*S. psittacus*	H	*A. hispidus*	O
Apogon sp.	Pl	*C. weberi*	Pl	**Pinguipedidae**		*A. stellatus*	O
A. aureus	Pl	*Dascyllus aruanus*	O	*Parapercis hexophtalma*	IFF	*Canthigaster coronata*	O
A. cyanosoma	Pl	*D. marginatus*	O	**Uranoscopidae**		*C. margaritata*	O
A. exostigma	Pl	*D. trimaculatus*	Pl	*Uranoscopus sulphureus*	IFF	*C. pygmaea*	O
A. fraenatus	Pl	*Neoglyphidodon melas*	C	**Blenniidae**		*Torquigener flavimaculosus*	O
A. nigrofasciatus	Pl	*Neopomacentrus miryae*	Pl	*Aspidontus taeniatus taeniatus*	O	**Diodontidae**	
Cheilodipterus lachneri	Pl	*Pomacentrus sulfureus*	O	*Cirripectes castaneus*		*Cyclichthys spilostylus*	IF
C. macrodon	Pl	*P. trichourus*	IFF	*Amanses scopas*	O		

were the most common feeding guild, followed by planktivores (20.8%) and omnivores (19.2%).

In terms of relative abundance, 58.1% of all fish specimens were planktivorous on coral reefs, and as much as 79.9% in the seagrass-dominated Al Mamlah Bay. Other important trophic groups on coral reefs were invertebrate- and fish-feeders (23.1%), omnivores fishes (11.6%) and herbivores (3.4%). These 3 groups showed a low relative abundance (5 to 6.5%) at Al Mamlah Bay.

Totale abundance of trophic groups (Fig. 3 & Table 5)

The total abundance of the various trophic groups at the different sites revealed patterns connected with the benthic habitat or disturbance at the respective sites. Those patterns were all statistically highly significant.

Corallivores were less abundant at the seagrass-dominated site than on coral reefs. Planktivores were more abundant at 12 m than at 6 m depth on both the coral reefs and at the seagrass-dominated site. The abundance of planktivores at 12 m depth was higher on undisturbed coral reefs than on disturbed reefs, and was higher in the seagrass meadow than on coral reefs.

In the seagrass-dominated Al-Mamlah Bay and on the disturbed coral reefs, herbivores were more abundant at 6 m than at 12 m depth. Comparison of herbivores in 6 m depth between disturbed and undisturbed coral reefs revealed a higher abundance for disturbed reefs.

The number of detritivores was higher on coral reefs than in the seagrass meadow. Disturbed coral reefs tended to have a larger population of detritivores than undisturbed reefs, especially on the shallow reef slope.

Invertebrate- and fish-feeders were more abundant on coral reefs, and their numbers were higher on undisturbed than on disturbed coral reefs, especially on the shallow reef slope.

Invertebrate-feeders had a larger population in the seagrass meadow.

In the seagrass-dominated Al-Mamlah Bay, piscivores were higher in abundance at 12 m than at 6 m. In addition, the population of piscivores at 12 m was larger than on coral reefs.

Omnivores tended to be more abundant on the deep reef slope than on the shallow reef slope, but there was no significant difference between sites.

Multivariate analysis

The cluster analysis and the MDS plot based on abundance of feeding guilds on coral reefs on the shal-

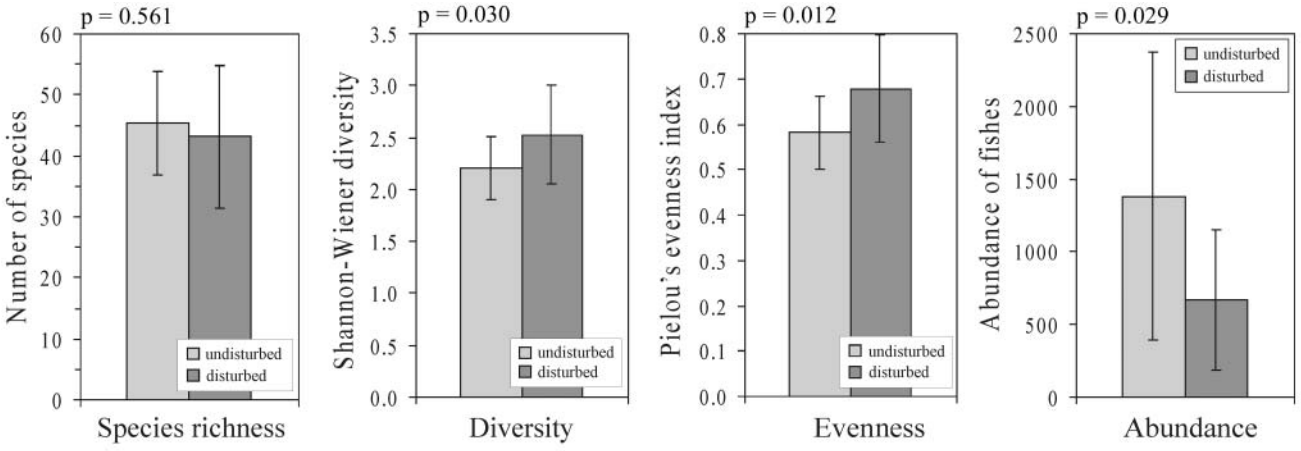

Fig. 2. Fish community parameters (species richness, diversity, eveness, abundance) of undisturbed and disturbed coral reefs at the Jordanian Red Sea coast, Gulf of Aqaba. Bold-face = significant values (1-way ANOVA)

low (6 m) and deep (12 m) reef slope revealed 2 clusters: (1) disturbed, and (2) undisturbed coral reefs (Fig. 4). Analysis of the shallow reef slope showed 2 mismatches (Samples 6a: Fig. 4), but these did not affect the general pattern. A dendrogram and MDS plot of the deep reef slope communities included 2 mismatches at disturbed reefs (Samples 1b and 2b) without affecting the division into the 2 groups. An ANOSIM test confirmed the pattern of both multivariate analyses (Fig. 4). The dendrogram and MDS plot for species abundance were more or less identical to the multivariate analysis of feeding guilds, and are therefore not presented here.

SIMPER analysis revealed that invertebrate- and fish-feeders (48.4%) and planktivores (41.3%) were the main feeding guilds responsible for differences in community structure between disturbed and undisturbed shallow reef slopes. Invertebrate feeders (4.2%), herbivores (3.1%) and omnivores (1.7%) contributed a minor percentage to the dissimilarity between the 2 groups (Table 6). On deep reef slopes, planktivores (64.2%) and invertebrate- and fish-feeders (23.5%) contributed most of the dissimilarity between undisturbed and disturbed sites, whereas omnivores (7.4%), herbivores (2.1%) and invertebrate-feeders (1.2%) played a minor role (Table 6).

Trophic structure of fish fauna on disturbed and undisturbed coral reefs (Fig. 5)

Fish communities on the shallow slope of disturbed coral reefs showed a higher relative abundance of planktivores and herbivores than undisturbed reefs, whereas the relative abundance of omnivores and fish and invertebrate feeders was reduced at the disturbed sites. On the deep reef slope the picture is not so clear. The relative abundance of planktivores and invertebrate- and fish-feeders was reduced at the disturbed coral reef, whereas omnivores and herbivores showed a higher relative abundance.

Table 4. Trophic composition of fish fauna in shallow water habitats along Jordanian Red Sea coast, Gulf of Aqaba

Feeding guilds	Species richness		Relative abundance (%)	
	n	%	Coral reef	Seagrass-dominated bay
Corallivores	7	3.5	0.8	0.1
Herbivores	17	8.6	3.4	6.5
Planktivores	41	20.8	58.1	79.9
Detritivores	2	1.0	0.5	0.1
Invertebrate- and fish-feeders	28	14.1	23.1	5.5
Invertebrate feeder	50	25.3	2.3	2.5
Omnivores	38	19.2	11.6	5.0
Piscivores	8	4.0	0.1	0.2
Unknown	7	3.5	0.0	0.2

DISCUSSION

Fish counts took place at the disturbed site in March and April 2000, and at the undisturbed sites in November 1999. The possibility of the differences detected being due to seasonal changes within the fish community was considered. Our study on the community structure of shore fishes of the Jordanian coast (Khalaf

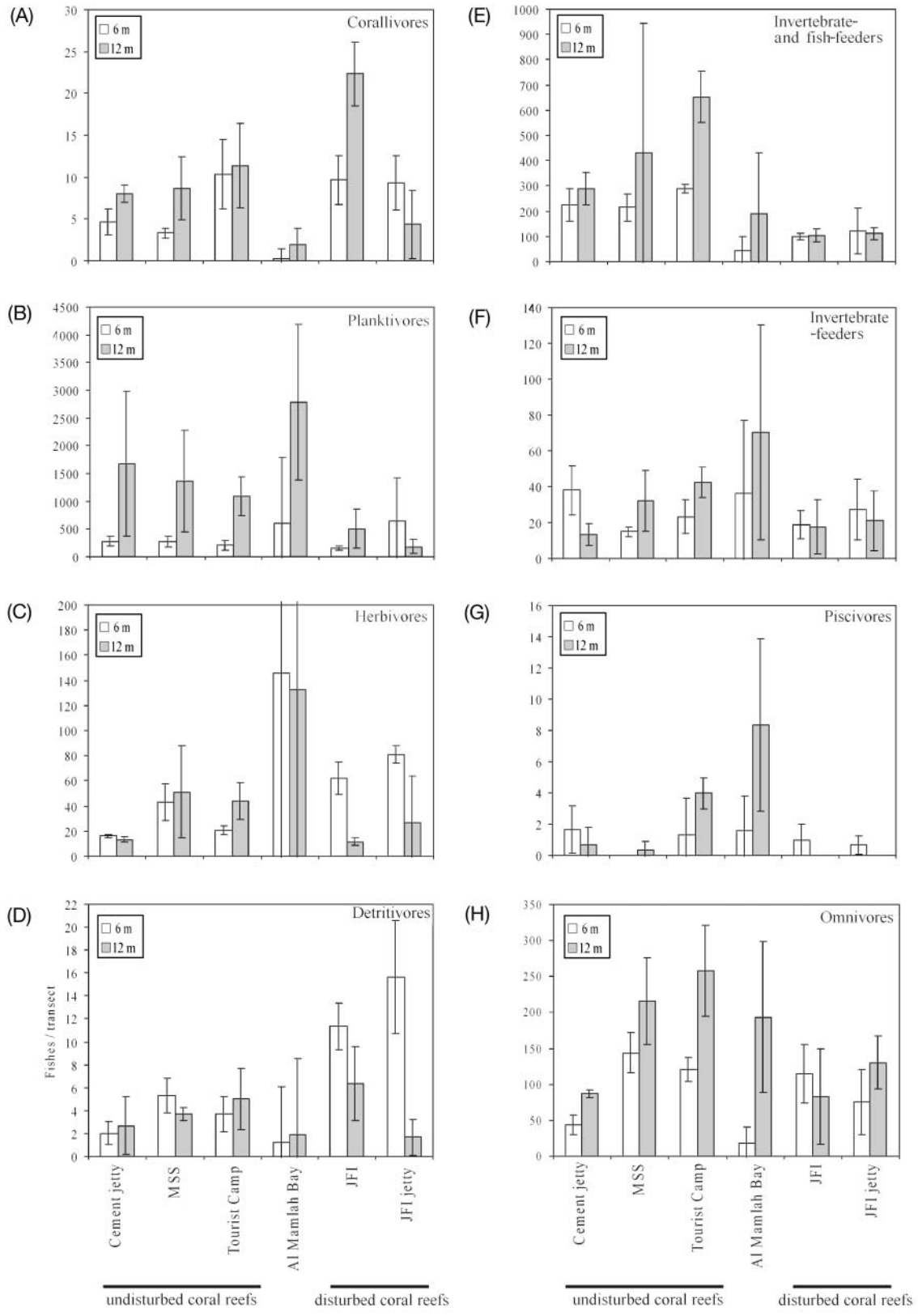

Fig. 3. Abundance of trophic fish groups (mean ± SD) at sites along Jordanian Red Sea coast, Gulf of Aqaba. (A) corallivores; (B) planktivores; (C) herbivores; (D) detritivores; (E) invertebrate- and fish-feeders; (F) invertebrate-feeders; (G) piscivores; (H) omnivores. Note different ordinate scales. JFI: Jordan Fertiliser Industries

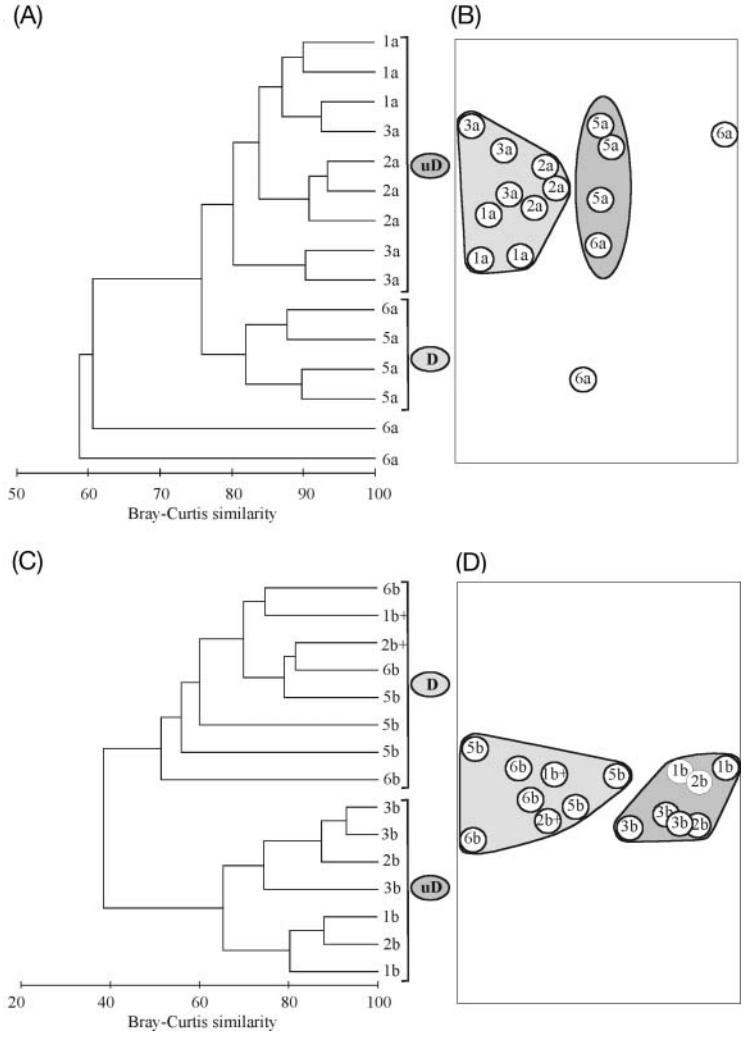

Fig. 4. Fish communities on disturbed and undisturbed coral reefs along Jordanian Red Sea coast, Gulf of Aqaba (based on abundance of feeding guilds—no pelagic or semi-pelagic species). (A, B) Dendrogram (A) and MDS plot (B) of shallow reef slope (6 m, Bray-Curtis similarity, standardisation, group average; stress = 0.05; ANOSIM: global R = 0.0553, p <0.001); (C, D) dendrogram (C) and MDS plot (D) of deep reef slope (12 m, Bray-Curtis similarity, group average; stress = 0.04; ANOSIM: global R = 0.493, p = 0.004). Sites numbered as in Fig. 1 (a = 6 m depth, b = 12 m depth). D: disturbed coral reefs; uD: undisturbed coral reefs; +: mismatch

& Kochzius 2002) revealed a strong spatial influence of habitat composition, but no temporal pattern. Studies on the colonisation of artificial reefs in Eilat (Rilov & Benayahu 1998, Golani & Diamant 1999) indicate that most recruitment takes place between January and May, with lower overall fish abundance in November. In contrast to these findings, total abundance was higher at the undisturbed sites in November than at the disturbed sites in March and April in our study. If temporal changes had been important, an opposite picture would have been expected. Therefore we can assume that temporal effects were not the reason for the observed differences.

Table 5. One-way ANOVA of abundance of feeding guilds at sites along Jordanian Red Sea coast, Gulf of Aqaba. Bold-face: significant p-values; *log(*x*+1)-transformed data; iv: inhomogenous variances; S: seagrass-dominated habitat; CR: coral reef; ud: undisturbed coral reef; d: disturbed coral reef; abbreviations of feeding guilds as in Table 3

Depth (habitat)	Feeding guilds							
	C	Pl	H	D	IFF	IF	Pi	O
S vs CR	**<0.001*** S < CR	iv	iv	**<0.001** S < CR	**0.002** S < CR	**0.020*** S > CR	iv	iv
12 m (S) vs 12 m (CR)	**<0.001*** S < CR	**<0.001** S > CR	0.124*	**<0.001*** S < CR	0.102	**<0.001*** S > CR	**<0.001*** S > CR	0.199
6 m vs 12 m (CR)	0.106	**0.009*** 6 m < 12 m	0.053*	0.885*	0.409	0.879	0.904	**0.035** 6 m < 12 m
6 m vs 12 m (S)	iv	**<0.001** 6 m < 12 m	**<0.001*** 6 m > 12 m	0.616	iv	iv	**<0.001*** 6 m < 12 m	iv
ud vs d	0.091	0.094	0.175	**0.035*** ud < d	**<0.001*** ud > d	0.245	0.164*	0.106
6 m vs 12 m (d)	0.406	0.847	**0.001** 6 m > 12 m	**0.001*** 6 m > 12 m	0.879	0.632	**0.022** 6 m > 12 m	0.691
6 m (ud) vs 6 m (d)	0.090	iv	**<0.001** ud < d	**<0.001** ud < d	**<0.001** ud > d	0.744	0.857	0.763
12 m (ud) vs 12 m (d)	iv	**0.014** ud > d	0.230	0.878	iv	0.242	0.058	0.072

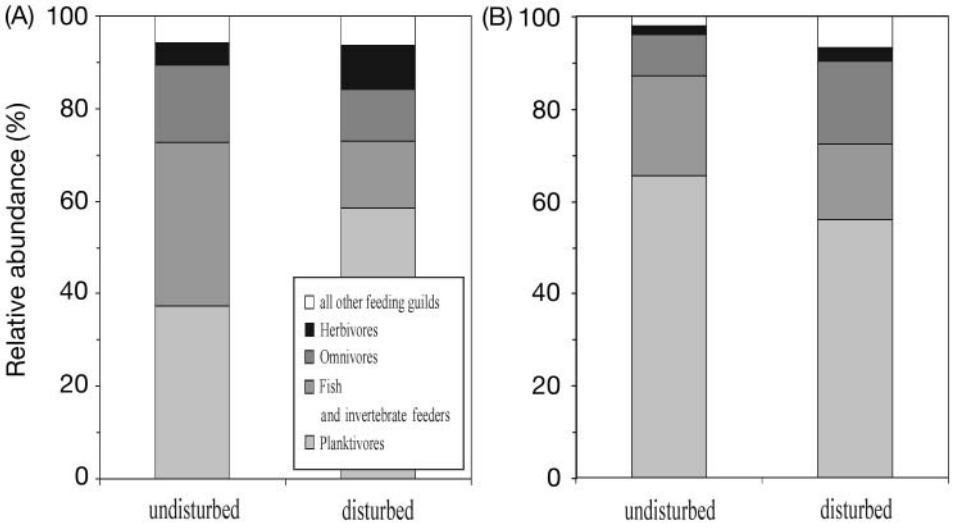

Fig. 5. Trophic composition of the fish fauna on disturbed and undisturbed coral reefs along Jordanian Red Sea coast, Gulf of Aqaba. (A) Shallow reef slope (6 m); (B) deep reef slope (12 m)

Trophic structure of the community

Planktivore fishes dominate the fish community on coral reefs in the Gulf of Aqaba. This finding corresponds with studies in Sri Lanka, the Great Barrier Reef, New Caledonia and the Gulf of Mexico (Williams & Hatcher 1983, Öhman et al. 1997, Pattengill et al. 1997, Rossier & Kulbicki 2000; Table 7). Zooplankton as a source of food, at least for diurnally active fishes, is fairly independent of the benthic habitat composition. Similar pattern of transport of the zooplankton result in a consistent dominance of planktivorous fishes on different coral reefs.

A comparison of our results with those of other studies revealed differences in the ranking and relative abundance of the other feeding guilds (Table 7). In Sri Lanka, New Caledonia, the Great Barrier Reef and the Gulf of Mexico, herbivores contribute a much higher proportion (2 to 7 times higher) to the fish community than they do in the Gulf of Aqaba. The relative abundance of herbivorous fishes was even lower at the seagrass-dominated site in the Gulf of Aqaba (Tables 4 & 7) than on the coral reef sites in other parts of the world.

Table 6. Contribution of feeding guilds to community shift between disturbed and undisturbed coral reefs on the Jordanian Red Sea coast, Gulf of Aqaba (no transformation of data)

Feeding guild	Contribution to dissimilarity (%) at: 6 m depth	12 m depth
Invertebrate- and fish-feeders	48.41	23.45
Planktivores	41.27	64.19
Invertebrate-feeders	4.22	1.13
Herbivores	3.14	2.07
Omnivores	1.72	7.37
Detritivores	0.59	0.21
Unknown	0.40	0.61
Corallivores	0.19	0.68
Piscivores	0.08	0.12

The relative abundance of piscivores is more than 10-fold higher on the coral reefs in Sri Lanka, New Caledonia, the Great Barrier Reef and the Gulf of Mexico than on the Jordanian coast. These differences could be due to various factors such as prey availability, shelter and fishing, but could also be due to

Table 7. Relative abundance (%) of feeding guilds of fishes on coral reefs

Feeding guild	Aqaba[a]	Sri Lanka[b]	Great Barrier Reef[c]	New Caledonia[d]	Gulf of Mexico[e]
Corallivores	0.8	1.3			
Herbivores	3.4	12.0	6.6	14.3	11.7–23.0
Planktivores	58.1	81.0	85.0	65.0	65.0
Omnivores	11.6	1.5			
Piscivores	0.1	2.5	3.6	1.0	1.3–2.8

[a]This study; [b]calculated from Öhman et al. (1997); [c]Williams & Hatcher (1983); [d]Rossier & Kulbicki (2000); [e]Pattengill et al. (1997)

Table 8. Trophic composition (%) of fish assemblages on coral reefs. *: sessile invertebrate browsers. No. of scleractinian coral species is also shown

Feeding guild	Aqaba[a]	Eilat[b]	Sanganeb atoll[c]	Sri Lanka[d]	Great Barrier Reef[e]	Tulear[f]	Moorea[f]	Moorea[g]	Reunion[g]	New Caledonia[g]	Gulf of Mexico[h]
Corallivores	3.5	3.5	7.4	8.1	4.6	6.2*	8.9*	11.0	7.0	8.0	
Herbivores	8.6	10.6	7.4	20.7	14.9	10.1	15.4	3.0	2.5	4.0	15.0
Planktivores	20.8	18.3	24.6	13.3	19.8	10.3	9.6	10.0	8.0	13.0	13.1
Detritivores	1.0	0.7	0.0	3.0				2.5	3.0	3.0	
Invertebrate- and fish-feeders	14.1	10.6	10.7	8.9	52.6	53.8	45.0	40.5	46.0	38.5	18.3
Invertebrate-feeder	25.3	22.5	22.1	20.7							
Piscivores	4.0	5.6	5.7	14.1	8.1	4.0	5.7	7.0	12.5	10.0	28.8
Omnivores	19.2	19.7	18.0	11.1		15.6	15.4	26.0	21.0	23.5	
Unknown	3.5	8.5	4.1								24.8
Scleractinian coral species (n)	138[i]		146[i]	118[j]	212[k]		72[l]		120[m]	108[n]	

[a]This study; [b]Rilov & Benayahu (2000); [c]Krupp et al. (1993); [d]Öhman et al. (1997); [e]Williams & Hatcher (1983); [f]Harmelin-Vivien (1989); [g]Letourneur et al. (1997); [h]Pattengill et al. (1997); [i]Antonius et al. (1990); [j]Rajasuriya et al. (1998); [k]Done (1982), [l]Adjeroud (1997); [m]Bouchon (1981); [n]UNEP/IUCN (1988)

methodological differences. Öhman et al. (1997) restricted their fish counts to 135 species, and Williams & Hatcher (1983) used explosive charges for sampling.

Besides relative abundance, the trophic species composition also reflects the trophic structure of the community (Table 8). Invertebrate feeders are the dominant feeding guild on coral reefs in terms of species richness (Jones et al. 1991), followed by planktivores and omnivores. Detrives comprise only a minor proportion of the ichthyofauna on coral reefs. The number of herbivores varies considerably within the fish communities of different geographical regions, and seems to be much lower around the oceanic islands of Moorea and Réunion and in New Caledonia.

The proportion of species belonging to particular feeding guilds is very similar between the 3 sites in the Red Sea (Aqaba, Eilat, Sanganeb atoll: Table 8), but differs somewhat from sites in the Indian and Pacific Oceans and the Gulf of Mexico (Table 8). The contribution of planktivorous species to fish assemblages in the Red Sea seems to be high in comparison to other coral reefs in the world, whereas piscivores play only a minor role. At the northern tip of the Gulf of Aqaba, the percentage of corallivorous species is only about half that in the central Red Sea and reefs in other parts of the Indo-Pacific. This might be due to lower scleractinian species richness in the Gulf compared to the central Red Sea (Antonius et al. 1990). However, no general correlation between the number of scleractinian corals and percentage of corallivorous species of a fish assamblage could be detected in the present study (Table 8).

Comparing the trophic structure of the ichthyofauna at the Jordanian coast with that of other coral reefs, we can conclude that: (1) the high relative abundance of planktivores is a general feature of the community structure of fishes on coral reefs; (2) most species on coral reefs are invertebrate feeders; (3) the relative abundance of feeding guilds other than planktivores seems to be strongly influenced by the benthic habitat; (4) the trophic species structure of fish communities on Red Sea coral reefs seems to be different from that on reefs in other parts of the Indo-Pacific Ocean.

Comparison between coral reefs and seagrass-dominated site

The reduced abundance of corallivores in the seagrass-dominated site at Al-Mamlah Bay is not surprising, since these fishes are strongly associated with live stony corals (Bouchon-Navaro et al. 1985, Jennings et al. 1996, Öhman & Rajasuriya 1998, Khalaf & Kochzius 2002). Despite the low coral cover and reduced shelter in Al-Mamlah Bay, the abundance of planktivorous fishes at 12 m depth is much higher than at all other study sites. In addition, the rich crustacean fauna of the seagrass meadows can support more invertebrate-feeders than coral reefs. Nocturnal feeding migrations of invertebrate-feeders from coral reefs into seagrasses are documented for the Atlantic as well as the Indo-Pacific (Weinstein & Heck 1979, Bell & Pollard 1989, Kochzius 1999). The higher prey availability at the seagrass-dominated Al-Mamlah correlates with a higher abundance of piscivores in the bay than at the coral reef sites.

Human impact

Univariate measures such as species richness, diversity and evenness were not able to demonstrate a negative impact of the industrial complex on the coral reef ichthyofauna. This situation is not uncommon, and has been reported in studies on the effect of coral mining (Shepherd et al. 1992) and coral bleaching (Lindahl et al. 2001). Investigations into the impact of dredging revealed a significant reduction in species richness on some reefs in French Polynesia, whereas other sites showed no difference from undredged areas (Harmelin-Vivien 1992). However, experimental coral disturbance led to a significant decline in fish species richness on the Great Barrier Reef (Lewis 1997). The higher diversity and evenness at the disturbed sites in the present study could be explained by the intermediate disturbance hypothesis (Connell 1978), i.e. an initial increase in diversity with increasing disturbance followed by a decrease at high levels of disturbance.

The abundance of fishes on disturbed reefs was half that on undisturbed reefs. In other geographical areas, significant declines in fish abundance have been caused by coral mining (Shepherd et al. 1992: the Maldives), turbidity and sedimentation due to dredging (Amesbury 1981: eastern Caroline islands), eutrophication (Chabanet et al. 1995: Indian Ocean) and experimental coral disturbance (Lewis 1997: Great Barrier Reef). However, disturbance by dredging in Moorea and Tahiti led to a decrease in fish abundance at some sites, whereas other reefs showed no significant difference (Harmelin-Vivien 1992). Mass mortality of bleached corals in Tanzania even triggered an increase in fish abundance, due to algal growth which supported a higher standing stock of herbivores (Lindahl et al. 2001).

Analysis of the trophic structure is very important when examining changes in the fish community due to human-induced disturbance. In our study, a higher abundance of detritivores was found on disturbed coral reefs, whereas the number of invertebrate- and fish-feeders was higher on undisturbed reefs. The reduction in invertebrate- and fish-feeders at disturbed sites can be explained by the loss of habitat structure due to degradation. The associated prey fauna of this feeding guild is reduced, and the disturbed reef cannot support a high number of invertebrate- and fish-feeders.

Herbivores were more abundant on the shallow slope of disturbed than undisturbed reefs, indicating a higher biomass of macroalgae on the slope. An increase in abundance of herbivorous fishes was reported after an increase in soft algae on Caribbean coral reefs, due to mass mortality of competing sea urchins (Robertson 1991). An increase in the abundance of some certain herbivorous fish species on degraded coral reefs has been described for bleached reefs by Lindahl et al. (2001) and after experimental coral disturbance by Lewis (1998). In contrast, no change in the abundance and biomass of some herbivores was detected on reefs impacted by the crown-of-thorns starfish *Acanthaster planci* with subsequent algal overgrowth (Hart et al. 1996).

There was a shift in the trophic composition of the ichthyofauna forwards planktivores on the shallow slope of disturbed reefs in our study. This could be due to the independence of planktivores from the benthic substrate in terms of food availability. Onshore transport of zooplankton depends on the oceanographic conditions and not on the condition of the reef. As long as enough shelter is available, these species can survive on a degraded coral reef (Lindahl et al. 2001). On the deep slope of the disturbed reefs in the present study, omnivores increased in relative abundance. This guild of fishes consisted of non-specialised feeders more able to cope with changes in the benthic habitat than invertebrate- and fish-feeders.

Apart from trophic considerations, recruitment to the degraded reef could also be reduced, through decreased settlement due to habitat loss or through higher mortality due to loss of shelter space (Shulman 1985, Schmitt & Holbrook 1999).

In summary, the following changes in the fish community were recorded on the coral reef fronting the industrial complex: (1) 50% reduction in fish abundance; (2) increased total abundance of herbivorous and detritivorous fishes; (3) decreased total abundance of invertebrate- and fish-feeders; (4) resultant changes in the trophic composition, such as increased relative abundance of planktivores.

These changes are probably the synergetic effects of coastal constructions, sedimentation, nutrient input, algal growth, coral destruction and heavy metal load. In the course of future urbanisation and industrialisation of the Jordanian Red Sea coast, increased coastal pollution is expected. Because of the short (27 km long) coastline, future industrial development should be restricted to already industrialised areas, in order to preserve the remaining coral reefs and seagrass meadows. Marine reserves such as the Red Sea Marine Peace Park and regional co-operation between countries bordering the Gulf of Aqaba are important for the protection of coastal ecosystems.

Acknowledgements. We would like to express our thanks to the foundations, institutions and to the individuals that have made our work possible: director and staff of the Marine Science Station, in particular O. Al-Momani for assistance in diving, and M. Badran for his comments on the manuscript; Authority of the Aqaba Special Economic Zone; Office of Ocean and Coastal Resource Management (OCRM/NOS, NOAA) and USAID; M. Crospy (NOOA); Red Sea Programme

on Marine Sciences (RSP), funded by the German Federal Ministry of Education and Research (BMBF, grant no. 03F0151A); Centre for Tropical Marine Ecology (ZMT), in particular G. Hempel and C. Richter for improving the manuscript with their comments; M. Birkicht for assistance in statistical analysis; P. Westhaus-Ekau for logistical support.

LITERATURE CITED

Abelson A, Shteinman B, Fine M, Kaganovsky S (1999) Mass transport from pollution sources to remote coral reefs in Eilat (Gulf of Aqaba, Red Sea). Mar Pollut Bull 38:25–29

Abu-Hilal AH (1985) Phosphate pollution in the Jordan Gulf of Aqaba. Mar Pollut Bull 16:281–285

Abu-Hilal AH (1987) Distribution of trace elements in nearshore surface sediments from the Jordan Gulf of Aqaba (Red Sea). Mar Pollut Bull 18:190–193

Abu Hilal AH (1997) Effects of coastal zone development and management on the coral reefs of the Jordan Gulf of Aqaba (Red Sea). In: NOAA (ed) Report of the Middle East Seas Regional Strategy Workshop for the International Coral Reef Initiative. Aqaba, Jordan, 21–25 September 1997. National Oceanic and Atmospheric Administration, Silver Springs, MD

Abu-Hilal AH, Badran MM (1990) Effect of pollution source on metal concentration in sediment cores from the Gulf of Aqaba. Mar Pollut Bull 21:190–197

Adjeroud M (1997) Factors influencing spatial patterns on coral reefs around Moorea, French Polynesia. Mar Ecol Prog Ser 159:105–119

Al-Moghrabi (2001) Unusual black band disease (BBD) outbreak in the northern tip of the Gulf of Aqaba (Jordan). Coral Reefs 19:330–331

Amesbury SS (1981) Effects of turbidity on shallow-water reef fish assemblages in Truk, eastern Caroline Islands. Proc 4th Int Coral Reef Symp 1:155–159

Antonius A, Scheer G, Bouchon C (1990) Corals of the Eastern Red Sea. Atoll Res Bull 334:1–22

Badran MI, Foster P (1998) Environmental quality of the Jordanian coastal waters of the Gulf of Aqaba, Red Sea. Aquat Ecosyst Health Manag 1:75–89

Bell JD, Pollard DA (1989) Ecology of fish assemblages and fisheries associated with seagrasses. In: Larkum AWD, McComb AJ, Shepherd SA (eds) Biology of seagrasses: a treatise on the biology of seagrasses with special reference to the Australian region. Elsevier, Amsterdam, p 565–609

Bell PRF (1992) Eutrophication and coral reefs—some examples in the Great Barrier Reef lagoon. Water Res 26: 553–568

Bouchon C (1981) Quantitative study of the scleractinian coral communities of a fringing reef of Réunion Island (Indian Ocean). Mar Ecol Prog Ser 4:273–288

Bouchon-Navaro Y, Bouchon C, Harmelin-Vivien ML (1985) Impact of coral degradation on a chaetodontid fish assemblage (Moorea, French Polynesia). Proc 5th Int Coral Reef Congr 5:427–432

Brock RE (1982) A critique of the visual census method for assessing coral reef fish populations. Bull Mar Sci 32: 269–276

Chabanet P, Dufor V, Galzin R (1995) Disturbance impact on reef fish communities in Réunion Island (Indian Ocean). J Exp Mar Biol Ecol 188:29–48

Clarke KR, Warwick RM (1994) Changes in marine communities: an approach to statistical analysis and interpretation. Natural Environment Research Council, Swindon, UK

Connell JH (1978) Diversity in tropical rain forests and coral reefs. Science 199:1302–1309

Done TJ (1982) Patterns in the distribution of coral communities across the Central Great Barrier Reef. Coral Reefs 1: 95–107

English C, Wilkinson C, Baker V (1994) Survey manual for tropical marine resources. Australian Institute of Marine Science, Townsville, QD

Fishelson L (1973) Ecology of coral reefs in the Gulf of Aqaba (Red Sea) influenced by pollution. Oecologia 12:55–67

Gladstone W, Tawfiq N, Nasr D, Andersen I, Cheung C, Drammeh H, Krupp F, Lintner S (1999) Sustainable use of renewable resources and conservation in the Red Sea and Gulf of Aden: issues, needs and strategic actions. Ocean Coast Manag 42:671–697

Golani D, Diamant A (1999) Fish colonization of an artificial reef in the Gulf of Eilat, northern Red Sea. Environ Biol Fish 54:275–282

Harmelin-Vivien ML (1989) Reef fish community structure: an Indo-Pacific comparison. In: Harmelin-Vivien ML, Bourlière F (eds) Vertebrates in complex tropical systems. Springer-Verlag, Berlin, p 21–60

Harmelin-Vivien M (1992) Impact des activités humaines sur les peuplements ichthyologiques des récifes coralliens de Polynésie Française. Cybium 16:279–289

Hart AM, Klumpp DW, Russ GR (1996) Response of herbivorous fishes to crown-of-thorns starfish *Acanthaster planci* outbreaks. II. Density and biomass of selected species of herbivorous fish and fish-habitat correlations. Mar Ecol Prog Ser 132:21–30

Hawkins JP, Roberts CN (1994) The growth of coastal tourism in the Red Sea: present and future effects on coral reefs. Ambio 23:503–508

Jennings S, Boullé DP, Polunin NVC (1996) Habitat correlates of the distribution and biomass of Seychelles' reef fishes. Environ Biol Fishes 46:15–25

Jones GP, Ferrell DJ, Sale PF (1991) Fish predation and its impacts on the invertebrates of coral reefs and adjacent sediments. In: Sale PF (ed) The ecology of fishes on coral reefs. Academic Press, San Diego, p 156–179

Khalaf MA, Disi AM (1997) Fishes of the Gulf of Aqaba. Marine Science Station, Aqaba

Khalaf MA, Kochzius M (2002) Community structure and biogeography of shore fishes in the Gulf of Aqaba, Red Sea. Helgol Mar Res 55:252–284

Kochzius M (1999) Interrelation of ichthyofauna from a seagrass meadow and coral reef in the Philippines. In: Séret B, Sire J-Y (eds) Proc 5th Indo-Pacific Fish Conf (Nouméa, 3–8 November 1997). Société Française d'Ichthyologie and Institut de Recherche pour le Développement, Paris, p 517–535

Krupp F, Paulus T, Nasr D (1993) Coral reef fish survey. In: Krupp F, Türkay M, El Hag AGD, Nasr D (eds) Comparative ecological analysis of biota and habitats in littoral and shallow sublittoral waters of the Sudanese Red Sea. Project report. Forschungsinstitut Senckenberg, Frankfurt, and Faculty of Marine Science and Fisheries, Port Sudan, p 63–82

Letourneur Y, Kulbicki M, Galzin R, Harmelin-Vivien M (1997) Comparaison des peuplements de poissons marins des récifs frangeants de trois îles océaniques de l'Indo-Pacifique (La Réunion, Moorea et la Nouvelle-Calédonie). Cybium 21(Suppl):129–145

Lewis AR (1997) Effects of experimental coral disturbance on the structure of fish communities on large patch reefs. Mar Ecol Prog Ser 161:37–50

Lewis AR (1998) Effects of experimental coral disturbance on

the population dynamics of fishes on large patch reefs. J Exp Mar Biol Ecol 230:91–110
Lindahl U, Öhman MC, Schelten CK (2001) The 1997/1998 mass mortality of corals: effects on fish communities on a Tanzanian coral reef. Mar Pollut Bull 42:127–131
Loya Y (1975) Possible effects of water pollution on the community structure of Red Sea corals. Mar Biol 29:177–185
Mahasneh D, Meinesz A (1984) Coastal management impact on the sublittoral zone of the Jordan coast of the Gulf of Aqaba. Proc Symp Coral Reef Env in the Red Sea, Jeddah, p 626–639
Mergner H (1981) Man-made influences on and natural changes in the settlement of the Aqaba reefs (Red Sea). Proc 4th Int Coral Reef Symp 1:193–207
Öhman MC, Rajasuriya A (1998) Relationships between structure and fish communities on coral and sandstone reefs. Environ Biol Fishes 53:19–31
Öhman MC, Rajasuriya A, Ólafsson E (1997) Reef fish assemblages in north-western Sri Lanka: distribution patterns and influence of fishing practises. Environ Biol Fishes 49: 45–61
Pattengill CV, Semmens BX, Gittings SR (1997) Reef fish structure at the Flower Gardens and Stetson Bank, NW Gulf of Mexico. Proc 8th Int Coral Reef Symp 1:1023–1028
Primer-E (2000) PRIMER 5. Plymouth Routines in Multivariate Ecological Research). PRIMER-E Ltd, Plymouth Marine Laboratory, Plymouth, UK
Rajasuriya A, Öhman MC, Johnstone RW (1998) Coral and sandstone reef-habitats in north-western Sri Lanka: patterns in the distribution of coral communities. Hydrobiologia 362:31–43
Riegl B, Velimirov B (1991) How many damaged corals in the Red Sea reef systems? A quantitative survey. Hydrobiologia 216/217:249–256
Rilov G, Benayahu Y (1998) Vertical artificial structures as an alternative habitat for coral reef fishes in disturbed areas. Mar Environ Res 45(4/5):431–451
Rilov G, Benayahu Y (2000) Fish assemblages on natural versus vertical artificial reefs: the rehabilitation perspective. Mar Biol 136:931–942
Robertson DR (1991) Increase in surgeonfish populations after mass mortality of the sea urchin *Diadema antillarum* in Panamá indicate food limitation. Mar Biol 111:437–444
Rossier O, Kulbicki M (2000) A comparison of fish assemblages from two types of algal beds and coral reefs in the south-west lagoon of New Caledonia. Cybium 24:3–26
Schmitt RJ, Holbrook SJ (1999) Settlement and recruitment of three damselfish species: larval delivery and competition for shelter space. Oecologia 118:76–86
Shepherd ARD, Warwick RM, Clarke KR, Brown BE (1992) An analysis of fish community response to coral mining in the Maldives. Environ Biol Fishes 33:367–380
Shulman MJ (1985) Recruitment of coral reef fishes: effects of distribution of predators and shelter. Ecology 66:1056–1066
StatSoft (1997) STATISTICA for Windows 5.1, StatSoft, Tulsa
Thompson AA, Mapstone BD (1997) Observer effects and training in underwater visual surveys of reef fishes. Mar Ecol Prog Ser 154:53–63
UNEP/IUCN (United Nations Environment Programme/International Union for Conservation of Nature and Natural Resources) (1988) Coral reefs of the world. UNEP Regional Seas Directories and Bibliographies. IUCN, Gland, Switzerland, and Cambridge, UK, and UNEP, Nairobi, p 145–151
Walker DI, Ormond RFG (1982) Coral death from sewage and phosphate pollution at Aqaba, Red Sea. Mar Pollut Bull 13: 21–25
Weinstein MP, Heck, KL (1979) Ichthyofauna of seagrass meadows along the Caribbean coast of Panama and in the Gulf of Mexico: composition, structure and community ecology. Mar Biol 50:97–107
Williams D McB, Hatcher AI (1983) Structure of fish communities on outer slopes of inshore. mid-shelf and outer shelf reefs of the Great Barrier Reef. Mar Ecol Prog Ser 10:239–250

Editorial responsibility: Gotthilf Hempel, Bremen, Germany

Submitted: May 3, 2001; Accepted: January 31, 2002
Proofs received from author(s): July 25, 2002

Vol. 239: 301–310, 2002 | MARINE ECOLOGY PROGRESS SERIES
Mar Ecol Prog Ser | Published August 23

Environmental and biological effects on the stable oxygen isotope records of corals in the northern Gulf of Aqaba, Red Sea

Saber Al-Rousan[1,2,*], Salim Al-Moghrabi[2], Jürgen Pätzold[1], Gerold Wefer[1]

[1]Fachbereich Geowissenschaften, Universität Bremen, 28359 Bremen, Germany
[2]Marine Science Station, PO Box 195, Aqaba, Jordan

ABSTRACT: Monthly $\delta^{18}O$ records of 2 coral colonies (*Porites* cf. *lutea and P.* cf. *nodifera*) from different localities (Aqaba and Eilat) from the northern Gulf of Aqaba, Red Sea, were calibrated with recorded sea surface temperatures (SST) between 1988 and 2000. The results show high correlation coefficients between SST and $\delta^{18}O$. Seasonal variations of coral $\delta^{18}O$ in both locations could explain 91% of the recorded SST. Different $\delta^{18}O$/SST relations from both colonies and from the same colonies were obtained, indicating that $\delta^{18}O$ from coral skeletons were subject to an extension rate effect. Significant $\delta^{18}O$ depletions are associated with high extension rates and higher values with low extension rates. The relation between coral skeletal $\delta^{18}O$ and extension rate is not linear and can be described by a simple exponential model. An inverse relationship extends over extension rates from 1 to 5 mm yr^{-1}, while for more rapidly growing corals and portions of colonies the relation is constant and the extension rate does not appear to have a significant effect. We recommend that $\delta^{18}O$ values be obtained from fast-growing corals or from portions in which the isotopic disequilibrium is fairly constant (extension rate >5 mm yr^{-1}). The results show that interspecific differences in corals may produce a significant $\delta^{18}O$ profile offset between 2 colonies that is independent of environmental and extension-rate effects. We conclude that the rate of skeletal extension and the species of coral involved have an important influence on coral $\delta^{18}O$ and must be considered when using $\delta^{18}O$ records for paleoclimatic reconstructions.

KEY WORDS: Stable oxygen isotopes · Coral extension rate · Coral calcification rate · *Porites* spp. · Gulf of Aqaba · Red Sea

INTRODUCTION

Massive-growing corals can be used as environmental recorder because their annual growth bands allow the reconstruction of accurate chronologies (Knutson et al. 1972). Massive hermatypic coral skeletons are excellent monitors of tropical water environments. Corals of this type live in the surface-ocean mixed layer, grow continuously at rates of several mm to cm per yr, and during growth incorporate isotopic species into their skeleton.

The stable oxygen isotopic composition ($\delta^{18}O$) of hermatypic corals has been utilised in numerous reconstructions of past sea surface temperatures (SST) and salinities (e.g. Charles et al. 1997, Gagan et al. 2000). Coral $\delta^{18}O$ reflects a combination of local SST and the $\delta^{18}O$ value of ambient seawater (Epstein et al. 1953, Wefer & Berger 1991). However, changes in coral growth rates may change the absolute isotopic values. Variations in the extension and calcification rates have an impact on the fractionation of stable isotopes and have long been a subject of discussion (Land et al. 1975, Goreau 1977, Weil et al. 1981, Pätzold 1986, McConnaughey 1989, de Villiers et al. 1995, Allison et al. 1996, Leder et al. 1996, Cohen & Hart 1997). Signif-

*E-mail: alrousan@uni-bremen.de

icant skeletal $\delta^{18}O$ depletion in faster-growing areas of coral skeleton compared to slower-growing areas were reported for the first time by Land et al. (1975). Allison et al. (1996) observed in *Porites lutea* from Phuket, south Thailand, that the growth rate/$\delta^{18}O$ relationship is linear at all extension rates, while McConnaughey (1989) found this relation in *Pavona clavus* from Galápagos only in parts of corals extending at a rate of less than 5 mm yr^{-1}. For more rapidly growing parts of the coral, extension rate does not appear to have a significant effect on $\delta^{18}O$.

Few studies have examined skeletal $\delta^{18}O$ variations within and among species. From studies on corals from Kaneohe Bay, Hawaii, Grottoli (1999) found that $\delta^{18}O$ values are constant over variable depths for a given species, and that this parameter exhibits interspecific variability. Species-specific offsets in $\delta^{18}O$ have also been reported by Weil et al. (1981) and Wellington et al. (1996).

In this study we examined skeletal $\delta^{18}O$ composition of 2 *Porites* colonies collected from the northern end of the Gulf of Aqaba: from Aqaba at a depth of 19 m (*Porites* cf. *lutea*) and from Eilat at 15 m (*P.* cf. *nodifera*). To evaluate the effect of extension rate that is independent of *in situ* temperature, variations in the $\delta^{18}O$ of seawater and specific-species effects, samples for $\delta^{18}O$ analysis were taken from each specimen along synchronous growth profiles with different extension rates. Previously published and unpublished coral $\delta^{18}O$ data from the area are also included in this study for comparison. However, the results from this study can be used to evaluate and correct coral $\delta^{18}O$ values from modern and fossil corals for extension rate effects.

MATERIALS AND METHODS

The study area is located at the northern end of the Gulf of Aqaba (Fig. 1), which is the northward extension of the desert-enclosed Red Sea. The maximum depth of the Gulf is 1830 m; its 180 km long and 5 to 26 km wide. Oligotrophic conditions prevail in the Gulf waters, and evaporation (350 cm yr^{-1}) greatly exceeds precipitation (3 cm yr^{-1}) (Reiss & Hottinger 1984).

A column of a *Porites* cf. *nodifera* colony was collected in front of the Interuniversity Institute in Eilat (29° 31′ N, 34° 56′ E) at a depth of 15 m in April 1996 (El-15), while another column of a *P.* cf. *lutea* colony (Aq-19) was collected in front of the Marine Science Station in Aqaba (29° 27′ N and 34° 90′ E) at a depth of 19 m in April 1999. Both coral columns were sectioned along their longitudinal axes to obtain slabs of about 4 mm thickness. X-radiographs were prepared to reveal annual density bands for determining sampling profiles (Fig. 2). Aragonite sub-samples were collected by low-speed drilling using a dentist drill with a 0.6 mm diameter bit. Distance between samples was about 1 mm and the drilling depth was 3 mm. A number of 7 to 12 samples (average 9) yr^{-1} from both corals were obtained along the maximum growth axis (main profile). In addition, we continuously sampled stable isotopic profiles drilled along lateral corallites from the sides of both colonies that showed low growth rate (Fig. 2).

The isotopic composition of the samples was measured with a Finnigan MAT 251 mass spectrometer at Bremen University. All values are reported in per mil relative to VPDB. The average measurement precision for $\delta^{18}O$ was ±0.07‰.

The chronologies of both corals were constructed by designating the maximum $\delta^{18}O$ value within each year as mid-March (the coldest month in the year according to recent SST records from Eilat and Aqaba). Linear interpolation of 12 equidistant values for the main profiles (6 for the side profiles) yr^{-1} between these maxima was applied, using AnalySeries 1.1 software package (Paillard et al. 1996). This procedure provided a monthly and bimonthly sampling resolution.

Absolute bulk density was measured by gamma-densitometry on a Multi Sensor Core Logger (Geotek) with a Cs^{137} source and 1 mm collimator at the Ocean Drilling Core Repository in Bremen. The method is based upon the attenuation of a gamma photon beam,

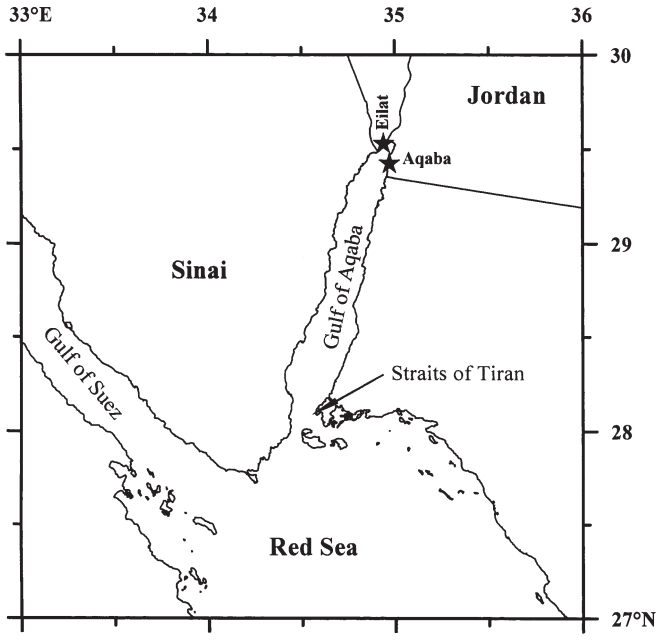

Fig. 1. Location map of the Gulf of Aqaba showing collection sites (★) of *Porites* spp. coral colonies from Aqaba and Eilat, northern Gulf of Aqaba

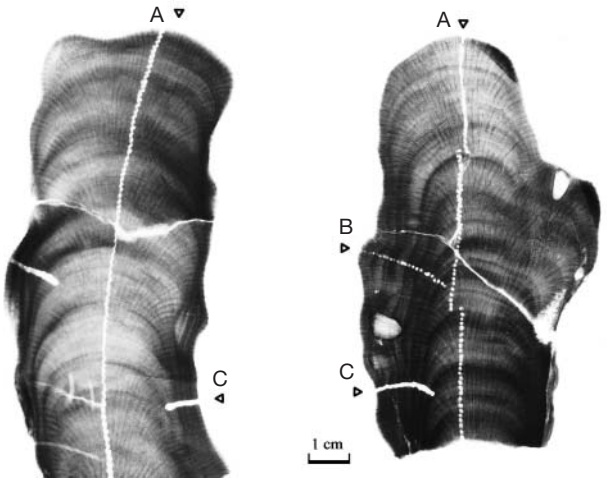

Fig. 2. *Porites* spp. X-radiograph-positive prints of the 2 coral slabs (Left: Aq-19; right: El-15) showing the skeletal density bands and the sampling profiles used for stable isotope analysis (Profiles A, B, and C) as indicated by the arrowheads

depending on the thickness and density of the skeleton material (Chalker & Barnes 1990). Annual mean bulk densities were calculated from the seasonal cycles of density variations which were measured along adjacent profiles near the drilled profiles.

The monthly temperature record from Aqaba was obtained between 1997 and 2000 (R. Manasreh pers. comm.). The measurements were based on biweekly measurements in the upper 1 m of the water column using an OS200 CTD instrument (precision 0.001°C). The measurements were performed in front of the Marine Science Station, 300 m away from the coral site.

Monthly measurements of SST from Eilat between 1988 and 2000 were used for comparison (A. Genin pers. comm.). The measurements were based on daily observations in the upper 20 cm of the water column (200 m distant from the site where the coral was collected) with a pre-calibrated mercury thermometer (precision 0.1°C) fixed in a bucket.

RESULTS

Seawater temperature records

No major significant differences were observed between the SST recorded in Aqaba and Eilat. At both locations, SST show the same regular seasonal cycle and have the same seasonal amplitude (5.5°C). They average 23.6°C, with maximum temperatures of 26.4°C (on average) in August–September, and minimum temperatures of 20.9°C (on average) in February–March (Fig. 3).

Salinity and $\delta^{18}O$ of seawater

Seawater $\delta^{18}O$ ($\delta^{18}O_w$) is related to changes in salinity as a response to changes in evaporation, precipitation and mixing of waters from different sources. This relation between $\delta^{18}O_w$ and salinity differs from ocean to ocean. In the Red Sea a change of 1‰ salinity causes a change of 0.29‰ in $\delta^{18}O_w$ according to Craig (1966) and Andrié & Merlivat (1989). At the northern end of the Gulf of Aqaba the salinity of the surface waters is close to 40.5‰, and varies by less than 0.5‰ throughout the year (Wolf-Vecht et al. 1992).

Manasreh (1998) reported that average minimum salinities of 40.34‰ occur during winter (February) and maximum salinities of 40.56‰ during summer (June). These minor variations in the surface seawater salinity throughout the year are considered to have little effect on the seasonal variation of the seawater $\delta^{18}O$ (Klein et al. 1992) (0.225‰ salinity = 0.065‰ $\delta^{18}O$: Craig 1966). Therefore, the seasonal $\delta^{18}O$ variation in the coral skeleton of the northern Gulf of Aqaba should be mainly controlled by SST (Heiss et al. 1999).

Calibration of $\delta^{18}O$ in coral skeletons

The x-radiograph-positive prints of the coral slabs reveal a clear and regular skeletal density-banding pattern. The alternating bands of high and low densities are annual, as confirmed by the strong seasonal cycle in $\delta^{18}O$.

The comparison between local SST records and the coral $\delta^{18}O$ time series is a necessary first step in the calibration of coral $\delta^{18}O$ records. The oxygen isotope profiles of both corals showed well-organized cyclic variations along the axis of maximum extension rate (fast-growing tops) (Profiles Aq-19A and El-15A: Fig. 4). $\delta^{18}O$ in the Aqaba coral ranged between –2.45 and –3.55‰ (average –3.10‰) and in the Eilat coral between –2.10 and –3.28‰ (average –2.79‰). Each $\delta^{18}O$ profile showed strong seasonal variations with similar amplitudes. These were on average 0.80‰ in Aqaba and 0.83‰ in Eilat. Both profiles correspond remarkably well to the monthly SST measurements in Aqaba and Eilat (Fig. 5). The correlation coefficients are rather high and range between –0.84 in the Eilat coral (in the time interval 1988 to 1995) and –0.81 in the Aqaba coral (in the time interval 1995 to 1999). Unfortunately no instrumental temperature data were available from Aqaba during the period 1988 to 1995.

Monthly records of $\delta^{18}O$ in both locations from the main growth profile (Aq-19A and AEl-15A) were cali-

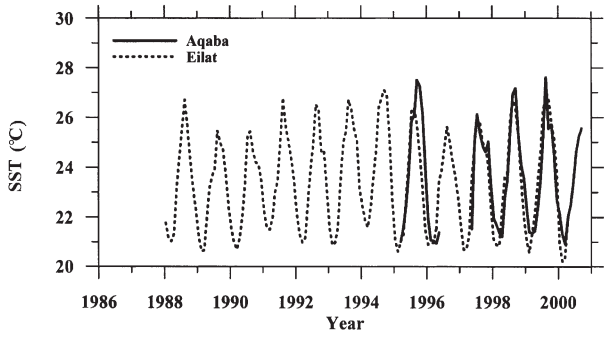

Fig. 3. Monthly recorded sea surface temperatures (SST) in Aqaba between 1997 and 2000 (R. Manasreh unpubl. data) and in Eilat between 1988 and 2000 (A. Genin unpubl. data)

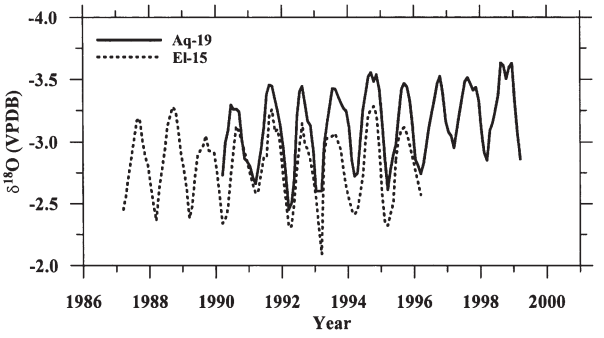

Fig. 4. *Porites* spp. Stable oxygen isotope profiles from samples drilled vertically along the axis of maximum extension rate of *P.* cf. *lutea* from Aqaba and *P.* cf. *nodifera* from Eilat between 1987 and 1999

brated with recorded SST, and the following equations are the results of the calculations:

$$SST\ (°C) = -5.93\ (\delta^{18}O_{coral}) + 4.63$$
$$r = -0.81\ (99.5\%\ level)\ Aqaba\ coral$$
$$SST\ (°C) = -5.75\ (\delta^{18}O_{coral}) + 7.30$$
$$r = -0.84\ (99.5\%\ level)\ Eilat\ coral$$

The $\delta^{18}O$/SST relationship from these equations varies between 0.168‰/°C from Aqaba and 0.174‰ /°C from Eilat coral. The correlations from the annual averages of the $\delta^{18}O$ record and the annual average SST of the 2 corals were low (–0.25 to –0.31) despite the fact that the annual $\delta^{18}O$ record follows that of the annual SST record.

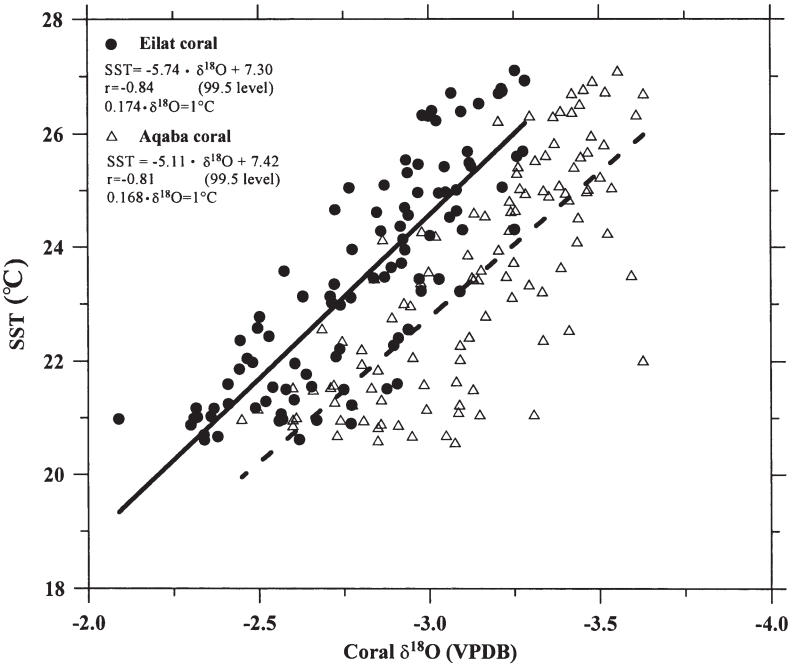

Fig. 5. *Porites* spp. Comparison of monthly variations in coral $\delta^{18}O$ (from profiles drilled vertically along axis of maximum extension rate) with monthly recorded sea surface temperatures (SST) at Aqaba and Eilat

Extension rate and skeletal $\delta^{18}O$

Comparison of the $\delta^{18}O$ records from Aqaba and Eilat (from the main profiles, Aq-19A and El-15A) for the period 1990 to 1995 shows that the Aqaba coral is several degrees more depleted in $\delta^{18}O$ than the Eilat coral. The offset between the 2 colonies ranged between 0.27 and 0.36‰ with an average of 0.29‰, and appears to be constant over the length of all years covered (Fig. 4).

Annual extension rates were determined from the seasonal cycle of $\delta^{18}O$ as the distance from the maximum $\delta^{18}O$ value (which represents the minimum recorded temperature) in a given year to the maximum value in the following year. The Eilat coral showed lower mean annual extension rates, ranging between 7 to 13 mm yr^{-1} (11.2 mm yr^{-1} on average), compared to 12 to 21 mm yr^{-1} (15.2 mm yr^{-1} on average) in the Aqaba coral.

We examined the relationship between annual extension rates and mean annual $\delta^{18}O$ in Aqaba and Eilat corals. The $\delta^{18}O$ values obtained along the slower extension rate profile (El-15A) were more enriched in $\delta^{18}O$ than the faster extension rate profile (Aq-19A).

Coral $\delta^{18}O$ from synchronous growth profiles

To evaluate the extension rate effect that is independent of the *in situ* temperature and variations in $\delta^{18}O$ of the seawater, $\delta^{18}O$ samples were taken from each specimen along synchronous growth profiles with different extension rates.

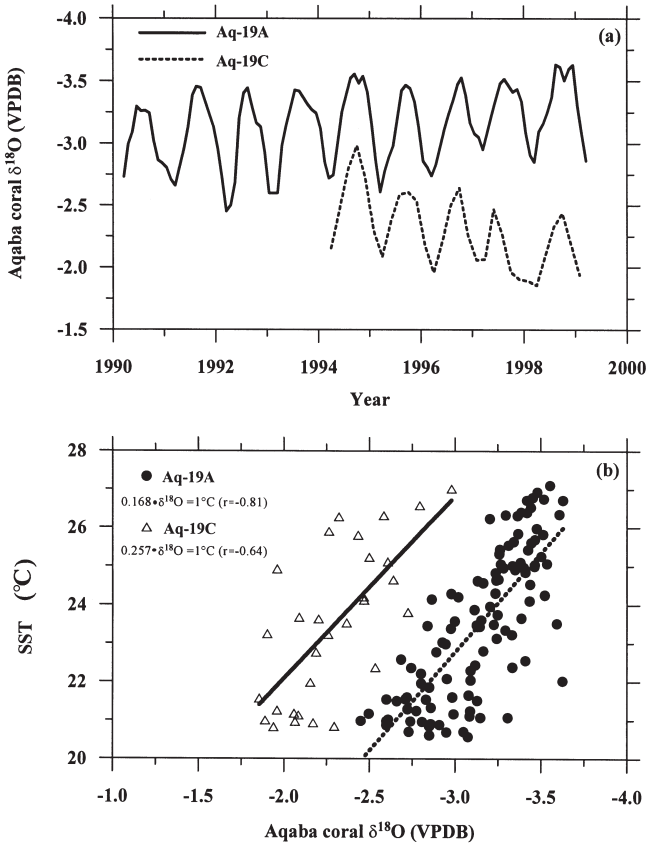

Fig. 6. *Porites* cf. *lutea.* (a) Seasonal variation in $\delta^{18}O$ (VPDB) composition of Aqaba coral along 2 different profiles; (b) linear relation between $\delta^{18}O$ and recorded sea surface temperatures (SST) along 2 different coral extension rate profiles (Aq-19A, 15.2 mm yr^{-1}; Aq-19C, 1.9 mm yr^{-1})

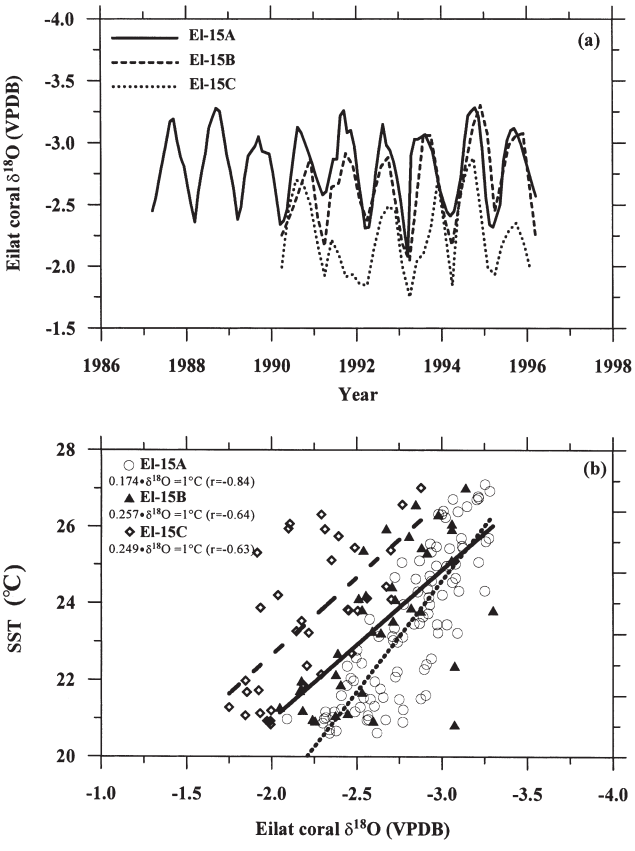

Fig. 7. *Porites* cf. *nodifera.* (a) Seasonal variation in $\delta^{18}O$ (VPDB) composition of Eilat coral along 3 different profiles; (b) linear relation between $\delta^{18}O$ and recorded sea surface temperatures (SST) along 3 different coral extension-rate profiles (El-15A, 11.2 mm yr^{-1}; El-15B, 3.9 mm yr^{-1}; El-15C, 2.3 mm yr^{-1})

The bimonthly $\delta^{18}O$ profile from the Aqaba coral (Aq-19C) with extension rates between 1 and 2.5 mm yr^{-1} (average 1.9 mm yr^{-1}) showed a seasonal amplitude of 0.73‰. Values ranged between −1.85 and −2.98‰ (average −2.29‰), similar to that obtained from the slowest growth profile of the Eilat coral (El-15C), 0.81‰ higher than the average value of the main profile from the same colony (Aq-19A) (Fig. 6a).

The bimonthly $\delta^{18}O$ profiles from the slower-growing sides of the Eilat coral (El-15B and El-15C) show strong seasonal variations of 0.82 and 0.89‰ seasonal amplitude, similar to that obtained from the main profile from the same colony (El-15A).

The $\delta^{18}O$ values from Profile El-15B ranged between −2.04 and −3.30‰, with an average of −2.68‰, which is 0.11‰ higher than that obtained from the main profile (Fig. 7a). The extension rate in this profile ranged between 2 and 5 mm yr^{-1} (average 3.9 mm yr^{-1}). Also, $\delta^{18}O$ values from the El-15C profile ranged between −1.75 and −2.87‰ (average −2.23‰), 0.15‰ higher than that from El-15B (Fig. 7a). The extension rate in this profile ranged between 1.5 and 3 mm yr^{-1} (average 2.3 mm yr^{-1}).

Calibration of $\delta^{18}O$ from these profiles with recorded SST at bimonthly intervals, produced different $\delta^{18}O$/SST equations (Figs. 6b & 7b) that varied between 0.21‰ $°C^{-1}$, 0.25‰ $°C^{-1}$ and 0.24‰ $°C^{-1}$, with correlation coefficients of 0.69, 0.64 and 0.63 from Aq-19C, El-15B, El-15C, respectively.

Relation between growth variables

Calcification rate was calculated as a product of linear extension and skeletal density (Chalker et al. 1985, Lough & Barnes 2000). Calcification values along all profiles ranged between 2.2 and 0.157 g cm^{-2} yr^{-1}, with an average of 0.92 g cm^{-2} yr^{-1}, and decreased from the top to the sides of the colonies due to decreases in the extension rates.

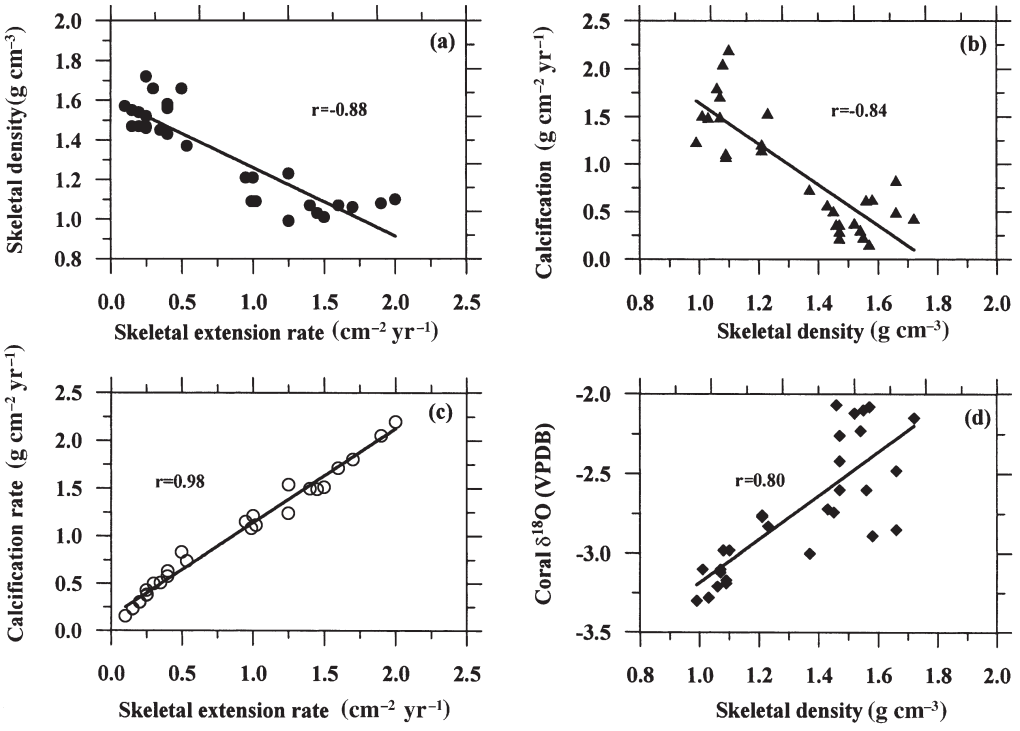

Fig. 8. *Porites* spp. Scatter diagram of average annual growth data for Aqaba and Eilat corals (combined data). (a) Density vs extension; (b) calcification vs extension; (c) calcification vs density; (d) density vs skeletal stable oxygen isotopes. Regression lines and correlation coefficients are shown

The relations between density, extension and calcification rate in this study (Fig. 8) are similar to the growth relations reported for other studies (Wellington & Glynn 1983, Dodge & Brass 1984, Scoffin et al. 1992, Lough & Barnes 2000). Average annual extension was inversely correlated with average annual density (r = 0.88) and significantly correlated with average annual calcification (r = 0.98). Average skeletal density was inversely correlated with average annual calcification (r = 0.84) and skeletal oxygen isotope (r = 0.80). Thus, we conclude that variations in average annual calcification were mostly caused by variations in extension rate, as found by Barnes & Lough (1993) and Lough & Barnes (2000).

DISCUSSION

Calibration of coral $\delta^{18}O$

Our $\delta^{18}O$/SST slopes from the main profiles of the Aqaba and Eilat corals (0.168 and 0.174‰/°C) are less than the widely accepted values of 0.22‰ for calcite (Epstein et al. 1953) and 0.23‰/°C for aragonite (Grossman & Ku 1986), and are similar to values determined by Gagan et al. (1994) for *Porites* sp. at a weekly resolution from the Great Barrier Reef (0.18‰/°C) and by Quinn et al. (1998) for a New Caledonia *Porites* sp. on a monthly scale (0.172‰/°C).

Felis et al. (1998) and Moustafa (2000) determined a value of 0.165‰/°C as the most reasonable for calibration for *Porites* sp. from Ras Umm Sid, Red Sea (using the IGOSS temperature data set). Heiss et al. (1999) also found a value of 0.166 and 0.187‰/°C from monthly resolution in horizontal and vertical profiles of a *P. lutea* colony from Aqaba.

On an annual timescale, the correlation coefficient decreased to −0.25 and −0.31. For New Caledonia corals, Quinn et al. (1998) reported that the correlation coefficient decreased from −0.87 on a seasonal timescale to −0.53 on an annual timescale. They explained this decrease as being due to salinity changes, whereby seasonal variations in salinity are small compared to those for temperature, while interannual changes in salinity are proportionally larger than their seasonal changes.

This may also be the situation in the northern Gulf of Aqaba. A regular measurement of seawater salinity over 4 yr (1997 to 2000) showed no systematic annual pattern (R. Manasreh, pers. comm. [2000]) and the average annual values differed from year to year. The interannual variations during this period were as much as 0.4‰, compared to 0.225‰ on a seasonal scale. The potential impact of 0.4‰ interannual salinity variation

on $\delta^{18}O$ of Red Sea water and hence on coral $\delta^{18}O$ is 0.12‰ (after Craig 1966). This effect could explain part of the difference in the seasonal and mean annual slopes of $\delta^{18}O$/SST.

The measured SST in Aqaba and Eilat reveal an average annual cycle of about 5.5°C. Using the gradient of 0.165‰/°C for coral $\delta^{18}O$-temperature dependence from the northern Red Sea (Felis et al. 1998, Moustafa 2000), the average seasonal coral $\delta^{18}O$ variation of 0.83‰ would reflect a temperature change of about 5.0°C, which is about 91% of the average seasonal SST amplitude. The expected variation of 0.065‰ $\delta^{18}O$ in seawater (related to a 0.225‰ change in salinity) constitutes 7.8% of the average seasonal coral $\delta^{18}O$ variation. This indicates that a large majority of the variations in coral oxygen isotope data can be explained by variations in the SST, and only a small fraction can be attributed to $\delta^{18}O$ variations of surface water.

It is obvious from our results that different $\delta^{18}O$/SST relations exist in different colonies and in different parts of the same colony. These variations are most probably biologically mediated, as outlined in the following subsection.

Effect of extension rate on skeletal $\delta^{18}O$ composition

Both main $\delta^{18}O$ profiles for the 2 colonies (Aq-19A and El-15A) show similar amplitudes (0.83 and 0.80‰, respectively), which implies that both corals respond similarly to environmental signals. The offset between the $\delta^{18}O$ profiles (~0.29‰ on average, with lower $\delta^{18}O$ values in the Aqaba coral) does not reflect changes in temperature and/or salinity between the 2 sites (similar physical environment) and is probably a biologically mediated signal.

Although the profiles from the coral sides (Aq-19C and El-15B, C) were sampled at lower resolution, they displayed roughly the same seasonal amplitude as the main profiles with a monthly sampling resolution. Analysis of $\delta^{18}O$ along the main and synchronous growth profiles revealed different trends in the $\delta^{18}O$ values (Figs. 5, 6b, 7b). These results indicate that the $\delta^{18}O$ values are subject to extension and calcification rate effects, i.e. the faster-growing profile (Aq-19A) is 0.29‰ more depleted in $\delta^{18}O$ than the slower-growing profile (El-15A). A trend of higher $\delta^{18}O$ content with slower extension rate was also observed in the synchronous growth profiles of both colonies (Aq-19C, El-15B, El-15C).

The relation between coral $\delta^{18}O$ and skeletal growth rate determined in this study is not linear and can be explained by a simple exponential model (Fig. 9):

$$\text{Coral } \delta^{18}O = -3.067 + \exp[1.069 + (-0.744) \times ER]$$
$$\text{Aqaba coral } r = 0.96$$
$$\text{Coral } \delta^{18}O = -2.795 + \exp[1.016 + (-0.757) \times ER]$$
$$\text{Eilat coral } r = 0.97$$

where ER is the coral extension rate (mm yr^{-1}), and $\delta^{18}O$ is ‰VPDB.

Coral $\delta^{18}O$ data from Aqaba and Eilat and from the same genus (*Porites*) with different extension rates—Coral S4 (6.8 mm yr^{-1}), Coral MB30 (3.3 mm yr^{-1}), Coral IS50 (2.0 mm yr^{-1}) and Coral S6 (14.8 mm yr^{-1}) (Klein et al. 1993, J. Pätzold & R. Klein unpubl. data), Aq-193 (20 mm yr^{-1}), Coral Aq-292 (5.3 mm yr^{-1}) and Coral Aq-424 (3.5 mm yr^{-1}) (Al-Rousan unpubl. data)—are also plotted in Fig. 9. The data fit the curve and support the reliability of the exponential model.

The inverse relationship between $\delta^{18}O$ and extension rate revealed by this model applies to growth rates of 1 to 5 mm yr^{-1} (Profiles Aq-19C, Aq-292, Aq-424, El-15B, El-15C, MB30, and IS50). For more rapidly growing corals and portions of corals (as in Profiles Aq-19A, Aq-193, El-15A, S4 and S6: Fig. 9), the relation is constant, and the extension rate does not appear to have a significant effect on coral $\delta^{18}O$.

These results are similar to those of McConnaughey (1989), who found an inverse relationship for Galápa-

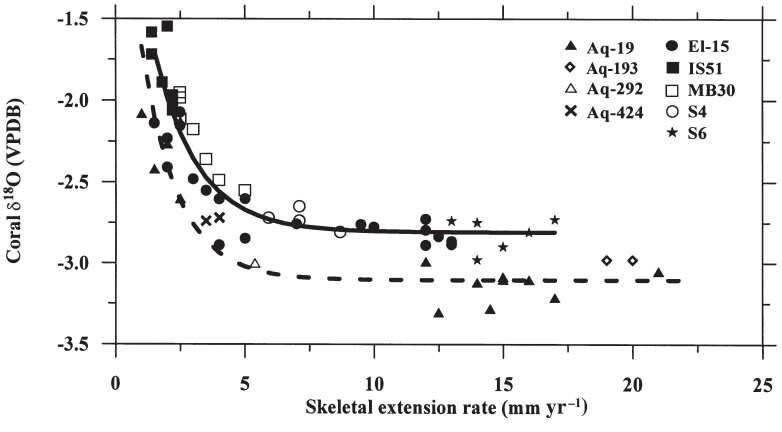

Fig. 9. *Porites* spp. Exponential relationship between skeletal $\delta^{18}O$ and skeletal extension rate of colonies sampled along vertical (main axis) and horizontal (coral sides) profiles of corals collected from the northern Gulf of Aqaba, Red Sea. Data for Corals IS51, MB30 and S4 are from Klein et al. (1993), data for S6 from J. Pätzold and R. Klein (unpubl. data), and for Aq-193, Aq-292 and Aq-424 from S. Al-Rousan (unpubl. data)

gos *Pavona clavus* corals that grew at rates of <5 mm yr^{-1}, and extension rate did not appear to have any significant effect on $\delta^{18}O$ composition at growth rates of >5 mm yr^{-1}. Quinn et al. (1998) also found a negative correlation in New Caledonia corals, and Allison et al. (1996) in corals from Phuket, South Thailand—but at all extension rates. Higher $\delta^{18}O$ and Sr/Ca values in slower growing transects were reported by de Villiers et al. (1995) for *Pavona clavus* from Galápagos. In contrast, Leder et al. (1996) found that the $\delta^{18}O$ content of rapidly growing portions (8 mm yr^{-1}) of a colony was 0.1 to 0.2‰ higher than that of the slowest growing portions (1.1 mm yr^{-1}), and explained this as a result of reduced sampling resolution in slower growing portions of the coral and not a result of variable kinetic effects.

We conclude that growth rate has an important effect on the isotopic composition of coral skeletons. Our results support the conclusion drawn by McConnaughey (1989) that the depletion of $\delta^{18}O$ is characteristic for kinetic fractionation associated with rapid calcification, and that isotope disequilibria tend to be fairly consistent in rapidly growing parts of photosynthetic corals. For this reason, we suggest that $\delta^{18}O$ should be measured in fast-growing portions where the extent of isotopic disequilibria is largest, since isotopic disequilibria are too variable in slow-growing parts.

Calcification rate and species-specific effects

As shown in Fig. 9, a $\delta^{18}O$ offset between Aqaba and Eilat colonies does exist. We calculated the calcification rate along the drilled profiles. Due to the high correlation between extension and calcification rate (Fig. 8c) the relation between calcification and $\delta^{18}O$ failed to explain the offset between the main $\delta^{18}O$ profiles for the 2 colonies. A similar exponential equation was produced (Fig. 10). We found that high extension profiles revealing low skeletal densities (Aq-19A) were depleted in $\delta^{18}O$ compared to low extension profiles showing high densities (El-15A) which may have had the similar calcification rate.

The offset between $\delta^{18}O$ profiles cannot always be explained as a function of extension and/or calcification rate. For this reason, both corals were taxonomically identified. Aq-19, Aq-193, Aq-292 and Aq-424 (which are depleted in $\delta^{18}O$ by ~0.29‰ compared to El-15) are *Porites* cf. *lutea*, while El-15 is *P.* cf. *nodifera*. Wellington et al. (1996) found that certain species are enriched or depleted in $\delta^{18}O$ relative to other species of the same genus living under the same environmental conditions, whereas Grottoli (1999) found for Hawaii corals that $\delta^{18}O$ varies among species. Species-specific offsets in $\delta^{18}O$ have been also reported by Weil et al. (1981). The $\delta^{18}O$ offset between coral species may reflect some genetic differences which alter the extent of isotopic disequilibria (Allison et al. 1996).

The results of this study show that the linear extension rate and species variation should be considered when interpreting coral $\delta^{18}O$ data for paleoclimatic studies. Further studies are also needed to study the variation of $\delta^{18}O$ of other *Porites* species.

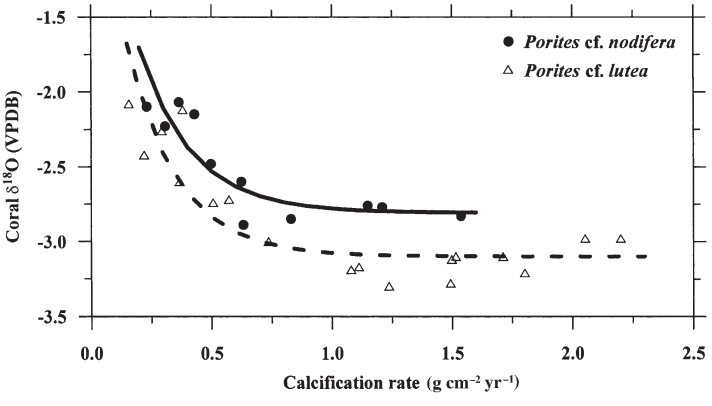

Fig. 10. *Porites* spp. Exponential relationship between skeletal $\delta^{18}O$ and skeletal calcification rate for 2 species collected from the northern Gulf of Aqaba, Red Sea

CONCLUSIONS

The high correlation between coral $\delta^{18}O$ and recorded SST (–0.84) in both Aqaba and Eilat in the northern Red Sea suggests that the great majority of the seasonal variations in coral oxygen isotopes can be explained by the SST variations, and only a small fraction can be attributed to $\delta^{18}O$ variations in the surface water. These results support the concept of using northern Red Sea corals as recorders of variability in SST. Interannual salinity variations in the Gulf of Aqaba (as recorded in recent studies) seem to be responsible for decreasing the correlation between coral $\delta^{18}O$ and SST on the annual timescale.

Different $\delta^{18}O$/SST relations from 2 different colonies and also from the same colonies were obtained, indicating that $\delta^{18}O$ of coral skeletons is subject to an extension rate effect. Significant $\delta^{18}O$ depletion occurs at high extension rates, and higher values at low extension rates. The relation between $\delta^{18}O$ and extension rate is not linear, and can be explained by a simple exponential model in which the inverse function extends over extension rates of 1 to 5 mm yr^{-1}. For more rapidly growing corals and portions

of coral colonies, the relation is constant, and the extension rate did not appear to have any significant effect on coral $\delta^{18}O$. The offset in $\delta^{18}O$ profiles cannot always be explained as a function of extension and/or calcification rate, and may result from interspecific differences between corals.

We suggest that $\delta^{18}O$ values from *Porites* spp. corals should be measured from fast-growing corals or portions of the colonies (growth rate of >5 mm yr^{-1}), in which the isotopic disequilibrium is fairly constant. Skeletal extension rate and coral species should be considered when interpreting and comparing coral paleoclimatic data from various coral species with different extension rates.

Acknowledgements. We wish to thank Y. Loya for coral sample collection at Eilat. Special thanks are also due to R. Manasreh and A. Genin for providing temperature records from Aqaba and Eilat. All isotopic measurements were carried out at Bremen University. We are grateful to M. Segl for stable isotope analysis and U. Röhl for introduction to the Multi Sensor Core Logger. This work is part of the Red Sea Programme (RSP, II), funded by the German Federal Ministry of Education, Science, Research, and Technology (BMBF).

LITERATURE CITED

Allison NT, Tudhope AW, Fallick AE (1996) Factors influencing the stable carbon and oxygen isotopic composition of *Porites lutea* coral skeletons from Phuket, south Thailand. Coral Reefs 15:43–57

Andrié C, Merlivat L (1989) Contribution des données isotopique de deutérium, oxygène-18, hélium-3 et tritium, à l'étude de la circulation de la Mer Rouge. Oceanol Acta 12:165–174

Barnes DJ, Lough JM (1993) On the nature and causes of density banding in massive coral skeletons. J Exp Mar Biol Ecol 167:91–108

Chalker BE, Barnes DJ (1990) Gamma densitometry for the measurement of coral skeleton density. Coral Reefs 9: 11–23

Chalker BE, Barnes DJ, Isdale PJ (1985) Calibration of X-ray densitometry for measurement of coral skeletal density. Coral Reefs 4:95–100

Charles CD, Hunter DE, Fairbanks RG (1997) Interaction between the ENSO and the Asian monsoon in a coral record of tropical climate. Science 277:925–928

Cohen AL, Hart SR (1997) The effect of colony topography on climate signals in coral skeleton. Geochim Cosmochim Acta 61:3905–3912

Craig H (1966) Isotopic composition and origin of the Red Sea and Salton Sea geothermal brines. Science 154:1544–1548

de Villiers S, Nelson BK, Chivas AR (1995) Biological controls on coral Sr/Ca and $\delta^{18}O$ reconstructions of sea surface temperatures. Science 269:1247–1249

Dodge RE, Brass GW (1984) Skeletal extension, density and calcification of the reef coral, *Montastrea annularis*: St. Croix, U.S. Virgin Islands. Bull Mar Sci 34:288–307

Epstein S, Buchsbaum R, Lowenstam HA, Urey HC (1953) Revised carbonate-water isotopic temperature scale. Geol Soc Am Bull 64:1315–1322

Felis T, Pätzold J, Wefer G, Fine M, Loya Y, Nawar AH (1998) First results of a coral-based history of recent climate in the northern Red Sea. Zentbl Geol Paläont Teil I :197–209

Gagan MK, Chivas AR, Isdale PJ (1994) High-resolution isotopic records from corals using ocean temperature and mass-spawning chronometers. Earth Planet Sci Lett 121: 249–258

Gagan MK, Ayliffe LK, Beck JW, Cole JE, Druffel ERM, Dunbar RB, Schrag DB (2000) New views of tropical paleoclimates from corals. Quat Sci Rev 19:45–64

Goreau TJ (1977) Coral skeletal chemistry: physiological and environmental regulation of stable isotopes and trace metals in *Montastrea annularis*. Proc R Soc Lond Ser B 196:291–315

Grossman EL, Ku TL (1986) Oxygen and carbon isotope fractionation in biogenic aragonite: temperature effects. Chem Geol (Isotope Geosci Sect) 59:59–74

Grottoli AG (1999) Variability of stable isotope and maximum linear extension in reef-coral skeletons at Kaneohe Bay, Hawaii. Mar Biol 135:437–449

Heiss GA, Dullo WC, Joachimski M, Reijmer J, Schuhmacher H (1999) Increased seasonality in the Gulf of Aqaba, Red Sea recorded in the oxygen isotope record of a *Porites lutea* coral. Senckenb Marit 30:17–26

Klein R, Pätzold J, Wefer G, Loya Y (1992) Seasonal variations in the stable isotopic composition and the skeletal density pattern of the coral *Porites lobata* (Gulf of Eilat, Red Sea). Mar Biol 112:259–263

Klein R, Pätzold J, Wefer G, Loya Y (1993) Depth-related timing of density band formation in *Porites* spp. corals from the Red Sea inferred from X-ray chronology and stable isotope composition. Mar Ecol Prog Ser 97:99–104

Knutson DW, Buddemeier RW, Smith SV (1972) Coral chronometers: seasonal growth bands in reef corals. Science 177: 270–272

Land LS, Lang JC, Barnes DJ (1975) Extension rate: a primary control on the isotopic composition of West Indian (Jamaican) scleractinian reef coral skeletons. Mar Biol 33: 221–233

Leder JJ, Swart PK, Szmant AM, Dodge RE (1996) The origin of variations in the isotopic record of scleractinian corals: I. Oxygen. Geochim Cosmochim Acta 60:2857–2870

Lough JM, Barnes DJ (2000) Environmental controls on growth of the massive coral *Porites*. J Exp Mar Biol Ecol 245:225–243

Manasreh RS (1998) Water circulation in the Gulf of Aqaba, Red Sea. MSc thesis, Yarmouk University, Irbid, Jordan

McConnaughey T (1989) ^{13}C and ^{18}O isotopic disequilibrium in biological carbonates. I. Patterns. Geochim Cosmochim Acta 53:151–162

Moustafa YA (2000) Paleoclimatic reconstructions of the northern Red Sea during the Holocene inferred from stable isotope records of modern and fossil corals and molluscs. Berichte Fachbereich Geowissenschaften Universität Bremen No. 153. Universität Bremen

Paillard D, Labeyrie L, Yiou P (1996) Macintosh Program Performs time-series analysis. EOS Trans Am Geophys Un 77(39):379

Pätzold J (1986) Temperature and CO_2 changes in tropical surface waters of the Philippines during the past 120 years: record in the stable isotopes of hermatypic corals; Berichte, Geologisches Paläontologisches Institut Universität Kiel, No. 12, Kiel

Quinn TM, Crowely TJ, Taylor FW, Henin C, Joannot P, Join Y (1998) A multicentury stable isotope record from a New Caledonia coral: interannual and decadal sea surface temperature variability in the southwest Pacific since 1657 A.D. Paleoceanography 13:412–426

Reiss Z, Hottinger L (1984) The Gulf of Aqaba: ecological micropaleontology. Springer-Verlag, Berlin

Scoffin TP, Tudhope AW, Brown BE, Chansang H, Cheeney RF (1992) Patterns and possible environmental controls of skeletogenesis of *Porites lutea*, south Thailand. Coral Reefs 11:1–11

Wefer G, Berger WH (1991) Isotope paleontology: growth and composition of extant calcareous species. Mar Geol 100: 207–248

Weil S, Buddemeier R, Smith S, Kroopnick P (1981) The stable isotopic composition of coral skeletons: control by environmental variables. Geochim Cosmochim Acta 45: 1174–1153

Wellington G, Glynn P (1983) Environmental influences on skeletal banding in eastern Pacific (Panama) corals. Coral Reefs 1:215–222

Wellington GM, Dunbar RB, Merlen G (1996) Calibration of stable isotope signature in Galápagos corals. Paleoceanography 11:467–480

Wolf-Vecht A, Paldor N, Brenner S (1992) Hydrographic indicators of advection/convection effects in the Gulf of Eilat. Deep-Sea Res 39:1393–1401

Editorial responsibility: Gotthilf Hempel, Bremen, Germany

Submitted: May 3, 2001; Accepted: January 31, 2002
Proofs received from author(s): August 9, 2002